The bromodomain inhibitor JQ1 as novel therapeutic option for type II testicular germ cell tumours

The role of SOX2 and SOX17 in regulating germ cell tumour pluripotency

Dissertation

zur

Erlangung des Doktorgrades (Dr.rer.nat.)

der

Mathematisch-Naturwissenschaftlichen Fakultät

der

Rheinischen Friedrich-Wilhelms-Universität Bonn

vorgelegt von

Sina Verena Jostes

aus

Kassel

Bonn, 2019

Angefertigt mit Genehmigung der Mathematisch-Naturwissenschaftlichen
Fakultät der Rheinischen Friedrich-Wilhelms-Universität Bonn

1. Gutachter: Prof. Dr. Hubert Schorle

2. Gutachter: Priv.-Doz. Dr. Reinhard Bauer

Tag der Promotion: 29. Juli 2019

Erscheinungsjahr: 2019

Eidesstattliche Erklärung

Hiermit erkläre ich, dass diese Dissertation von mir selbst und ohne unerlaubte Hilfe angefertigt wurde. Es wurden keine anderen als die angegebenen Hilfsmittel benutzt. Ferner erkläre ich, dass die vorliegende Arbeit an keiner anderen Universität als Dissertation eingereicht wurde.

Teile dieser Arbeit wurden bereits in folgenden Publikationen veröffentlicht:

The bromodomain inhibitor JQ1 triggers growth arrest and apoptosis in testicular germ cell tumours in vitro and in vivo. Jostes S, Nettersheim D, Fellermeyer M, Schneider S, Hafezi F, Honecker F, Schumacher V, Geyer M, Kristiansen G, Schorle H**.** *J Cell Mol Med. 2016 Dec 27*

Epigenetic drugs and their molecular targets in testicular germ cell tumours.
Jostes S, Nettersheim D, Schorle H. *Nat Rev Urol*. *2019 Feb 14*

Bonn, 2019

Sina Verena Jostes

List of Abbreviations

AFP	Alpha-fetoprotein
AP	Alkaline Phosphatase
BETi	BET Inhibitor
BMP	Bone Morphogenic Protein
BRD	Bromodomain
ChIP	Chromatin Immunoprecipitation
CRISPR	Clustered Regularly Interspaced Short Palindromic Repeats
DAPI	6-Diamidino-2-Phenylindole Dihydrochloride
DNA	Deoxyribonucleic acid
DNMT	*De novo* Methyltransferase
EAU	European Association of Urology
EC	Embryonal Carcinoma
ESC	Embryonic Stem Cell
ESMO	European Society for Medical Oncology
FACS	Fluorescence-Activated Cell Sorting
GCNIS	Germ Cell Neoplasia In Situ
GSEA	Gene Set Enrichment Analysis
HAT	Histone Acetyltransferase
HCG	Human Chorionic Gonadotropin
HDAC	Histone Deacetylase
HDACi	HDAC Inhibitor
HOMER	Hypergeometric Optimization of Motif EnRichment
I.p.	Intraperitoneally
IP	Immunoprecipitation
iPSC	Induced Pluripotent Stem Cell
LDH	Lactate Dehydrogenase
MSigDB	Molecular Signatures Database
PARP	Poly (ADP-ribose) Polymerase
PGC	Primordial Germ Cell
qRT-PCR	Quantitative real-time PCR
RA	Retinoic Acid
RPLND	Retroperitoneal Lymph Node Dissection
SAM	Synergistic Activation Mediator
SDS	Sodium dodecyl sulfate
TET	Ten-Eleven Translocaton Enzyme
TGCT	Testicular Germ Cell Tumour
TSS	Transcription Start Site
WNT	Wingless/Integrated
YST	Yolk-Sac-Tumour

Table of Contents

List of Figures

List of Tables

Summary I

Type II testicular germ cell tumours (TGCTs) represent the most common malignancy in young men (19-35 years). They are classified as seminoma or embryonal carcinoma (EC; the stem cell population of non-seminomas). TGCTs are highly sensitive to radio- and chemotherapy, however 1-5% of TGCTs may develop resistance mechanisms to standard therapy regimens. Epigenetic drugs open a new avenue to cancer therapy and may present a promising alternative to treat recurrent TGCTs. JQ1 is an inhibitor of the BET family of bromodomain reader proteins. In TGCT cell lines, JQ1 treatment leads to upregulation of stress markers (i.e. *CDKN1C*, *DDIT4*, *TSC22D1*, *TXNIP*), induction of the differentiation marker *HAND1*, and downregulation of pluripotency-associated genes (i.e. *LIN28*, *DPPA4*, *UTF1*) [1]. This results in growth arrest and apoptosis in cisplatin-sensitive and cisplatin-resistant EC cells (at doses ≥ 100 nM) and seminoma cells (at doses ≥ 250 nM) [1, 2]. In line, EC xenografts in nude mice show reduced tumour burden when treated with JQ1 (50 mg / kg) compared to solvent controls. Additionally, JQ1-treated tumours showed reduced blood vessel count (lower CD31+), possibly due to JQ1-mediated downregulation of *VEGFB.* Altogether, this reflects the therapeutic potential of bromodomain inhibition for TGCTs. However, similar to TGCT cells, somatic control cells (here: Sertoli cells) responded with cell cycle arrest and apoptosis to JQ1 treatment. Thus, a more detailed analysis of possible side effects of JQ1 administration is recommended, before commissioning the drug for clinical use. Interestingly, JQ1 treatment had similar effects on TGCT cells as the HDAC inhibitor romidepsin (i.e. induction of stress markers *GADD45A*, *GADD45B*, *RHOB*, *ID2*) [1-3]. I now showed that JQ1 and romidepsin may elicit additive or synergistic effects on cytotoxicity levels of TGCT cells *in vitro* and *in vivo*. Since a combination of both drugs may, however, also increase potential side effects, the exact efficacy vs toxicity relationship of this treatment strategy needs further evaluation.

Summary II

TGCTs can be characterized as seminoma or EC. While seminomas display limited differentiation capacities, ECs display features of pluri- to totipotency. Previous data suggests that pluripotency in EC cells is maintained by cooperative binding of SOX2-OCT4 to the canonical (SOX2/OCT4) motifs at pluripotency genes. Indeed, SOX2 binding in EC cells is enriched at canonical motifs and SOX2 target genes showed significant overlap with embryonic stem cell signatures. In contrast, seminomas lack expression of SOX2, but display high levels of OCT4 and SOX17. In embryonic stem cells cooperative binding of SOX17-OCT4 to the compressed (SOX17/OCT4) motif on DNA induces endodermal differentiation. However, seminomas maintain an undifferentiated state, indicated by expression of pluripotency genes and lack of expression of typical differentiation markers. We therefore asked, whether the SOX17-OCT4 complex in seminoma cells binds to canonical (SOX2/OCT4) binding sites to regulate and maintain seminoma pluripotency. High-throughput chromatin immunoprecipiation (ChIP)-sequencing analysis revealed that the majority of genes bound by SOX17 in seminoma cells has functions in neuronal differentiation and that 26% of SOX17 peaks contain the compressed (SOX17/OCT4) binding motif. These findings are is in disagreement with the latent pluripotent state of seminoma cells. However, a small subset of SOX17-bound genes has roles in pluripotency maintenance (e.g. *NANOG, POU5F1* (*OCT4*), *PRDM1* and *TFAP2C*) and 10% of SOX17 peaks include the described canonical (SOX2/OCT4) binding motif. This suggests that, next to somatic genes, SOX17 regulates pluripotency genes in seminoma cells by binding to the canonical motif. In line, CRISPR/Cas9-mediated deletion of SOX17 in TCam-2 resulted in a strong reduction of OCT4 and TFAP2C protein levels, as well as alkaline phosphatase activity. qRT-PCR analysis showed that loss of SOX17 induces differentiation into trophoblast-like lineages. I conclude that SOX17 shares a similar role in seminoma cells as in primordial germ cells (PGC), which is to maintain a latent pluripotent state and to suppress cellular differentiation (i.e. via downstream activation of the PGC specifiers *PRDM1* and *TFAP2C* and by direct activation of pluripotency genes such as *NANOG* and *POU5F1*).

1. Introduction

1.1. Male germ cell development

Germ cells are the founder cells of new life. They harbour all necessary genetic and epigenetic information, which is propagated from one generation to the next. Like in other mammals, human germ cells are formed early during embryogenesis. These germ cells then later undergo meiosis to form haploid spermatocytes (in males) or oocytes (in females).

1.1.1. Transcription factors determining male germ cell fate

Human germ cell development is initiated two weeks after fertilization with the formation of primordial germ cells (PGCs). Similar to PGCs in primates, it is believed that human PGCs are specified in the nascent amnion, which expresses BMP4 and WNT3A at high levels [4]. Both signalling molecules are crucial for human germ cell development [4]. Recent data suggests that WNT signalling leads to *EOMES* induction, which in turn transactivates *SOX17*, resulting in upregulation of *BLIMP1* [5]. At the same time BMP2 (expressed in the extraembryonic mesoderm) and BMP4 activate *TFAP2C* expression [5]. Together, SOX17, BLIMP1 and TFAP2C form a tripartite transcription factor network and the core circuitry for human germ cell specification [5-7] (**Fig. 1**). Each factor exerts unique, but also overlapping roles in activating the germ cell program and in sustaining the epigenetic program of PGCs, thereby maintaining pluripotency and suppressing somatic differentiation [8]. Once specified, human PGCs migrate along the hindgut to the genital ridges. During this migration PGCs are stalled in G2 phase of the cell cycle, while they undergo global DNA demethylation and imprinting erasure [9]. 4-6 weeks following implantation of the embryo in the uterus, PGCs arrive in the genital ridge where they continue to amplify by mitosis [9]. From now on the male germ cells are referred to as gonocytes and express the following markers: MAGE-A4, DAZL, KIT, PLAP, POU5F1, TFAP2C, UTF1, VASA [10]. Approximately 6 months after birth the undifferentiated gonocytes (A_{dark}-spermatogonia) settle at the basal membrane of the seminiferous tubules of the testis, where they lose their pluripotent state and develop further into A_{pale}-spermatogonia [3, 11]. These remain quiescent until the age of ~ 10 years, when spermatogenesis starts

with the development of B-spermatogonia, which differentiate further into primary spermatocytes and subsequently undergo two rounds of meiotic division to become haploid spermatids [12]. During meiosis the developing spermatocytes lose contact with the basal membrane and migrate toward the lumen of the seminiferous tubules [12]. Finally, the haploid round spermatids differentiate into mature, motile spermatozoa (a process referred to as spermiogenesis) [13]. This process starts within the seminiferous tubules, from which the elongated spermatozoa are transported via the rete testis into the epididymis, where they mature and are stored [14]. The whole process of spermatogenesis (including spermiogenesis) in humans consumes approximately 74 days [15].

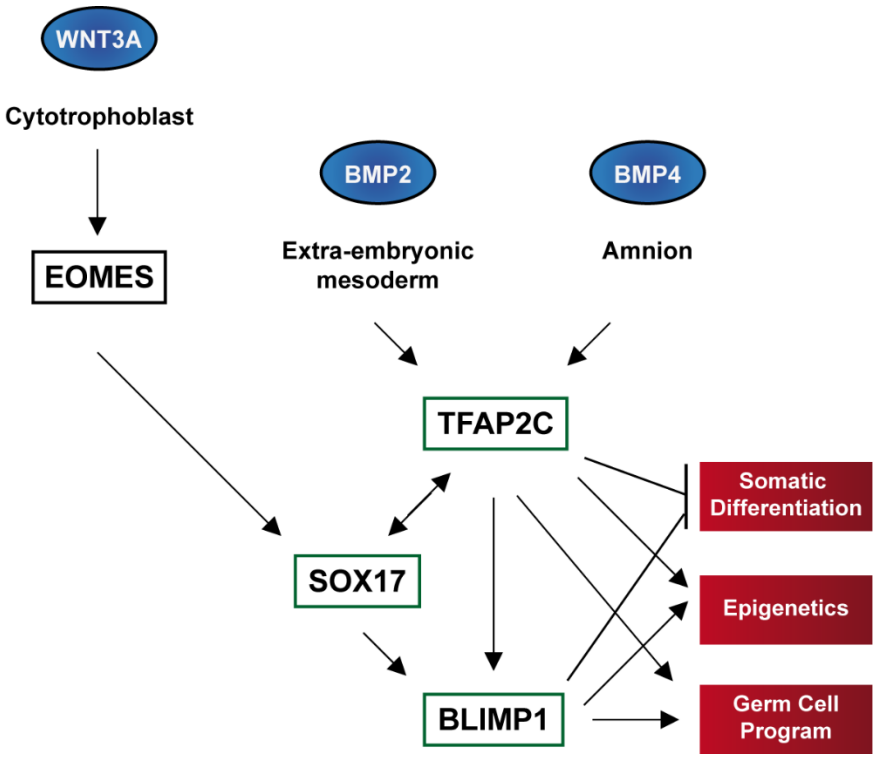

Figure 1: Germ cell specification in the human system. Modified from [8]
BMP2 and BMP4 are released from extra-embryonic mesoderm and the nascent amnion, triggering human germ cell development by activating *TFAP2C* expression [4, 5]. Further, WNT signalling activates expression of *EOMES*, which transactivates *SOX17*, resulting in upregulation of *BLIMP1* [5]. SOX17, TFAP2C and BLIMP1 form a tripartite transcription factor network, regulating epigenetic reprogramming, germ cell fate and suppression of somatic differentiation.

1.2. Malignant germ cell development

Testicular germ cell cancer is the most common form of cancer among males between 15 and 35 years [16]. It comprises a heterogeneous group of neoplasms that originates from male germ cells and is therefore anatomically distributed along the migration route of PGCs [17, 18]. Although the exact cause of germ cell cancer is unknown, it is believed that environmental factors, e.g. endocrine disruptors, may contribute to the risk of developing germ cell cancer [19]. Germ cell cancer incidence is globally increasing, however the development of novel chemotherapeutic treatment regimens has led to a drastic decline in mortality rates [20]. There are three types (I-III) of testicular germ cell tumours (TGCTs), which can be discriminated according to their anatomical site, stage of maturation and pattern of genomic imprinting [21] (**Fig. 2**).

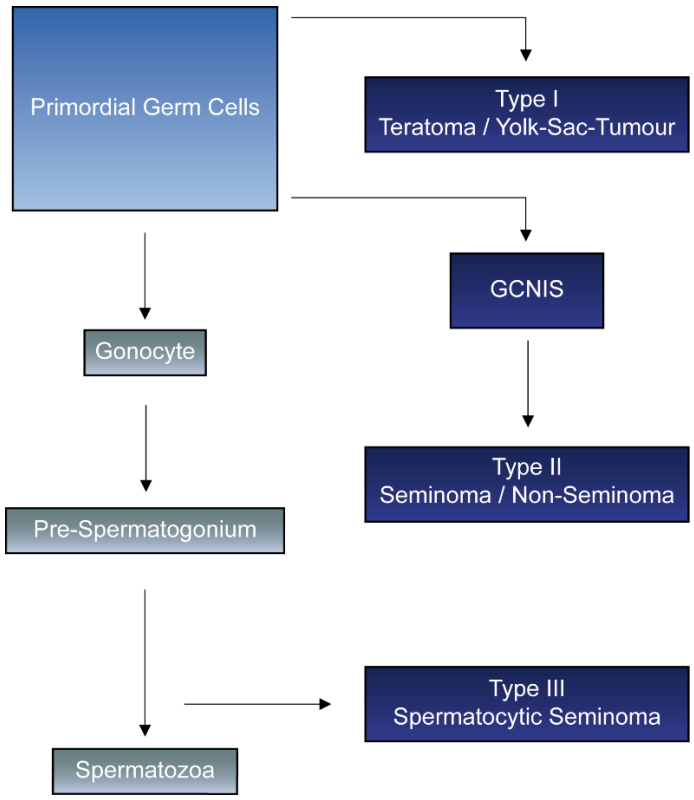

Figure 2: Male testicular germ cell tumours (type I-III). Modified from [8, 21]
Type I TGCTs comprise of teratoma and yolk-sac-tumour of children and infants. They putatively arise early during primordial germ cell development. Type II TGCTs comprise of seminomas and non-seminomas of adolescents and adults. These tumours arise from a common precursor lesion, the germ cell neoplasia in situ (GCNIS), which develops from an error in late primordial germ cell (PGC) maturation. Type III TGCTs are spermatocytic seminomas, which frequently occur in older men and develop from late spermatogonia or spermatocytes.

1.2.1. Type I testicular germ cell tumours

Type I TGCTs account for 1-2% of solid tumours in children [22]. The vast majority of type I TGCTs may either be classified as teratoma or yolk-sac-tumour (YST) according to tumour histology and marker expression [21]. YSTs are defined by high levels of alpha-fetoprotein (AFP) and morphologically present as endodermal or yolk-sac-like tissue [23]. These tumours account for ~ 50% of testicular tumours in children [24, 25]. Pediatric teratomas are the second most common testicular tumours in children with a relative frequency of ~ 15% [24, 26]. Pre-pubertal teratomas present as well-differentiated (mature) and are of benign nature [25, 26]. They are usually derived from cells of all three embryonic germ layers (endoderm, mesoderm, ectoderm). Chromosomal abnormalities frequently found in pediatric YSTs and teratomas are loss of 1p, 4 and 6q, and gain of 1q, 12(p13) and 20q [27]. Since type I TGCTs show a partially erased imprinting pattern, it is believed that they develop early during germ cell development [28] (**Fig. 2**), however risk factors remain poorly understood.

1.2.2. Type II testicular germ cell tumours

Type II TGCTs comprise of seminomas and non-seminomas [21]. These tumours are found in young adolescents and adults and are the most frequent cause of cancer in young men [29]. Type II TGCTs are characterized by high levels of the pluripotency marker OCT4 and gain of the 12 p chromosomal region [30]. Both seminomas and non-seminomas arise from a common precursor lesion called germ cell neoplasia in situ (GCNIS) [31]. It is generally accepted that GCNIS formation occurs as a consequence of an arrest in late PGCs development, due to the acquisition of genetic mutations or epigenetic aberrations (**Fig. 2**) [10, 30-32]. We believe that GCNIS may additionally arise from adult stage spermatogonial cells via reacquisition of the germ cell pluripotency program, although not formally proven [10]. This is supported by the observation that pluripotent cells can be derived from adult murine and human testicular cells [10]. GCNIS are non-invasive and asymptomatic and therefore only rarely diagnosed [31]. 8-10 years after puberty, however, they transform into a malignant seminoma or non-seminoma (**Fig. 3**).

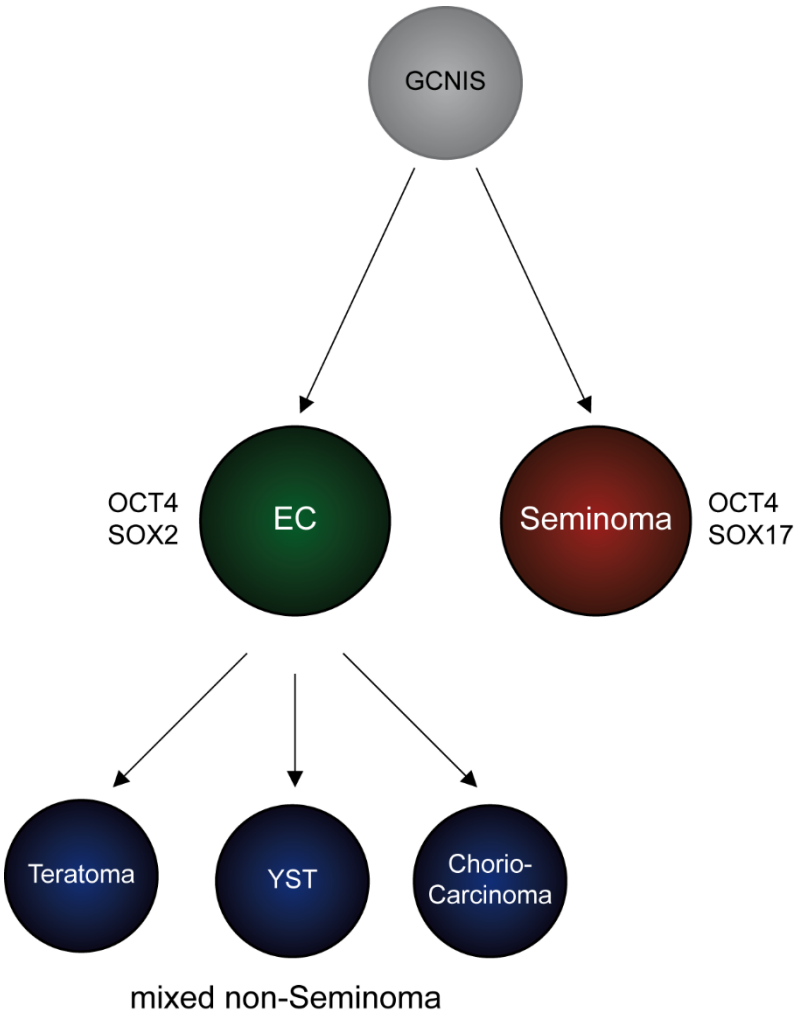

Figure 3: Overview of type II testicular germ cell tumours. Modified from [8, 21]
Type II TGCTs comprise of seminomas and non-seminomas. Both subtypes arise from the GCNIS precursor lesion. Non-seminomas initially present as ECs. ECs are pluri- to totipotent and can further differentiate into embryonic (teratoma) and extraembryonic tissues (YST, choriocarcinoma).

Seminomas are highly similar to PGCs and GCNIS in terms of their overall marker expression (they express LIN28, OCT4, NANOG, PRDM1, TFAP2C and cKIT) and epigenetic profile (global hypomethylation) [10]. Non-seminomas initially present as embryonal carcinomas (ECs) (**Fig. 3**). ECs are described as the stem cell compartment of non-seminomas [10]. These cells are pluri- to totipotent and are therefore able to differentiate into embryonic (teratoma) and extra-embryonic tissues (choriocarcinoma or YST) (**Fig. 3**) [10]. Similar to seminomas, ECs express TFAP2C, GDF3, DPPA3, OCT4 and NANOG at high levels, but additionally express DNMT3B, DNMT3L, NODAL, CRIPTO, CD30 and SOX2 [10]. A major distinction between seminomas and

embryonal carcinomas is the differential expression of the biomarkers and transcription factors SOX2 (EC) and SOX17 (seminoma) [33, 34] (**Fig. 3**). Chromosomal abnormalities that frequently occur in seminomas and non-seminomas are loss of 1p, 11, 13, 18 and gain of 7, 8, 12p, 21 and X [27]. 12 p gain is the most frequent chromosomal alteration in Type II TGCTs, which is why overexpression of pluripotency associated genes (e.g. *NANOG*, *GDF3*, *DPPA3*) encoded in this region is a common event in these tumours [35].

1.2.3. Type III testicular germ cell tumours

Type III TGCTs are spermatocytic seminomas [21]. These tumours are rare (0.3-0.8 per one million men affected) and predominantly occur in men older than 50 years [36]. Spermatocytic seminomas display partial imprinting [21]. Since this imprinting pattern resembles the one of spermatogonia or spermatocytes, it is generally believed that these tumours develop at later stages during male germ cell development [21] (**Fig. 2**). Gain of chromosome 9 is a common karyotypic alteration in these tumours [36]. Looijenga *et al.* proposed the transcriptional regulator DMRT1, which is encoded on chromosome 9, as a driving factor for the development of spermatocytic seminomas [37].

1.3. Model systems for type II testicular germ cell tumours

Several cell lines have successfully been derived from type II TGCTs and established for *in vitro* culture, reviewed in Nettersheim *et al.* (2016) [10] (**Table 1**). Further, xenotransplantation of these cell lines into the flank, brain or testes of immunodeficient Crl:CD1-Foxn1^{nu} (CD-1 nude) mice allows for *in vivo* tumour analysis. However, changes in the cellular microenvironment following xenotransplantation may cause a shift in cell fate (**Table 1**). For example, the seminoma-like cell line TCam-2 grows as EC after injection into the flank of nude mice, while transplantation into the testis results in seminoma growth [10] (**Table 1**).

Table 1: Type II TGCT cell lines. From [10]

Cell Line	Origin	Growth *in vitro* as	Growth *in vivo* as	Reference
TCam-2	Seminoma	Seminoma	EC (flank), CIS / Seminoma (testis)	[38]
JKT-1	Seminoma, EC	Seminoma / EC intermediate	Seminoma	[39]
SEM-1	Seminoma	Seminoma / EC intermediate	Mediastinal GCC	[40]
1411HP	Seminoma, EC, Teratoma, YST	EC	EC, YST	[41]
169A/218A/228A/ 240A	EC	EC	Not determined	[42]
1777N	Retriperitoneal metastasis of non-seminoma	EC	EC	[43]
2102EP	EC, Teratoma	EC	EC	[44]
833Ke	Seminoma, EC, Teratoma, Choriocarcinoma	EC	EC	[45]
GCT27	EC, Teratoma	EC	EC, Teratoma, YST	[46]
GCT35	EC, Teratoma	EC	EC, YST	[46]
GCT44/46/72	EC, Teratoma	EC	YST	[46]
GCT48	EC, Teratoma	EC	EC	[46]
H12.1/.5/.7	Seminoma, EC, Teratoma, Choriocarcinoma	EC	EC	[47]
NCCIT	EC, Teratoma	EC	EC, Teratoma	[48]
NEC-8/-14/-15	EC, YST, Choriocarcinoma	EC	EC, Teratoma	[49]
SuSa	EC, Teratoma	EC	Not determined	[50]
TERA1/2	EC, Teratoma	EC	EC	[51]
577MF/L/RPLN	Metastasis of non-seminoma	Undifferentiated carcinoma	Teratoma	[52]
BeWo	Choriocarcinoma	Choriocarcinoma	Choriocarcinoma	[53]
JAR	Choriocarcinoma	Choriocarcinoma	Choriocarcinoma	[54]
JEG-3	Choriocarcinoma	Choriocarcinoma	Choriocarcinoma	[55]

1.3.1. The seminoma-like cell line TCam-2

The only seminoma-like cell line that has been adapted to cell culture is the TCam-2 cell line [38, 56] (**Table 1**). Two other cell lines have been isolated from seminoma patients (JKT-1, SEM-1), however SEM-1 cells show characteristics of both seminoma and non-seminoma components, while JKT-1 lack the typical characteristics of a type II TGCT (such as gain of the 12p chromosomal region) [40, 56, 57]. Other attempts for the *in vitro* cultivation of seminoma cells have failed, since these cells undergo spontaneous cell death (anoikis) when isolated from their microenvironment [58]. However, it is still unclear what determines the survival of TCam-2 cells *in vitro*. Thorough analysis has demonstrated that TCam-2 cells display expression of the early germ cell and TGCT markers OCT4, NANOG, TFAP2C and LIN28, and the seminoma markers SOX17, PRDM1 (nuclear expression) and KIT [10]. At the same time TCam-2 lack expression of EC markers SOX2 and CD30 [38, 59]. Furthermore, TCam-2 cells show an aneuploid karyotype with the characteristic gain of the 12p region [38]. Morphologically, TCam-2 cells appear polygonal and flat in shape, with a large cytoplasm and a round nucleus [56, 60]. Further, TCam-2 cells have a relatively long doubling time of approximately 58 hours, which is reminiscent of migratory PGCs [56].

1.3.2. The EC cell lines NCCIT, NT2/D1 and 2102EP

The NCCIT cell line is a pluripotent EC cell line derived from a mixed germ cell tumour [48] (**Table 1**). NCCIT are positive for alkaline phosphatase and the pluripotent stem cell markers TRA-1-60 and TRA-1-81 [48]. They show epithelial-like morphology and form dense cell clusters upon *in vitro* cultivation. When exposed to retinoic acid (RA), NCCIT cells differentiate into cells of all three germ layers, mimicking teratoma growth [48]. When transplanted into nude mice, NCCIT cells differentiate into mixed non-seminoma [48].

The NT2/D1 (NTERA-2 cl.D1) cell line was derived by cloning the pluripotent EC line NTERA-2. NTERA-2 were established from a nude mouse xenograft of the Tera-2 cell line (**Table 1**). Similar to NCCIT cells, NT2/D1 grow in tight colonies and appear epithelial-like [61]. In response to RA NT2/D1 cells differentiate into neuronal lineages

[62]. When transplanted into nude mice, NT2/D1 cells grow as mixed non-seminoma [63].

2102EP cells resemble undifferentiated EC cells and stain positive for alkaline phosphatase and the pluripotency markers SSEA-4, TRA-1-60 and TRA-1-81 [64] (**Table 1**). Although 2102EP cells resemble human ES cells on transcriptome level and express a number of core pluripotency genes (*TDGF1*, *DNMT3A*, *DNMT3B*, *POU5F1*, *NANOG*, *GDF3*, *UTF1*, *SOX2*), these cells lack the capacity to differentiate [64, 65]. This suggests that 2102EP cells have acquired additional mutations restricting their differentiation capacities, therefore characterizing 2102EP cells as nullipotent [65]. When transplanted into nude mice, 2102EP cells grow as EC.

1.4. Transcription factors determining type II TGCT cell fate

Seminomas and ECs can be discriminated by their differential expression of SOX17 (seminoma: high, EC: low) and SOX2 (seminoma: low, EC: high) [33]. Both factors belong to the SOX family of transcription factors. SOX factors have important roles in orchestrating stem cell self-renewal and differentiation [66]. Along with OCT4, KLF4 and MYC, SOX2 is also well known for its function in the generation of induced pluripotent stem cells (iPSC) and stem cell maintenance [67]. In contrast, SOX17 is a known specifier of endodermal lineage decisions [68].

1.4.1. SOX and POU transcription factors in type II TGCTs

In mouse ES cells it was shown that SOX2 and SOX17 partner with the POU transcription factor OCT4 and act as opposing forces in regulating cell fate decisions [69]. SOX2 and OCT4 dimerize and bind to the canonical (SOX2/OCT4) binding motif on the DNA, which is composed of the SOX and OCT4 binding motifs separated by a single basepair [69, 70], (**Fig. 4 A**). SOX17 and OCT4 dimerize and bind to the compressed motif, which is similarly composed of the SOX and OCT4 binding motifs, but lacking the central basepair separating the two motifs [69], (**Fig. 4 B**). In both human and mouse embryonic stem cells (ESCs) SOX2-OCT4 binding to the canonical motif results in upregulation of pluripotency and stemness-associated genes [70]. In contrast, binding of the SOX17-OCT4 complex to the compressed motif results in

upregulation of endodermal-associated genes [69, 71, 72]. Interestingly, the group of Prof. Jauch demonstrated that in mouse ESCs the SOX17-OCT4 heterodimer can also bind to the canonical (SOX2/OCT4) motif (**Fig. 4 C**), however with reduced affinity compared to binding to the compressed (SOX17/OCT4) motif: 13.6% canonical motif, 33.5% compressed motif [69]. In contrast, SOX2/OCT4 heterodimer formation on the compressed motif is not possible, due to sterical hindrance (**Fig. 4 D**).

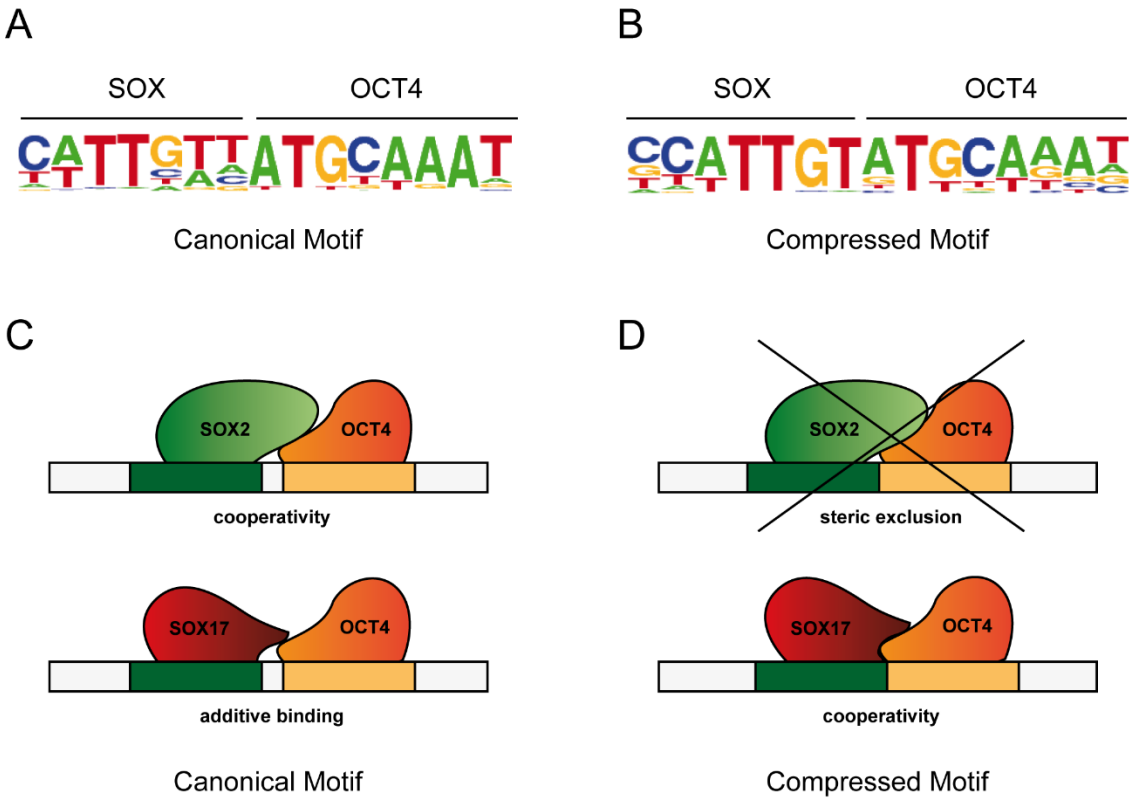

Figure 4: SOX2/OCT4 and SOX17/OCT4 DNA binding motifs. Modified from [69, 72]

(A) The canonical motif is composed of the SOX and OCT4 motif, separated by a single basepair. Binding of SOX2-OCT4 to this motif regulates pluripotency.

(B) The compressed motif is composed of the SOX and OCT4 motif, lacking the central basepair separating the two motifs. Binding of SOX17-OCT4 to this motif regulates endodermal differentiation.

(C) Similar to SOX2-OCT4, the SOX17-OCT4 complex is able to bind to the canonical motif (additive binding).

(D) SOX2-OCT4 cannot bind to the compressed motif, due to sterical hindrance.

Since EC cells show high expression of core pluripotency genes (*POU5F1 (OCT4)*, *SOX2*, *NANOG*, *KLF4* and *ZIC3*), it was suggested that self-renewal and pluripotency in EC cells is also maintained by cooperative binding of the SOX2/OCT4 complex to the regulatory regions of these genes. In contrast, seminoma cells display high levels of OCT4 and the transcription factor SOX17, therefore Nettersheim *et al*. hypothesized that SOX17 in seminomas is replacing for the lack of SOX2 in regulating pluripotency genes [60]. Seminomas maintain a latent pluripotent cell state and do not undergo endodermal differentiation, thus it was suggested that SOX17 together with OCT4 in seminoma cells regulates pluripotency by binding to the canonical motif [60] (**Fig. 4 C**).

1.4.2. The plasticity of type II TGCTs

It was a long-standing belief that seminoma cells were not able to differentiate, due to expression of the PGC program, which is inhibiting the differentiation. However, Nettersheim *et al.* demonstrated in 2011 that *in vitro* cultivation of the seminoma-like cell line TCam-2 in medium supplemented with TGFβ1, EGF and FGF4 results in conversion into a mixed non-seminomateous or choriocarcinoma-like phenotype [73] (**Fig. 5**). This differentiation process was initiated by inhibition of BMP signalling and subsequent downregulation of BLIMP1 expression [73]. Since BLIMP1 normally associates with the histone methyltransferase PRMT5 to regulate symmetrical dimethylation of arginine 3 on histone H2A and/or H4 tails [74] (which is characteristic for TCam-2 and PGC cells), loss of BLIMP1 additionally led to reduction in H2a/H4 dimethylation [73].

In a different study it was shown that xenotransplantation of TCam-2 cells into the murine flank or brain results in transition into an EC-like phenotype [75] (**Fig. 5**). This differentiation process was also initiated by inhibition of BMP signalling, leading to activation of NODAL signalling and acquisition of a pluripotent state [75]. At the same time DNMT3B-mediated *de novo* methylation silenced seminoma-specific genes, leading to an EC-like epigenetic signature [75]. It was shown that SOX2-/- TCam-2 cells xenotransplanted in the murine flank grow as seminoma-like with a few cell foci displaying mixed non-seminoma morphology [60] (**Fig. 5**). SOX2 upregulation was indispensable for this seminoma to EC transition, demonstrating that SOX2 is a key determinant of EC cell fate [60]. EC cells are able to differentiate further into a mixed

non-seminoma cell fate (teratoma, yolk-sac-tumour or choriocarcinoma) (**Fig. 5**). This can be observed upon xenotransplantation of EC lines into the murine system or in patient tumour samples that have been diagnosed with both EC and mixed non-seminoma components (**Fig. 5**).

However, so far it was questionable whether a direct conversion of EC to seminoma fate was possible (**Fig. 5**). Nettersheim *et al.* suggested that cultivation of EC cells in "4i"-medium (+GSK3 inhibitor, +MEK inhibitor, +P38-kinase inhibitor, +JNK inhibitor) supplemented with TGF-β1 and bFGF may induce seminoma-like cell fate under simultaneous overexpression of the PGC and seminoma specifier SOX17 [76] (**Fig. 5**). In a previous study, Irie *et al.* could already demonstrate successful derivation of PGC-like cells from ESCs under these conditions [6].

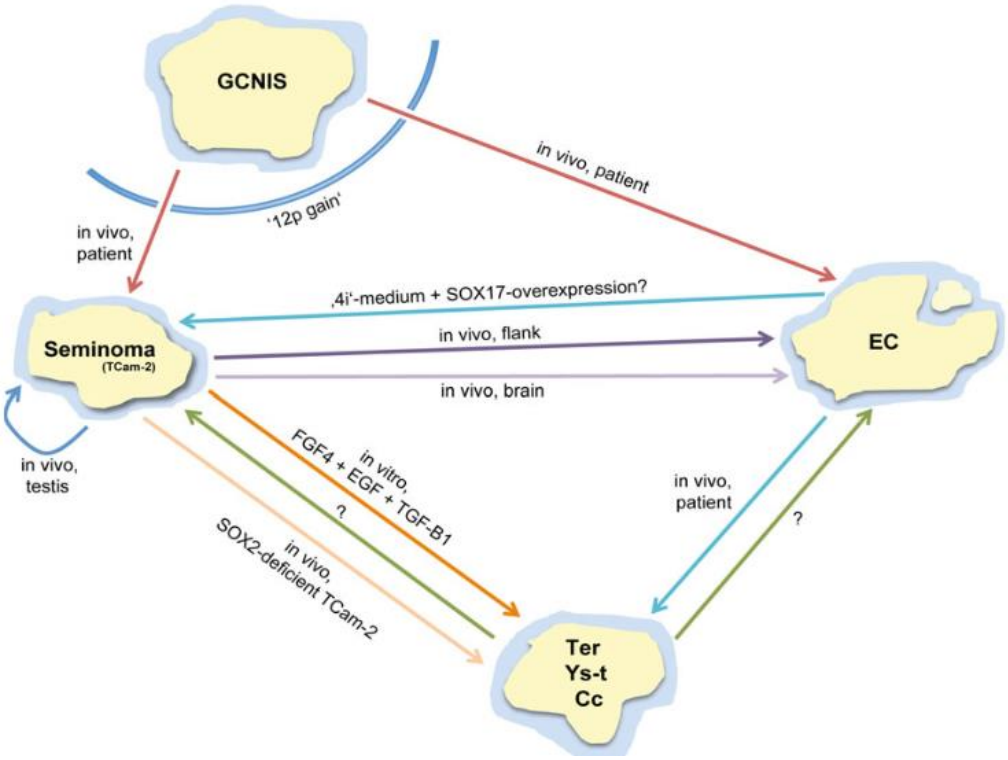

Figure 5: The plasticity of type II TGCTs. From [76]
Seminoma cells grow seminoma-like when transplanted into the murine testis. Xenotransplantation of seminoma cells into the flank or brain of nude mice results in seminoma to EC transition. SOX2-deficient TCam-2 cells keep a seminoma-like cell fate or differentiate into mixed non-seminoma when transplanted into the murine flank. EC cells may further differentiate into mixed non-seminoma *in vivo* or in the patient (Ter = teratoma, Ys-t = YST, Cc = choriocarcinoma). EC to seminoma transition may be achieved by cultivation of seminoma cells in "4i"-medium supplemented with TGFβ1 and FGF4 under simultaneous overexpression of SOX17.

1.5. Treatment of type II TGCTs

Type II TGCTs are diagnosed according to histological appearance and AFP, lactate dehydrogenase (LDH) and human chorionic gonadotropin (HCG) serum levels [77]. In all cases, radical orchiectomy (removal of the testis) is the first line of treatment [77]. Additionally, tumour serum markers are determined both before and after orchiectomy to ensure correct tumour classification and staging [77]. Following the EAU and ESMO guidelines of clinical practice for Type II TGCTs three stages of seminomas and non-seminomas can be distinguished and the following treatment strategies have to be adjusted accordingly [77, 78].

1.5.1. Treatment of stage I-III seminoma and non-seminoma

Stage I seminomas (low risk: absence of rete testis invasion and tumour size < 4 cm, high risk: presence of rete testis invasion or tumour size ≥ 4 cm) are typically treated by surveillance [78]. In case of relapse, low-risk tumours are alternatively treated with radiotherapy [78]. The majority of low-risk patients (70%) respond very well to this treatment, since seminoma cells are highly sensitive to radiotherapy [78]. In case of relapse following salvage radiotherapy, tumours can additionally be treated by chemotherapy [78]. High-risk tumours are directly treated by chemotherapy [77, 78]. Stage II/III seminomas are typically treated by 3-4 cycles of chemotherapy and / or radiotherapy [77]. In case of relapse, tumour tissue may be surgically removed, if feasible, and patients may be treated by either salvage chemotherapy or localised radiotherapy [78].

Stage I non-seminomas are preferably treated by surveillance [77]. However, about 30% of patients show relapse after being treated with surveillance alone [77]. Patients may then additionally be treated by chemotherapy and / or retroperitoneal lymph node dissection (RPLND) [77]. In case of post-chemotherapy relapse patients are treated by salvage chemotherapy [77]. Stage II/III non-seminomas are treated by chemotherapy and, if applicable, additional RPLND [77]. In case of residual disease or relapse, tumour tissue may be surgically removed and patients may be treated by salvage chemotherapy [77]. 4-8 weeks following therapy, AFP, LDH and HCG serum levels are determined and patients are checked for residual tumour masses by X-ray, CT scan or MRI [77]. However, 2-3% of type II TGCT patients remain AFP, LDH or HCG-positive

and / or show relapse shortly or even ≥ 2 years after therapy [78]. Patients with tumours resistant to standard therapeutic approaches should be included in clinical trials for individualized therapy and next-generation drugs.

1.6. Epigenetic therapies as alternative treatment option

The principles of epigenetics were first described by Conrad H. Waddington in 1956, when he demonstrated acquisition of the bithorax phenotype in a population of *Drosophila melanogaster* in response to an environmental stimulus [79, 80]. Today, it is well-established that certain phenotypic changes do not involve alterations of the primary DNA sequence, but can solely be explained by chemical modifications on the DNA or on those proteins responsible for DNA compaction (histones) (**Fig. 6**) [79]. These chemical modifications (i.e. DNA methylation, histone acetylation, histone methylation) alter the accessibility of DNA and therefore may ultimately result in changes in gene expression [79]. Epigenetic modifications are carried out by three different classes of enzymes (I-III): writers (I), readers (II) and erasers (III) [79] (**Fig. 6**). Writers add chemical modifications to histones tails or DNA, erasers remove these modifications and readers recognize and bind these modifications in order to recruit other components of the transcriptional machinery to shut on or to shut off gene expression [79].

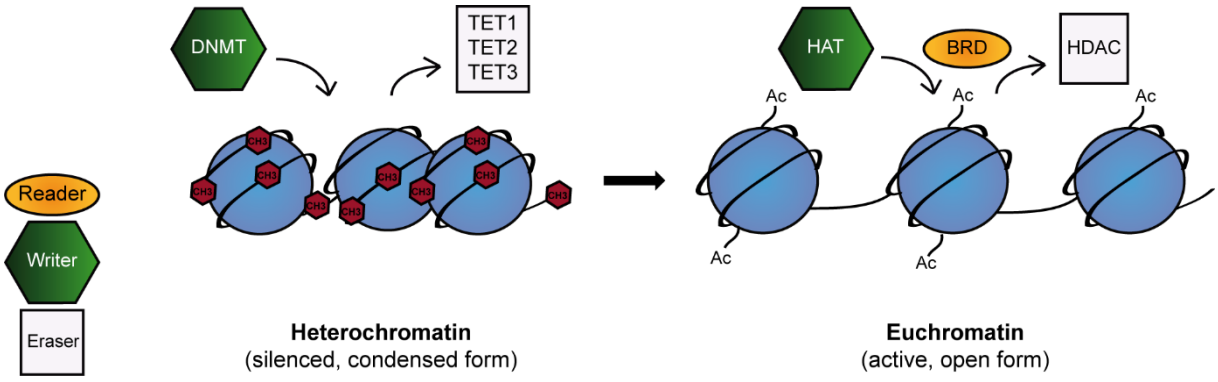

Figure 6: The chromatin landscape. Modified from [79]
Silent or condensed chromatin is called heterochromatin. In this state of compaction the DNA is highly methylated and histones are deacetylated. Active or open chromatin is called euchromatin. In this state DNA is unmethylated and histones are highly acetylated. DNA methylation is carried out by *de novo* methyltransferases (DNMTs) and erased by ten-eleven translocation (TET) enzymes. Histone acetylation is carried out by histone acetyltransferases (HATs), erased by histone deacetylases (HDACs) and recognized or 'read' by bromodomain (BRD) proteins.

1.6.1. HDAC inhibitors

Histone deacetylases (HDACs) are important players of the epigenetic machinery. These enzymes remove acetyl groups from histone tails, thus producing hypo-acetylated chromatin regions [79]. In contrast, histone acetyl transferases (HATs) add acetyl groups to histone tails, thus producing hyper-acetylated chromatin regions [79]. In general, hypo-acetylated regions mark transcriptionally silent chromatin, while hyper-acetylated regions mark transcriptionally active chromatin [81]. The balance between HDAC and HAT proteins fundamentally regulates chromatin state and compaction [81]. In humans, there are 18 HDAC proteins that can be categorized into four classes (Class I: HDAC1-3, HDAC8; Class II: HDAC4-7, HDAC9-10; Class III: SIRT1-7; Class IV: HDAC11) based on sequence similarity [79, 82]. Overrepresentation of a number HDAC proteins was shown to correlate with poor prognosis in cancer, for example in neuroblastoma (HDAC8, HDAC10), lung (HDAC1-3, HDAC5, HDAC10), gastric (HDAC1-3, HDAC4, HDAC10) or liver cancer (HDAC1-3, HDAC5, HDAC6) [82]. Due to the oncogenic role of HDAC proteins, a number of HDAC inhibitors (HDACi) have been developed for cancer therapy (**Table 2**).

Table 2: Overview of selected HDAC inhibitors. From [83]

Class	HDAC Inhibitor	Target HDAC Class	Clinical Status
hydroxamic acids	Trichostatin A	Pan	Preclinical
	SAHA	Pan	approved for cutaneous T-cell lymphoma
	Belinostat	Pan	approved for peripheral T-cell lymphoma
	Panabinostat	Pan	approved for multiple myeloma
	Givinostat	Pan	phase II clinical trials
	Resminostat	Pan	phase I and II clinical trials
	Abexinostat	Pan	phase II clinical trial
	Quisinostat	Pan	phase I clinical trial
	Rocilinostat	II	phase I clinical trial
	Practinostat	I, II, IV	phase II clinical trial
	CHR-3996	I	phase I clinical trial
short chain fatty acids	Valproic acid	I, IIa	approved for epilepsia, bipolar disorders and migraine
	Butyric acid	I, II	phase II clinical trials

	Phenylbutyric acid	I, II	phase I clinical trials
benzamides	Entinostat	I	phase II clinical trials
	Tacedinaline	I	phase III clinical trial
	4SC202	I	phase I clinical trial
	Mocetinostat	I, IV	phase II clinical trials
cyclic tetrapeptides	Romidepsin	I	approved for cutaneous T-cell lymphoma
sirtuins inhibitor	Nicotinamide	all class III	phase III clinical trial
	Sirtinol	SIRT 1 and 2	Preclinical
	Cambinol	SIRT 1 and 2	Preclinical
	EX-527	SIRT 1 and 2	cancer preclinical, phase I and II clinical trials

In general, HDAC inhibitors were shown to induce cell cycle arrest, apoptosis and / or differentiation in tumour cells [83]. These effects often could be enhanced when HDACi treatment was combined with already approved treatment regimens like the demethylating agent 5-aza-2'-deoxycytidine or the chemotherapeutic drugs bortezomib and cisplatin [83].

1.6.2. BET inhibitors

The Bromo- and Extra-Terminal domain (BET) family belongs to the class of epigenetic readers or BRD proteins [79]. Members of this family include BRD2, BRD3, BRD4 and BRDT [84]. BRD proteins recognize acetylated lysine chains on histone tails and thereby shape the transcriptome either directly or indirectly by interaction with other chromatin-remodelling enzymes or transcriptional co-factors [85]. Similar to HDACs, also the malfunction of BRD proteins has been implicated in cancer development. It was demonstrated that the development of NUT-midline carcinoma underlies an oncogenic fusion of nuclear protein in testis (NUT) with the BRD4 reader protein [86]. Similarly, BRD4 was shown to be an important driver of *MYC* expression, an oncogene which is frequently upregulated in cancer [87-89]. In ESCs BRD4 is required for pluripotency regulation and maintenance [1, 90, 91]. To date, a number of BET inhibitors (BETi) have been developed for cancer therapy, which have reached clinical trials [79, 92] (**Table 3**). In general, these BETi have shown to induce growth arrest

and apoptosis in different tumour settings [93-96]. In particular, BETi mediate anti-tumoural effects by disruption of BRD4 occupancy at super-enhancers that feature key oncogenic drivers, such as *MYC* [79, 97]. To date, there is a number of pre-clinical studies showing that BETi-mediated cytotoxicity can be synergistically enhanced by simultaneous administration of HDACi, providing a rationale for combination therapy [1, 95, 98].

Table 3: Overview of selected BET inhibitors. Modified from [92]

BET Inhibitor	Target BET Member	Clinical Status
ABBV-075	BRD2/3/4, BRDT	I
CPI-0610	BRD4	I
FT-1101	BRD2/3/4, BRDT	I
GSK525762/I-BET762	BRD2/3/4, BRDT	I/II
GSK2820151/I-BET151	BRD2/3/4	I
OTX015/MK-8628	BRD2/3/4	I
PLX51107	BRD4	I
ZEN003694	BRD2/3/4, BRDT	I

Parts of this chapter have been discussed in:

Epigenetic drugs and their molecular targets in testicular germ cell tumours
Jostes S, Nettersheim D, Schorle H.
Nature Reviews Urology. 2019 Feb 14

2. Materials and Methods

2.1. Materials

2.1.1. Mouse strains

Mouse Strain	Description	Company
Crl:NU-Foxn1nu	Immunodeficient mouse. The animal lacks a thymus and is therefore unable to produce T-cells.	Charles River Laboratories

2.1.2. Cell lines

Cell Line	Standard Growth Medium	Reference
2102EP	DMEM (+ 10% FBS, 50 U/ml P/S, 2 mM L-glutamine)	Prof. Dr. L. Looijenga, Erasmus MC, Daniel den Hoed Cancer Center, Josephine Nefkens Institute, Rotterdam, Netherlands
2102EP-R	DMEM (+ 10% FBS, 50 U/ml P/S, 2 mM L-glutamine)	Dr. F. Honecker, Breast and Tumor Center, ZeTup Silberturm, St Gallen, Switzerland
FS1	DMEM (+ 20% FBS, 50 U/ml P/S, 2 mM L-glutamine, 1x NEAA)	Dr. Valerie Schumacher, Nephrology Research Center, Boston, USA
HEK-293T	DMEM (+ 10% FBS, 50 U/ml P/S, 2 mM L-glutamine)	Dr. Michael Peitz, Bonn University, Institute of Reconstructive Neurobiology, Bonn, Germany
MPAF	DMEM (+ 10% FBS, 50 U/ml P/S, 2 mM L-glutamine, 1x NEAA)	Dr. Michael Peitz, Bonn University, Institute of Reconstructive Neurobiology, Bonn, Germany
NCCIT	DMEM (+ 10% FBS, 50 U/ml P/S, 2 mM L-glutamine)	Prof. Dr. L. Looijenga, Erasmus MC, Daniel den Hoed Cancer Center, Josephine Nefkens Institute, Rotterdam, Netherlands
NCCIT-R	DMEM (+ 10% FBS, 50 U/ml P/S, 2 mM L-glutamine)	Dr. F. Honecker, Breast and Tumor Center, ZeTup Silberturm, St Gallen, Switzerland
NT2/D1	DMEM (+ 10% FBS, 50 U/ml P/S, 2 mM L-glutamine)	Prof. Dr. L. Looijenga, Erasmus MC, Daniel den Hoed Cancer Center, Josephine Nefkens Institute, Rotterdam, Netherlands

NT2/D1-R	DMEM (+ 10% FBS, 50 U/ml P/S, 2 mM L-glutamine)	Dr. F. Honecker, Breast and Tumor Center, ZeTup Silberturm, St Gallen, Switzerland
TCam-2	RPMI (+ 10% FBS, 50 U/ml P/S, 2 mM L-glutamine)	Dr. Janet Shipley, Institute of Cancer Research, Sutton, England

2.1.3. Chemicals and reagents

(2-Hydroxypropyl)-β-cyclodextrin (HP-β-CD)	Sigma-Aldrich, St. Louis, USA
6-Diamidino-2-phenylindole dihydrochloride (DAPI)	AppliChem, Darmstadt, Germany
Acetic acid	AppliChem, Darmstadt, Germany
Acrylamide Mix	Roth, Karlsruhe, Germany
Ammonium persulfate (APS)	Carl Roth, Karlsruhe, Germany
Bovine Serum Albumin (BSA)	Sigma-Aldrich, München, Germany
Coomassie Brilliant Blue	Biomol, Hamburg, Germany
Diagenode Crosslink Gold	Diagenode
Dimethylsulfoxide (DMSO)	Sigma-Aldrich, München, Germany
dNTPs	Thermo Fisher Scientific, Waltham, USA
Ethanol	VWR, Darmstadt, Germany
Ethylene diamine tetra acetic acid (EDTA)	Sigma-Aldrich, München, Germany
Formaldehyde (37 %) for ChIP	AppliChem, Darmstadt, Germany
Formaldehyde (4%) for immunofluorescence and immunohistochemistry	Merck, Darmstadt, Germany
JQ1	Jay Bradner, Dana Farber Institute, USA
Methanol	VWR, Darmstadt, Germany
Oligonucleotide (Primer)	Sigma-Aldrich, München, Germany
PageRuler Prestained Protein Ladder	Thermo Fisher Scientific, Waltham, USA
Paraffin Wax Paraplast Plus	McCormick Scientific, St Louis, USA
Phosphate buffered saline (PBS) tablets	AppliChem, Darmstadt, Germany
PMS	Sigma-Aldrich, St. Louis, USA
Ponceau S	Sigma-Aldrich, St. Louis, USA
Propidium Idodide (PI)	Sigma-Aldrich, St. Louis, USA
RNAse A	AppliChem, Darmstadt, Germany
Romidepsin	Celgene, Signal Pharmaceuticals, San Diego, USA
Roti-Load (4× concentrated)	Carl Roth, Karlsruhe, Germany
Rotiphorese Gel 30	Carl Roth, Karlsruhe, Germany

Skimmed milk powder	Nestle, Soest, Germany
Sodium Chloride (NaCl)	Merck, Darmstadt, Germany
Sodium dodecyl sulfate (SDS)	Sigma-Aldrich, St. Louis, USA
Tetramethylethylenediamine (TEMED)	VWR, Darmstadt, Germany
TG-SDS running buffer, 10× liquid concentrate	Amresco, Solon, USA
Tris-HCl	Roth, Karlsruhe, Germany
Triton X	AppliChem, Darmstadt, Germany
Tween 20	AppliChem, Darmstadt, Germany
XTT (sodium salt)	Sigma-Aldrich, St. Louis, USA
β-Mercaptoethanol	Sigma-Aldrich, St. Louis, USA

2.1.4. Kits

Alkaline Phosphatase Detection Kit	Merck, Darmstadt, Germany
BCA protein assay kit	Thermo Fisher Scientific, Waltham, USA
Dynabeads® Protein G	Thermo Fisher Scientific, Waltham, USA
Genomeplex® Single Cell Whole Genome Amplification Kit (WGA4)	Sigma-Aldrich, St. Louis, USA
Maxima First Strand cDNA synthesis Kit	Thermo Fisher Scientific, Waltham, USA
Maxima SYBR Green Master Mix	Thermo Fisher Scientific, Waltham, USA
PE Annexin V Apoptosis Detection Kit I	BD Biosciences, Heidelberg, Germany
ProFection® Mammalian Transfection System	Promega, Mannheim, Germany
RNeasy Mini Kit	Qiagen, Hilden, Germany
Simple ChIP® Enzymatic Chromatin IP Kit (Magnetic Beads)	Cell Signaling Technology, Danvers, USA
SuperSignal West Pico Chemiluminescent Substrate	Thermo Fisher Scientific, Waltham, USA
TruSeq ChIP Library Preparation Kit	Illumina, San Diego, USA

2.1.5. Buffers and recipes

1 × Western blot transfer buffer	700 ml H_2O, 200 ml methanol, 100 ml 10× Western blot transfer buffer
10 × Western blot transfer buffer	24.2 g Tris base, 144.1 g glycine, 5 ml 20 % SDS, H_2O ad 1 l

12% SDS Gel	12% Separation Gel: 1.6 ml H_2O, 2.0 ml Rotiphorese Gel 30, 1.3 ml 1.5 M Tris (pH 8.8), 50 µl 10% SDS, 50 µl 10% APS, 2 µl TEMED Stacking Gel: 2.1 ml H_2O, 500 µl Rotiphorese Gel 30, 380 µl 1.0 M Tris (pH 6.8), 30 µl 10% SDS, 30 µl 10% APS, 3 µl TEMED
Coomassie Brilliant Blue staining solution	0.25 g Coomassie Brilliant Blue, 10 ml acetic acid, 45 ml MetOH, 45 ml H_2O
Coomassie destaining solution	10 ml acetic acid, 45 ml MetOH, 45 ml H_2O
Low pH glycine buffer	100 mM Glycine pH 2.5 (adjusted with HCl)
PBST	1 PBS Tablet, 1000 ml H_2O, 1 ml Tween 20
Ponceau S staining solution	0.5 g Ponceau S, 5 ml acetic acid, H_2O ad 500 ml
RIPA buffer	10 mM Tris-Cl (pH 8.0), 1 mM EDTA, 1% Triton X-100, 0.1% sodium deoxycholate, 0.1% SDS, 140 mM NaCl, 1 mM phenylmethylsulfonyl fluoride
Western blot stripping buffer	5 ml 20 % SDS, 3.125 ml 1 M Tris (pH 8.8), 390 µl β-Mercaptoethanol, H_2O ad 50 ml

2.1.6. Consumables

1.5 ml microcentrifuge tube	Sarstedt, Nümbrecht, Germany
100 µl PCR reaction tubes	Axygen, California, USA
2 ml microcentrifuge tube	Sarstedt, Nümbrecht, Germany
384-well PCR plates for qRT-PCR	4titude, Wotton, United Kingdom
96-well plates	BD Biosciences, Le Pont de Claix, France
Blotting papers	Macherey-Nagel, Düren, Germany
Cell culture dishes and plates	TPP, Trasadingen, Austria
FACS tubes	BD Biosciences, Heidelberg, Germany
Falcon tubes (15 ml and 50 ml)	Greiner, Kremsmünster, Austria
Filter tips (10 µl, 100 µl, 200 µl, 1000 µl)	Nerbe Plus, Winsen/Luhe, Germany
Parafilm M	Pechiney Plastic Packaging, Chicago, USA
Pipette tips (10 µl, 100 µl, 200 µl, 1000 µl)	Greiner Bio-One, Kremsmünster, Austria
Pipette tips (filtered)	Nerbe Plus, Winsen, Germany
qPCR seals	4titude, Wotton, United Kingdom
Roti-PVDF membrane	Carl Roth, Karlsruhe, Germany
Steri-pipette	Corning, Amsterdam, Netherlands

2.1.7. Cell culture accessories

0.05 % Trypsin-EDTA	Thermo Fisher Scientific, Waltham, USA
Advanced DMEM	Thermo Fisher Scientific, Waltham, USA
Dulbecco's Modified Eagle Medium (DMEM)	Thermo Fisher Scientific, Waltham, USA
Fetal bovine serum (FBS)	Sigma-Aldrich, St. Louis, USA
FuGene® HD Transfection Reagent	Promega, Mannheim, Germany
Hygromycin B	Santa Cruz, Dallas, Texas
L-Glutamine	Thermo Fisher Scientific, Waltham, USA
Matrigel Matrix	Corning, Corning, USA
MEM Non-Essential Amino Acids Solution (NEAA)	Thermo Fisher Scientific, Waltham, USA
Penicillin/Streptomycin (P/S)	Thermo Fisher Scientific, Waltham, USA
Phosphate Buffered Saline (PBS)	Thermo Fisher Scientific, Waltham, USA
Poly-l-lysine	Thermo Fisher Scientific, Waltham, USA
RPMI 1640 Medium (RPMI)	Thermo Fisher Scientific, Waltham, USA

2.1.8. Equipment

Autostainer 480 S	Thermo Fisher Scientific, Waltham, USA
Balance PT 120	Sartorius, Göttingen, Germany
BioAnalyser 2100	Agilent Technologies, Santa Clara, USA
Blot documentation ChemiDoc MP	Bio-Rad Laboratories, Hercules, USA
Centrifuge 5415 D	Eppendorf, Hamburg, Germany
Centrifuge 5417 R	Eppendorf, Hamburg, Germany
Centrifuge Biofuge fresco	Thermo Fisher Scientific, Waltham, USA
Centrifuge Galaxy mini	VWR, Darmstadt, Germany
Centrifuge Megafuge 1.0	Thermo Fisher Scientific, Waltham, USA
Centrifuge Multifuge 3SR	Thermo Fisher Scientific, Waltham, USA
Cool centrifuge	Eppendorf AG, Hamburg, Germany
Electrophoresis power supply EV243	PEQLAB, Erlangen, Germany
FACS Canto™	BD Biosciences, Heidelberg, Germany
Illumina High Seq 2500	Illumina, San Diego, USA
Illumina Human HT-12 v4 Bead Chip	Illumina, San Diego, USA
iMark Microplate Absorbance Reader	Bio-Rad Laboratories, Hercules, USA
Incubator Cytoperm2	Thermo Fisher Scientific, Waltham, USA
Incubator Heracell 240i	Thermo Fisher Scientific, Waltham, USA
Leitz Labovert cell culture microscope	Leica Microsystems, Wetzlar, Germany
Magnetic separation rack	Active Motif, La Hulpe, Belgium

Microscope Axiovert 40 C	Carl Zeiss, Oberkochen, Germany
Microscope DM IRB	Leica Microsystems, Wetzlar, Germany
Microscope Labovert FS	Leica Microsystems, Wetzlar, Germany
Microwave NN 5256	Panasonic, Wiesbaden, Germany
Nano Drop 1000 Spectrophotometer	Thermo Fisher Scientific, Waltham, USA
Orbital shaker 3005	Gesellschaft für Labortechnik, Burgwedel, Germany
PCR machine	PTC-200 MJ Research, Waltham, USA
Pipette controller accu-jet	BRAND, Wertheim, Germany
Pipette Set Research	Eppendorf AG, Hamburg, Germany
Power Supply Consort E143	Sigma-Aldrich, München, Germany
Real-Time PCR ViiA7	Thermo Fisher Scientific, Waltham, USA
Sample mixer HulaMixer	Thermo Fisher Scientific, Waltham, USA
SDS-Page electrophoresis chamber Mini-PROTEAN Tetra Cell	Bio-Rad Laboratories, Hercules, USA
Shaking incubator Innova 4000	Eppendorf, Hamburg, Germany
Sterile workbench BSB 6A	Gelaire, Sydney, Australia
Sterile workbench Herasafe	Thermo Fisher Scientific, Waltham, USA
Thermal cycler 2720	Thermo Fisher Scientific, Waltham, USA
Thermomixer compact	Eppendorf AG, Hamburg, Germany
Tissue-Tek® VIP	Sakura Finetek Europe B.V., Alphen aan den Rijn, Netherlands
Trans Blot Turbo blotting chamber	Bio-Rad Laboratories, Hercules, USA
Ultrasonic bath Bioruptor	Diagenode, Seraing, Belgium
Vortex mixer Bio Vortex V1	PEQLAB, Erlangen, Germany
Vortex mixer Top-Mix 94323	Heidolph Instruments, Schwabach, Germany
Waterbath TW8	Julabo, Seelbach, Germany

2.1.9. Antibodies

Primary antibodies

Antibody	Application	Company	# Number
BRD2	Western Blot	Sigma Aldrich	HPA042816
BRD3	Western Blot	AbCam	ab50818
BRD4	Western Blot	Active Motif	39909
CD31	Immunohistochemistry	PECAM	SZ31
Cleaved PARP	Western Blot	AbCam	ab4830

GATA3	Immunofluorescence	Santa Cruz	sc268
GDF3	Western Blot	AbCam	ab38547
Goat IgG	ChIP	Santa Cruz	sc2028
HDAC1	Western Blot	Santa Cruz	sc81598
Ki67	Immunohistochemistry	Dako	MIB-1
LIN28A	Western Blot	R&D	AF3757
MYC	Western Blot	Cell Signaling	5605
NANOG	Western Blot	Santa Cruz	sc134218
OCT3/4 (C-10)	Western Blot, Immunofluorescence, co-IP	Santa Cruz	sc5279
Rabbit IgG	ChIP	Cell Signaling	2729
SOX17	ChIP, Western Blot	R&D	AF1924
SOX2	ChIP	AbCam	ab59776
SOX2	Western Blot	R&D	MAB2018
TFAP2C	Western Blot, Immunofluorescence	Santa Cruz	sc8977
β-ACTIN	Western Blot	Sigma Aldrich	a5441

Secondary antibodies

Antibody	**Application**	**Company**	**# Number**
Alexa-Fluor anti-goat secondary antibody	Immunofluorescence	Thermo Fisher Scientific	A11055
Alexa-Fluor anti-mouse secondary antibody	Immunofluorescence	Thermo Fisher Scientific	A11005
Alexa-Fluor anti-mouse secondary antibody	Immunofluorescence	Thermo Fisher Scientific	A11037
HRP-conjugated anti-goat secondary antibody	Western Blot	Dako	P0160
HRP-conjugated anti-mouse secondary antibody	Western Blot	Dako	P0260
HRP-conjugated anti-rabbit secondary antibody	Western Blot	Dako	P0448

2.1.10. qRT-PCR primers

Target Gene	Forward (5'->3')	Reverse (5'->3')
ALPL	AACATCAGGGACATTGACGTG	GTATCTCGGTTTGAAGCTCTTCC
ATF3	AAGAACGAGAAGCAGCATTTGAT	TTCTGAGCCCGGACAATACAC
BRD2	CTACGTAAAGAAACCCCGGAAG	GCTTTTTCTCCAAAGCCAGTT
BRD3	CCTCAGGGAGATGCTATCCA	ATGTCGTGGTAGTCGTGCAG
BRD4	AGCAGCAACAGCAATGCTGAG	GCTTGCACTTGTCCTCTTCC
BRDT	GCTCGGACACAGGAACTCATACG	CCACCATTGCTTCTCTCCTCCTC
CDKN1C	GCGGCGATCAAGAAGCTGT	GCTTGGCGAAGAAATCGGAGA
CDX2	TTCCCATCTGGCTTTTTCTG	AGAGAAGAGCTGGGGAGGAG
EOMES	CGGCCTCTGTGGCTCAAA	AAGGAAACATGCGCCTGC
GAPDH	TGCCAAATATGATGACATCAAGAA	GGAGTGGGTGTCGCTGTTG
GATA3	TCTGACCGAGCAGGTCGTA	CCTCGGGTCACCTGGGTAG
HAND1	AATCCTCTTCTCGACTGGGC	TGAACTCAAGAAGGCGGATG
KIT	CGTTCTGCTCCTACTGCTTCG	CCCACGCGGACTATTAAGTCT
LIN28	TGTAAGTGGTTCAACGTGCG	TGTAAGTGGTTCAACGTGCG
NANOG	GATTTGTGGGCCTGAAGAAA	AAGTGGGTTGTTTGCCTTTG
NANOS3	ACAAGGCGAAGACACAGGAC	AGGTGGACATGGAGGGAGA
POU5F1	GGGAGATTGATAACTGGTGTGTT	GTGTATATCCCAGGGTGATCCTC
PRDM1	GGGTGCAGCCTTTATGAGTC	CCTTGTTCATGCCCTGAGAT
PRDM14	ACACGCCTTTCCCGTCCTA	GGGCAGATCGTAGAGAGGCT
RHOB	GGGACAGAAGTGCTTCACCT	CGACGTCATTCTCATGTGCT
SOX17	GATGCGGGATACGCCAGTGAC	GCTCTGCCTCCTCCACGAAG
SOX2	ATGCACCGCTACGACGTGA	CTTTTGCACCCCTCCCATT
SPRY4	TCTGACCAACGGCTCTTAGAC	GTGCCATAGTTGACCAGAGT
TFAP2C	CCCACTGAGGTCTTCTGCTC	AGAGTCAC ATGAGCGGCTTT
THY1	ATCGCTCTCCTGCTAACAGTC	CTCGTACTGGATGGGTGAACT
αHCG	GTGCAGGATTGCCCAGAAT	CTGAGGTGACGTTCTTTTGGA

2.1.11. Primers for ChIP validation

Name	Forward	Reverse	Reference
DPPA4	ACCCAGACAAAAGTCACCCC	AAGTCTCCTCCCACTTCCTG	[99]
LEFTY2	TCTCCACTCAGACCCTCAGA	GGCAGCCTGAAGAGTTTTGT	[99]
LIN28A	GGGTTGGGTCATTGTCTTTTAG	AAAGGGTTGGTTCGGAGAAG	[100]
NANOG	GCTCGGTTTTCTAGTTCCCC	CCCTACTGACCCACCCTTG	[3]
PRDM1	GAGAAGCAGGAATGCAAGGTC	GGTCGGAGGCAGTAATTAGTGG	[101]
PRDM14	CCTAGACTGAGGCTCGTTACT	ATGCCTGCCTATTGATGAGC	[99]
SOX2	GGATAACATTGTACTGGGAAGGGACA	CAAAGTTTCTTTTATTCGTATGTGTGAGCA	[102]

2.1.12. Plasmids

Name	Purpose	gRNA Sequence (5'→3')	Reference
Lenti-SAMv2	Transcriptional activation of endogenous genes	-	Addgene number: 75112
MS2-P65-HSF1_Hygro	Transcriptional activation of endogenous genes (see Lenti-SAMv2)	-	Addgene number: 61426
pEGFP-N3	GFP expressing control vector	-	Clontech number: 6080-1
pMD2.G	envelope expressing plasmid for lentiviral production	-	Addgene number: 12259
psPAX2	gag / pol expressing plasmid for lentiviral production	-	Addgene number: 12260
PX330-SOX17gRNA1	SOX17 Knockout in TCam-2 cells (backbone: **P**X330-U6-Chimeric_BB-CBh-hSpCas9)	ACGGGTAGCCGTCGAGCGG	Cloned from addgene number: 42230

PX330-SOX17gRNA2	SOX17 Knockout in TCam-2 cells (backbone: **P**X330-U6-Chimeric_BB-CBh-hSpCas9)	GGCACCTACAGCTACGCGC	Cloned from addgene number: 42230
SOX17 SAM gRNA1	SOX17 Overexpression in NCCIT cells (backbone: Lenti-SAMv2)	CTGCCCCCGGGAAAACTAGC	Cloned from addgene number: 75112
SOX17 SAM gRNA2	SOX17 Overexpression in NCCIT cells (backbone: Lenti-SAMv2)	GTGGGGTTGGACTGGGACGT	Cloned from addgene number: 75112

2.1.13. Software and databases

Name	**Purpose**	**Reference**
CRISPR.mit.edu	CRISPR design tool, selection of gRNAs and off-target prediction	http://crispr.mit.edu *Note: this tool is not available any more*
Ensembl	Analysis and visualization of genomic data	http://www.ensembl.org/
Genetrail 2 (1.6)	Statistical analysis of molecular signatures (i.e. Gene Ontology, KEGG Pathways)	https://genetrail2.bioinf.uni-sb.de/
Graphpad Prism version 5.03 for Windows	Customization and design of graphs, bar charts and scatter plots	San Diego, California, USA
HOMER Motif Analysis	Motif discovery and next generation sequencing analysis for ChIP-seq	http://homer.ucsd.edu/homer/ [103]
Illustrator CS3 for Windows	Graphics illustration and design tool	Adobe, San Jose, CA, USA
ImageJ	Analysis and graphical illustration of immunohistochemical stainings	http://imagej.nih.gov/ij/
Molecular Signatures Database (MiSigDB)	Compute overlap with other gene sets by gene set enrichment analysis	http://software.broadinstitute.org/gsea/msigdb/
NCBI	Collection of biomedical and genomic information	http://www.ncbi.nml.nih.gov/

Papers 3.257 for Windows	Reference software	Mekentosj B.V., Dordrecht, Netherlands
Serial Cloner 2.6 for Windows	Provides assistance for DNA cloning and vector mapping	http://serialbasics.free.fr/Serial_Cloner.html/
STRING	Analyse and predict protein-protein interactions	https://string-db.org
Venny 2.1	Create Venn diagram representing the overlap of different datasets	http://bioinfogp.cnb.csic.es/tools/venny/ [104]

2.2. Molecular biological methods

2.2.1. Standard cell culture conditions

Cells were grown at 37°C and 7.5% CO_2 and passaged two times / week in order to keep sub-confluent conditions. For passaging, cells were washed with PBS and incubated with 0.05% Trypsin-EDTA for 3-5 min at 37°C. Trypsin was inactivated by addition of standard growth medium. One part of the cell suspension was then transferred into a new cell culture flask containing fresh standard growth medium.

2.2.2. Transfection

24 h prior to transfection, cells were seeded at a defined cell number in 6-well plates. Transfection mixtures were prepared using FuGene® HD Transfection Reagent in a 1:5 ratio (1 µg DNA, 5 µl FuGene) in 100 µl standard growth medium (w/o P/S, w/o FBS, w/o L-glutamine) and incubated for 15 min. Cells were supplemented with fresh standard growth medium (w/o P/S) and the transfection mix was added for overnight incubation. Next day, cells were washed 1x with PBS and supplemented with fresh complete standard growth medium.

2.2.3. Protein isolation

For protein isolation, cells were harvested using 0.05% Trypsin-EDTA and cell suspension was pelleted by centrifugation at 12.000 rpm for 5 min. To remove residual media components the cell pellet was washed 1x with PBS and then resuspended in 1x RIPA buffer for protein isolation. The protein lysate was incubated for 10 min on ice and then pelleted by centrifugation at 10.000 rpm for 10 min at 4°C. The supernatant was stored at -20°C or -80°C.

2.2.4. Western blot analysis

Prior to Western blot analysis, protein concentrations were determined using the BCA protein assay kit. Typically, 20 µg protein (diluted in 1 x Roti-load) were loaded per lane on a 12% SDS-PAGE (sodium dodecyl sulfate polyacrylamide gel electrophoresis) gel together with PageRuler Prestained Protein Ladder and separated by electrophoresis.

Proteins were then transferred onto a Roti-PVDF membrane in 1 x Western blot transfer buffer using the semi-dry Trans Blot Turbo blotting chamber. Successful transfer was confirmed by staining with Ponceau S or Coomassie Brilliant Blue staining solution. Membranes were rinsed in distilled H_2O or destained using Coomassie destaining solution and then blocked in 5% skimmed milk powder / BSA in PBST. Membrane was then incubated with primary antibody overnight at 4°C or for 3 hours at room temperature. Membrane was then washed 3x in PBST and incubated with HRP-conjugated secondary antibody either overnight at 4°C or for 1 hour at room temperature. After three additional washing steps in PBST, signal was detected using SuperSignal West Pico Chemiluminescent Substrate on a Blot documentation ChemiDoc MP. For detection of a second protein, membrane was afterwards incubated with 1 x Western blot stripping buffer for 25 min at 65°C to remove bound antibodies. The membrane was then washed once in PBST and again processed as described above.

2.2.5. Co-immunoprecipitation

For co-immunoprecipitation (co-IP), typically 50 µl (= 1.5 mg) of Dynabeads® Protein G were coated with 10 µg of primary antibody, according to the manufacturer's instructions. After washing the beads-antibody complex with PBS pH 7.4 (+0.02% Tween 20) 1 mg of whole protein lysate were added and incubated with the beads under constant rotation for 30 min at room temperature. After three washing steps, the beads-antibody-antigen complexes were eluted in 15 µl low pH glycine buffer + 5 µl Roti-Load for 5 min at 95 °C. The beads were then separated from the antibody-antigen complex in a magnetic rack and the clear supernatant was loaded on a 12% SDS-PAGE gel for visualization. 20 µg protein lysate served as 2% input sample.

2.2.6. RNA isolation

For RNA isolation, cells were harvested using 0.05% Trypsin-EDTA and cell suspension was pelleted by centrifugation at 12.000 rpm for 5 min. To remove residual media components the cell pellet was washed 1x with PBS and then RNA was isolated using the RNeasy Mini Kit. RNA concentration and purity was assessed using a Nano

Drop 1000 Spectrophotometer. A 260/280 nm ratio of 1.8-2.2 was generally accepted as ‘pure’ for RNA.

2.2.7. cDNA synthesis and qRT-PCR

Typically, 500 ng of total RNA were reverse-transcribed into complementary DNA (cDNA) using the Maxima Reverse Transcriptase Kit according to the instructions specified by the manufacturer. For qRT-PCR, 7.58 ng of cDNA were pipetted in technical triplicates with Maxima SYBR Green qPCR Master Mix. For qRT-PCR primer details, see **2.1.10**. qRT-PCR was performed using the ViiA7 RealTime PCR System. Quantitative values were obtained from the Ct and *GAPDH* was used as housekeeping gene.

2.3. JQ1 Project

2.3.1. JQ1 treatment of cell lines

For JQ1 treatment, cells were seeded at a defined cell number in 6-well plates. After 24 hours cells were treated with 100, 250 or 500 nM of JQ1 dissolved in DMSO. As negative control, cells were treated with equal amounts of DMSO only.

2.3.2. AnnexinV-7-AAD FACS

For AnnexinV-7AAD FACS, cells were washed with PBS and then harvested using 0.05% Trypsin-EDTA. Cells were collected in FACS tubes and then stained with PE Annexin V and 7-AAD using the PE Annexin V Apoptosis Detection Kit I. Samples were measured in a FACS Canto™.

2.3.3. PI-FACS

For PI FACS analysis, cells were washed with PBS, harvested using 0.05% Trypsin-EDTA and collected in a 1.5 ml microcentrifuge tube. Cells were then pelleted by centrifugation for 3 min at 5000 rpm. Then, cells were washed with PBS and again pelleted for 3 min at 5000 rpm. The remaining pellet was resuspended in 300 µl PBS

and 700 µl ice-cold methanol was added dropwise for fixation, while gently vortexing. The samples were either stored at -80 °C or further processed for FACS analysis. For this, samples were again centrifuged for 3 min at 5000 rpm and the resulting pellet was resuspended in 1 ml of DNA staining solution (2.5 µg / ml PI + 0.5 mg / ml RNAse A) in PBS. Cells were stained for 15 min in the dark and then measured using a FACS Canto™.

2.3.4. XTT assay

The effects of JQ1 and romidepsin treatment on cell viability and cell proliferation were determined by XTT assay. For this, cells were seeded into 96-well plates at a density of 3000 cells / well in 80 µl standard growth medium. The next day different concentrations of JQ1 and / or romidepsin were added in 20 µl standard growth medium. After 24 / 48 / 72 / 96 hours of treatment 50 µl XTT medium (1 mg / ml in standard growth medium) + 1 µl PMS (1.25 mM in PBS) were added to each well. Absorbance was measured 4 hours later in an iMark microplate absorbance reader (450 nm vs. 650 nm). Samples were measured in four technical replicates.

2.3.5. Illumina humanHT-12 v4 expression array

For Illumina HumanHT-12 v4 microarray analysis, total RNA was extracted and RNA quality was assessed by gel electrophoresis in a BioAnalyser 2100. Samples were processed by the Institute for Human Genetics, Bonn, Germany, and measured on an Illumina Human HT-12 v4 Bead Chip. Bioinformatic analysis and data normalization was done by Andrea Hofman, Institute for Human Genetics, Bonn, Germany.

2.3.6. JQ1 treatment of TGCT-xenografted nude mice

For xenotransplantation 1 x 10^7 cells were resuspended in 500 µl of 4°C cold Matrigel and injected into the flank of Crl:NU-Foxn1nu mice. During the procedure, samples were kept on ice at all times to avoid hardening of Matrigel. Tumours were then grown for 2 weeks. Afterwards, mice were treated with JQ1 (+ Romidepsin) to analyse drug efficacy *in vivo*. JQ1 was administered at a dosage of 50 mg / kg on 5 days / week intraperitoneally. 10% HP-β-CD solution was used as a vehicle in order to improve drug solubility. For combination treatment, mice were injected intraperitoneally with 50

mg / kg JQ1 + 0.5 mg / kg romidepsin 3 days / week in 10% HP-β-CD solution. As control, mice were injected with solvent only. Injection volume was 10 µl / g of body weight. Tumour burden was continuously measured using a calliper.

2.3.7. Tumour dissection for IHC staining

Tumours were dissected at defined time points and fixed in 4% formaldehyde at 4°C overnight. Afterwards tissues were processed in paraffin wax using a Tissue-Tek® VIP. For immunohistochemistry, 4 µm sections were cut from embedded tissues and then stained in-house using a semi-automatic Autostainer 480 S. Antibody details are given in **2.1.9**. Ki67 and CD31 stainings were quantified from three individual tumours and significance was calculated using a two-tailed t-test.

2.4. Identification of SOX2 and SOX17 targets in TGCT cells

2.4.1. Fixation and chromatin preparation

For ChIP qPCR chromatin was prepared from 1 x 10^7 cells / IP. For this, cells were fixed in 15 cm cell culture dishes for 30 min at room temperature using Diagenode Crosslink Gold. After two washing steps with PBS cells were fixed again for 10 min in 1% formaldehyde (in PBS). For ChIP-seq analysis cells were fixed for 10 min in 1% formaldehyde (in PBS) only. Crosslinking of proteins to DNA is a critical step, since poor crosslinking results in low yield, while over-fixation will reduce shearing efficiency and negatively affect the reverse cross-linking procedure.

2.4.2. Chromatin immunoprecipitation (ChIP)

Chromatin immunoprecipitation was typically carried out using 200 µg chromatin lysate and 5 µg antibody. The protocol was then performed using the Simple ChIP® Enzymatic Chromatin IP Kit. 2% Input (= 2 µg chromatin) and IgG-IP served as controls. For verification of successful chromatin immunoprecipitation 10 µl of IP samples were amplified using the Genomeplex® Single Cell Whole Genome Amplification Kit (WGA4) and subjected to qPCR. Primers were selected according to already published information on SOX2-OCT4 binding sites, see **2.1.11**.

2.4.3. ChIP-sequencing and bioinformatics analysis

ChIP-seq libraries were generated and processed by Microsynth (Microsynth AG, Balgach, Switzerland). Libraries were prepared using the TruSeq ChIP Library Preparation Kit. Samples were sequenced on the Illumina High Seq 2500 using 30 M single-end reads (1 x 75 bp). Reads were mapped to the human genome (hg38) and data was analysed using HOMER (Hypergeometric Optimization of Motif EnRichment) Software (http://homer.ucsd.edu/homer/). Peak count frequency was analysed with help of the Core Unit for Bioinformatics Analysis, Bonn.

2.4.4. SOX17-knockout in TCam-2 cells

For the generation of TCam-2 Δ SOX17 cells, TCam-2 cells were transfected with 250 ng PX330-SOX17gRNA1 + 250 ng PX330-SOX17gRNA2 using FuGENE® HD transfection reagent in a 1:5 ratio (= 1 µg DNA : 5 µl FuGENE reagent). SOX17 single guide RNAs (gRNAs) were designed and selected using the CRISPR.mit.edu tool. As control, cells were transfected with 500 ng pEGFP-N3.

2.4.5. Immunofluorescence

For immunofluorescence, cells were typically grown in 12-well or 24-well plates. At the desired time point, cells were washed with PBS and then fixed in 4% formaldehyde for 10 min at room temperature. Afterwards, cells were permeabilized using 0.5% Triton X diluted in PBS for 5 min at room temperature. After two washing steps in PBS, cells were blocked in 2% BSA diluted in PBS for 1 hour at room temperature. Afterwards, cells were incubated with primary antibody diluted in blocking solution (500 µl for 12-well plate, 250 µl for 6-well plate) for 2 hours at room temperature or 4°C overnight. After three washing steps in PBS, cells were incubated with Alexa Fluor® secondary antibody diluted in blocking solution for 1 hour at room temperature or 4°C overnight. Again, cells were washed three times in PBS and then counterstained with DAPI in PBS for 5 min at room temperature. Cells were then washed three times in PBS and staining was evaluated under the fluorescent microscope.

2.4.6. Alkaline phosphatase staining

Alkaline phosphatase (AP) staining can be used to discriminate pluripotent cells (AP-positive) from differentiated cell types (AP-negative). For detection of AP activity, cells were typically seeded in 6-well plates. At the desired time point of analysis, cells were fixed for 1 min in 4% formaldehyde and stained for AP activity using the Alkaline Phosphatase Detection Kit. AP-expressing cells will appear red-violet, while AP-negative cells appear colourless.

2.4.7. SOX17 overexpression in EC cells

Overexpression of SOX17 in NCCIT cells was achieved using the CRISPR/Cas9 Synergistic Activation Mediator (SAM) system that was established by the Zhang Lab [105]. It includes a catalytically inactive Cas9-VP46 fusion protein, the single guide RNA incorporating two MS2 RNA aptamers and a MS2-P65-HSF1 activation helper protein. For efficient overexpression two viral particles were generated: I) The MS2-P65-HSF1 helper virus containing the HSF1 and P65 activation domains and II) the SOX17 SAM virus coding for the gRNA specific for the SOX17 upstream regulatory region and the Cas9-VP64 fusion protein.

2.4.8. Virus production

Lentiviral particles were generated using calcium-phosphate precipitation. For this, HEK-293T were seeded onto poly-l-lysine coated 10 cm dishes and medium was changed to Advanced DMEM containing 2% FBS. Transfection mixtures were prepared using the ProFection® Mammalian Transfection System according to the following scheme:

	10 cm dish
2 M CaCl2	61.5 µl
Lentiviral Vector DNA	18.5 µg
Helper DNA (psPAX2)	9.25 µg
Envelope DNA (pMD2.g)	9.25 µg
Fill up with H20 to	600 µl
2x HBS Buffer	600 µl

Transfection mixtures were then added dropwise to ensure an even distribution on the plate. 5-6 hours later the medium was changed to Advanced DMEM containing 5% FBS. Next morning, the medium was again changed to fresh Advanced DMEM containing 5% FBS (6 ml / 10 cm dish). Virus supernatant was harvested after 24 and 48 hours and sterile-filtered using a pore size of 0.45 µm.

2.4.9. Generation of MS2-P65-HSF1 helper cell lines

MS2-P65-HSF viral particles were generated according to **2.4.8**. For lentiviral plasmid details (MS2-P65-HSF1) see **2.1.12**. Cell lines were then transduced with 500 µl MS2-P65-HSF1 virus supernatant and afterwards selected for stable vector integration under growth in 50 mg / ml hygromycin B medium for 2 weeks.

2.4.10. Transduction of helper cell lines with SOX17 SAM virus

SOX17 SAM virus was prepared using equimolar amounts of SOX17 SAM gRNA1 and SOX17 SAM gRNA2, see **2.1.12**. Virus supernatant was generated according to **2.4.8.** Cell lines were then transduced with 100, 200 or 500 µl SOX17 SAM virus. SOX17 overexpression was verified by qRT-PCR and Western blot analysis.

3. Results I

As previously described, TGCTs are highly sensitive to chemotherapeutic agents and radiotherapy [106]. However, despite cure rates of ≥ 95% TGCTs may develop resistance mechanisms to standard therapy regimens. These subtypes are difficult to treat and even multiple cycles of high-dose chemotherapy can remain ineffective. In this aspect epigenetic drugs open a new avenue to cancer therapy and may present a promising alternative to standard therapies [79]. Demethylating agents (5-aza, SGI-110), histone demethylase inhibitors (CBB1003, CBB1007, CBB3001) and HDAC inhibitors (romidepsin) have already shown promising effects in pre-clinical studies [3, 79, 107, 108]. Additionally, the bromodomain inhibitor JQ1 was tested for its efficacy in TGCT cell lines, demonstrating cytotoxic effects (G0/G1 arrest, apoptosis) in EC cells at doses ≥ 100 nM and seminoma cells at doses ≥ 250 nM [1, 2, 79]. The apoptosis and cell cycle arrest of EC and seminoma cells following JQ1 treatment reflects the therapeutic potential of bromodomain inhibition for TGCTs. The first aim of this thesis was to analyse the molecular effects of the bromodomain inhibitor JQ1 in TGCT cell lines in more detail.

3.1. TGCT cell lines and somatic control cells express the JQ1 targets BRD2, BRD3 and BRD4

JQ1 is an inhibitor of the BET family of bromodomain proteins (BRD2, BRD3, BRD4 and BRDT). Since JQ1 treatment markedly induced growth arrest and apoptosis in the TGCT cell lines TCam-2, NCCIT, NT2/D1 and 2102EP [1, 2], I asked, which BET members were expressed and could be inhibited by JQ1 in these cell lines. First, mRNA expression in seminoma (TCam-2), EC (NCCIT, NT2/D1, 2102EP) and cisplatin-resistant EC (NCCIT-R, NT2/D1-R, 2102EP-R) cells was analysed (**Fig. 7 A**). Sertoli (FS1) and fibroblast (MPAF) served as controls (**Fig. 7 A**). Across all cell lines analysed, we found highest mRNA expression for *BRD2* and lower expression for *BRD3* and *BRD4*, while *BRDT* expression was absent. Protein levels of BRD2, BRD3 and BRD4 were similarly detected in TCam-2, NCCIT, NT2/D1, 2102EP and FS1 cells (**Fig. 7 B**). To see whether expression of *BRD2*, *BRD3* and *BRD4* can also be confirmed *in vivo*, I performed a meta-analysis of previously published microarray data of TGCT tissues [109]. *BRD2*, *BRD3* and *BRD4* were equally expressed in normal

testis tissue (NTT), GCNIS tissue, seminoma (SEM) tissue and EC tissue samples (**Fig. 7 C**). Also *BRDT* was expressed in all analysed tissues (**Fig. 7 C**). According to literature, *BRDT* should only be expressed in spermatocytes and early spermatids [110]. The *BRDT* expression detected in TGCT and normal testis tissues might come from *BRDT*-expressing germ cells present in the isolated tissues.

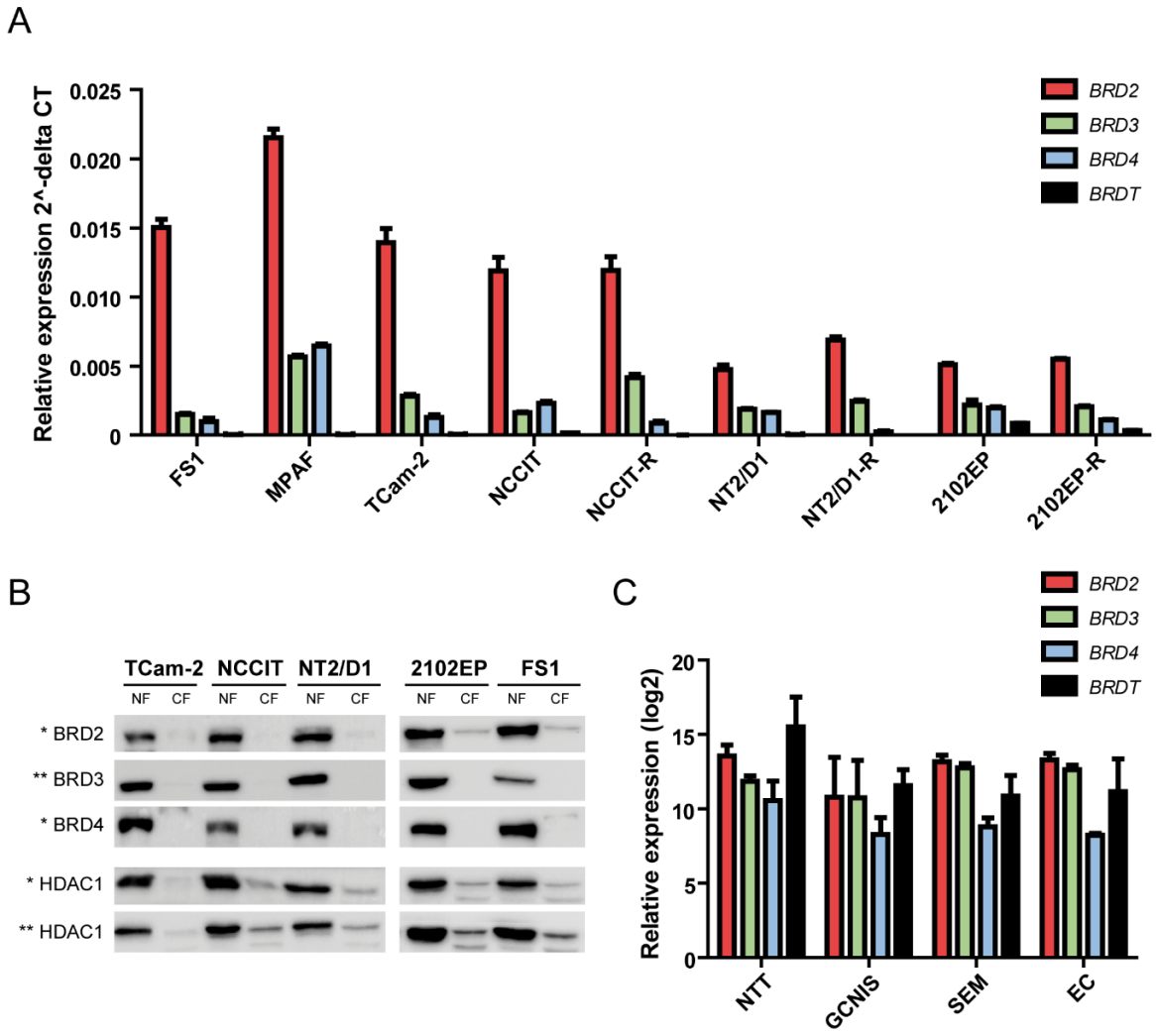

Figure 7: Expression of BRD2, BRD3, BRD4 and BRDT in TGCT cell lines and somatic control cells. Modified from [2]

(A) mRNA expression of *BRD2*, *BRD3*, *BRD4* and *BRDT* in human TGCT cell lines (TCam-2, NCCIT(-R), NT2/D1(-R), 2102EP(-R)), Sertoli cells (FS1) and human fibroblasts (MPAF), determined by qRT-PCR. Expression levels were normalized to *GAPDH* as housekeeping gene.

(B) Western blot of BRD2, BRD3 and BRD4 protein levels in nuclear (NF) and cytoplasmic fractions (CF) of TGCT cell lines (TCam-2, NCCIT, NT2/D1, 2102EP) and Sertoli cells (FS1). HDAC1 served as loading control.

(C) mRNA expression of *BRD2*, *BRD3*, *BRD4* and *BRDT* in normal testis tissue (NTT) (n = 4), germ cell neoplasia in situ (GCNIS) (n = 3), seminoma (SEM) (n = 4) and embryonal carcinoma (EC) (n = 3) tissue, as determined by cDNA microarray analysis. Error bars indicate standard deviation from the mean.

Altogether, these data show that the BET members BRD2, BRD3 and BRD4 are mutually expressed across seminoma and EC cell lines and tissues, including the cisplatin-resistant subclones. Thus, BRD2, BRD3 and BRD4 may be inhibited by JQ1 treatment in these cells and therefore responsible for the JQ1-mediated cytotoxicity in TGCT cell lines reported previously [1]. However, expression of BRD2, BRD3 and BRD4 was also detected in normal testis tissue and somatic control cells (FS1, MPAF). Therefore it is still unclear, which side effects JQ1 treatment will have on the testicular microenvironment *in vivo*. Previous experiments could already demonstrate cytotoxic effects of JQ1 treatment in the Sertoli cell line FS1 [1], indicating that JQ1 elicits side effects in surrounding tissues.

3.2. JQ1 induces apoptosis and cell cycle arrest in TGCT cells and in cisplatin-resistant EC cells

Previous work reported that JQ1 induces apoptosis and G0/G1 arrest in EC lines (2102EP, NCCIT, NT2/D1) at concentrations ≥ 100 nM and seminoma cells (TCam-2) at concentrations ≥ 250 nM [1]. This was shown by AnnexinV/7AAD FACS and PI FACS analysis, respectively [1]. In addition, reduction of cell viability in TGCT cells was confirmed by Western blot analysis detecting cleaved PARP (Poly (ADP-ribose) polymerase) levels. 500 nM JQ1 treatment resulted in a strong increase in cleaved PARP levels in seminoma (TCam-2) and EC cells (NCCIT, NT2/D1, 2102EP) already after 24 hours (**Fig. 8 A**). The normal function of PARP is to repair DNA damage [111]. Excessive DNA damage, however, results in cleavage of PARP rendering the enzyme inactive [111]. In fact, cleaved PARP is considered a hallmark of apoptotic cells [111]. Therefore, rising levels of cleaved PARP levels demonstrate the cytotoxicity of JQ1 in TGCT cell lines.

Since 95% of all TGCT patients are already successfully treated by standard therapy regimens (chemo- or radiotherapy), we were particularly interested in the efficacy of JQ1 in cells displaying cisplatin-resistance. Therefore, I additionally analysed the effects of JQ1 on cell viability and cell cycle of cisplatin-resistant EC cell lines (NCCIT-R, NT2/D1-R, 2102EP-R). Similar to cisplatin-sensitive cells [1], cisplatin-resistant EC lines undergo apoptosis (**Fig. 8 B**) and G0/G1 arrest (**Fig. 8 C**) following JQ1 treatment. In EC lines NCCT-R and NT2/D1-R apoptosis and G0/G1 arrest was detected already

after 16 hours of JQ1 treatment. A prolonged exposure time of 20 hours led to similar effects in 2102EP-R. Since the same trend was observed in parental NCCIT, NT2/D1 and 2102EP cells [1], it can be concluded that JQ1 shows therapeutic effects in both cisplatin-sensitive and cisplatin-resistant cells.

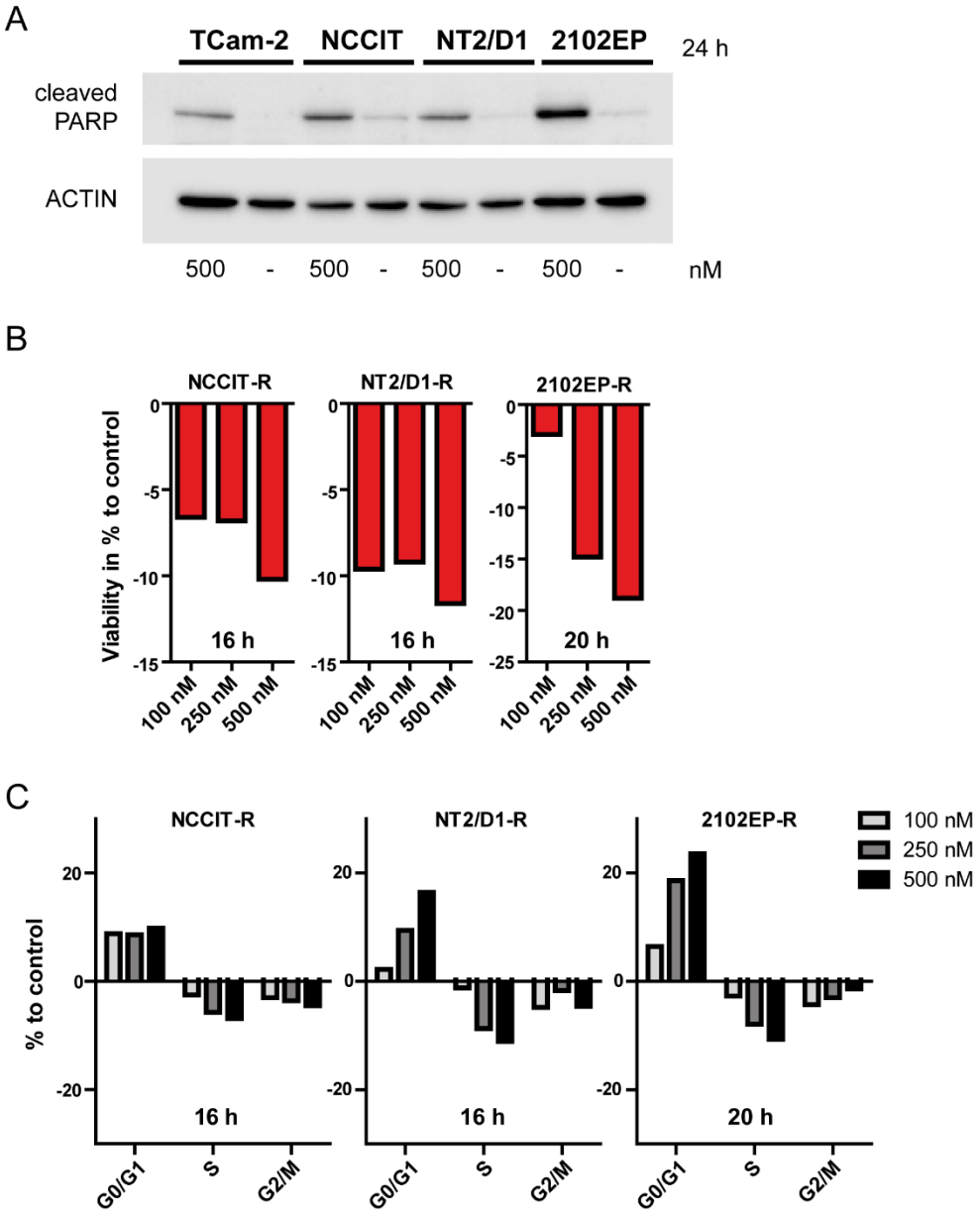

Figure 8: JQ1 induces apoptosis and G0/G1 arrest in cisplatin-sensitive and cisplatin-resistant TGCT cells

(A) Western blot of cleaved PARP levels in 500 nM JQ1-treated TGCT cell lines compared to solvent controls (-). ACTIN was used as loading control.

(B) Cell viability (in % to control) of JQ1-treated cisplatin-resistant EC lines as determined by AnnexinV-7AAD FACS analysis. Time after JQ1 treatment is given in hours (h) below.

(C) Cell Cycle (in % to control) of JQ1-treated cisplatin-resistant EC lines as determined by PI FACS analysis. Time after JQ1 treatment is given in hours (h) below.

3.3. The molecular effects of JQ1 treatment in TGCT cells

Microarray data showed that JQ1 treatment of EC (NCCIT) and seminoma (TCam-2) cells leads to upregulation of stress markers (*CDKN1C*, *DDIT4*, *TSC22D1*, *TXNIP*, *ATF3*, *RHOB*, *BTG1*, *JUN*), strong induction of the differentiation marker *HAND1*, and downregulation of pluripotency-associated genes (*LIN28*, *DPPA4*, *UTF1*, *ZSCAN10*) as well as germ-cell related markers (*SPRY4*, *THY1*) [1]. We hypothesized that deregulation of these genes is responsible for the JQ1-mediated cytotoxicity in TGCT cell lines. To confirm the microarray data and to determine whether these deregulations are common for all TGCT cells, I measured mRNA expression of *CDKN1C*, *ATF3*, *RHOB*, *HAND1*, *POU5F1*, *LIN28, SPRY4* and *THY1* in seminoma (TCam-2) and EC cells (NCCIT, NT2/D1, 2102EP). A common effect of JQ1 treatment across all TGCT cell lines was the downregulation of germ cell – associated genes *SPRY4* and *THY1* (**Fig. 9**). Further, I verified induction of the stress markers *CDKN1C*, *ATF3* and *RHOB* in the pluripotent EC lines NCCIT and NT2/D1 cells after 100 nM JQ1 treatment (**Fig. 9**). Additionally, strong induction of the differentiation marker *HAND1* and downregulation of pluripotency genes *POU5F1* and *LIN28* suggested loss of pluripotency and induction of differentiation in pluripotent EC cells (**Fig. 9**). In contrast, the nullipotent EC line 2102EP showed mild induction of *CDKN1C*, *ATF3* and *RHOB*, but only at higher JQ1 concentrations (750 nM). Downregulation of pluripotency markers *POU5F1* and *LIN28* and upregulation of *HAND1* was similarly seen only at higher JQ1 concentrations (750 nM) in this cell line (**Fig. 9**). It is tempting to speculate that 2102EP cells are less sensitive to JQ1-induced deregulation, due to their nullipotent character. In contrast to the pluripotent EC lines NCCIT and NT2/D1, 2102EP cells lack the ability to differentiate into mixed non-seminoma cells. In comparison, the seminoma-like cell line TCam-2 shows induction of stress markers *CDKN1C*, *ATF3* and *RHOB,* mild upregulation of the differentiation marker *HAND1* and downregulation of pluripotency, indicated by loss of *LIN28* expression (**Fig. 9**). mRNA levels of *POU5F1*, however, remained unchanged in TCam-2 cells (**Fig. 9**).

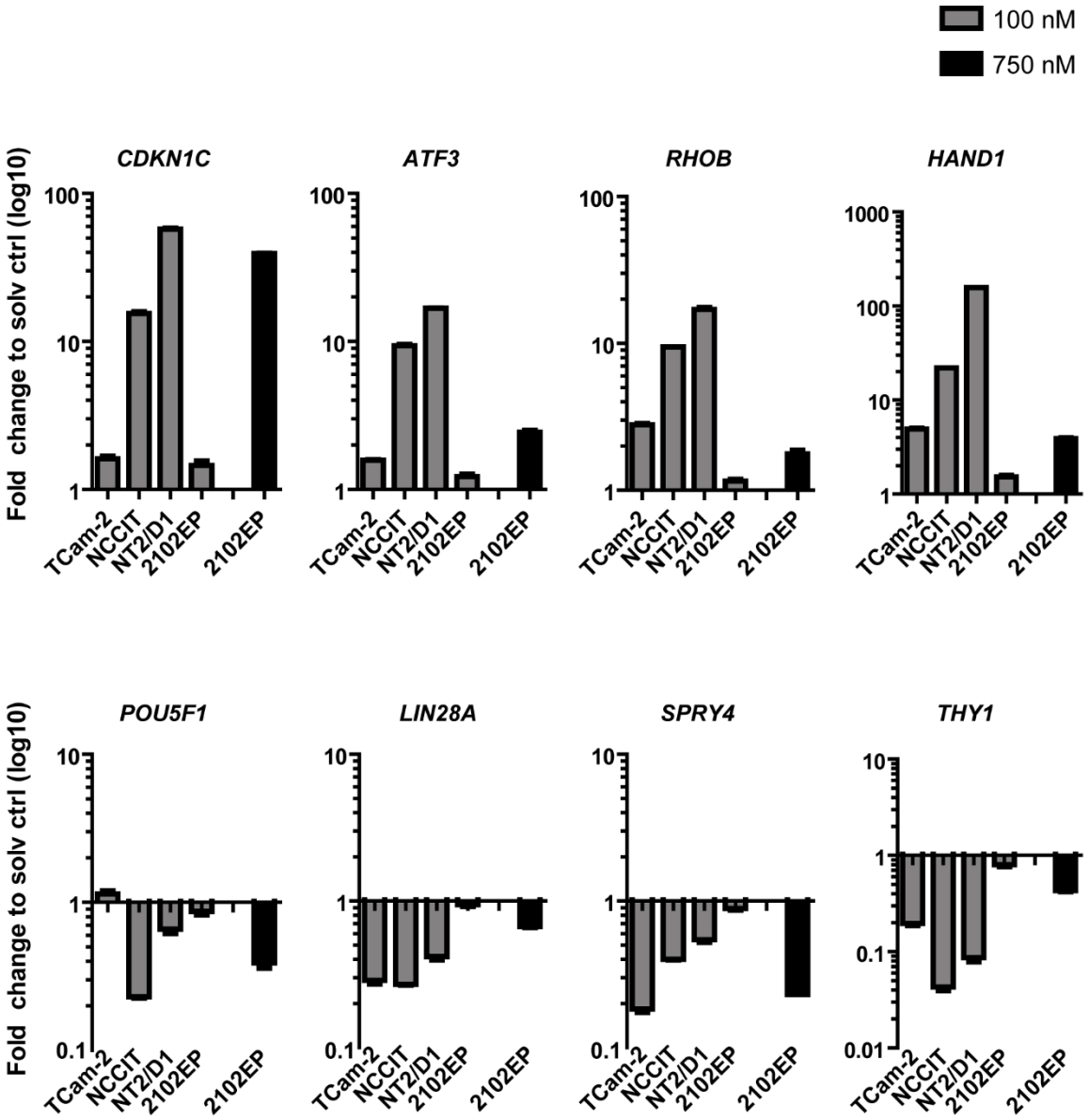

Figure 9: Upregulation of stress markers and downregulation of pluripotency genes in TGCT cells following JQ1 treatment. Modified from [2]
Verification of cDNA microarray data by qRT-PCR. Expression values were calculated as fold change compared to solvent control and normalized against *GAPDH* as housekeeping gene.

To confirm the downregulation of pluripotency after JQ1 treatment in TGCT cells on protein level, I screened for changes in POU5F1 (OCT4) and LIN28 expression, as well as levels of the stem cell marker and BMP inhibitor GDF3. I detected downregulation of GDF3 and POU5F1 in EC lines (NCCIT, NT2/D1) and mild downregulation of LIN28 in the seminoma line TCam-2, which is consistent with the microarray and qRT-PCR data [1] (**Fig. 9-10**). Although the effects of JQ1 on

pluripotency marker expression are not identical between seminoma (TCam-2) and EC (NCCIT, NT2/D1) cell lines, I was able to confirm an overall downregulation of pluripotency in both TGCT subtypes on RNA and protein level.

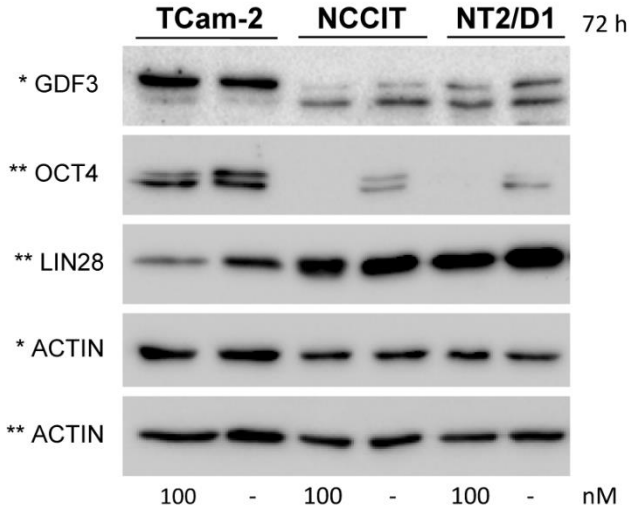

Figure 10: Downregulation of pluripotency in TGCT cell lines. Modified from [2]
GDF3, POU5F1 and LIN28 protein levels in 100 nM JQ1-treated TGCT cell lines compared to solvent controls (-). ACTIN was used as loading control and for data normalization.

Notably, the overall state of pluripotency differs between seminoma and EC cells. While seminoma cells share the latent pluripotent character of early PGCs, EC cells show features of totipotency similar to early ESCs. Hence, EC cells are capable of differentiating into cells of embryonic and extra-embryonic lineages. In contrast, seminoma cells express some of the well-known pluripotency and stem cell markers (e.g. POU5F1, LIN28), but are highly restricted in their differentiation potential. For a long time it was believed that seminoma cells can not differentiate at all, however in a previous publication by our group it was shown that seminoma cells can differentiate into mixed non-seminomatous lineages in presence of TGF-β, EGF and FGF4 [73]. Due to the differences in the differentiation potential of seminomas and ECs, however, I proceeded with analysing the effects of JQ1 specifically on TGCT pluripotency in more detail. Since the pluripotent EC lines NCCIT and NT2/D1 showed much higher sensitivity to JQ1 than the TCam-2 cell line or the nullipotent 2102EP cell line, I

speculated that JQ1-mediated cytotoxicity may in part be mediated via downregulation of pluripotency of these cells.

Gene set enrichment analysis (GSEA) of the previously obtained microarray data [1] revealed enrichment of stem cell signatures among downregulated genes in TCam-2 (LIM_MAMMARY_STEM_CELL_UP, BENPORATH _ES_1) (**Table 4**) and an even more prominent enrichment of stem cell signatures among downregulated genes in NCCIT (BENPORATH_ES_1, BENPORATH_NANOG_TARGETS, KORKOLA_ CORRELATED_WITH_POU5F1, BENPORATH_SOX2_TARGETS, BHATTACHA RYA_EMBRYONIC_STEM_CELL, CONRAD _STEM_CELL, BENPORATH_ES_2) (**Table 5**). Since the EC cell line NCCIT is capable of differentiating into cells of embryonic and extra embryonic lineages I additionally analysed the list of genes upregulated following JQ1 treatment by gene ontology analysis. In line with the downregulation of pluripotency in this cell line, gene ontology analysis demonstrated enrichment of biological processes associated with embryonic differentiation among genes induced by 100 nM JQ1 (**Table 6**). Categorization of these genes into embryonic lineages reveals that the majority of these processes are associated with mesoderm differentiation (**Fig. 11**). In summary, this shows that JQ1 treatment of TGCT cells results in downregulation of pluripotency or stem cell associated genes. According to the GSEA, this downregulation is more significant in the pluripotent EC line NCCIT ($p \geq 2.41E-59$) compared to the latent pluripotent seminoma cell line TCam-2 ($p \geq 7.5E-13$) and downregulation of pluripotency in NCCIT goes in hand with upregulation of differentiation markers (mainly mesoderm).

Table 4: GSEA of genes downregulated in TCam-2 cells 72 hours after JQ1 treatment

Gene Set Name	P-value
SMID_BREAST_CANCER_LUMINAL_B_DN	1.77E-16
HOSHIDA_LIVER_CANCER_SUBCLASS_S1	1.82E-13
LEI_MYB_TARGETS	4.14E-13
CHICAS_RB1_TARGETS_CONFLUENT	5.56E-13
RODWELL_AGING_KIDNEY_UP	7.05E-13
LIM_MAMMARY_STEM_CELL_UP	7.5E-13
SERVITJA_ISLET_HNF1A_TARGETS_UP	1.47E-12
BENPORATH_ES_1	4.39E-12
SMID_BREAST_CANCER_BASAL_UP	4.59E-12
VERHAAK_AML_WITH_NPM1_MUTATED_DN	6.36E-12

Table 5: GSEA of genes downregulated in NCCIT cells 72 hours after JQ1 treatment

Gene Set Name	P-value
BENPORATH_ES_1	2.41E-59
BENPORATH_NANOG_TARGETS	1.34E-23
KORKOLA_CORRELATED_WITH_POU5F1	1.71E-19
BENPORATH_SOX2_TARGETS	5.9E-19
KRIEG_HYPOXIA_NOT_VIA_KDM3A	2.28E-18
ELVIDGE_HYPOXIA_UP	1.27E-15
BHATTACHARYA_EMBRYONIC_STEM_CELL	1.71E-15
CONRAD_STEM_CELL	7.56E-15
BENPORATH_ES_2	1.00E-14
ELVIDGE_HYPOXIA_BY_DMOG_UP	1.1E-14

Table 6: Gene ontology analysis of genes upregulated in NCCIT cells 72 hours after JQ1 treatment

Process	q-value
heart morphogenesis	1.83e-13
regionalization	6.62e-12
regulation of cellular response to growth factor stimulus	5.90e-11
cardiac chamber development	9.06e-11
cardiac ventricle development	1.25e-10
appendage development&limb development	1.39e-10
cardiac chamber morphogenesis	1.39e-10

mesenchymal cell development	1.39e-10
regulation of transmembrane receptor protein serine threonine kinase signaling pathway	1.39e-10
stem cell development	1.39e-10
mesenchymal cell differentiation	2.29e-10
mesenchyme development	3.21e-10
appendage morphogenesis&limb morphogenesis	4.22e-10
cardiac septum development	1.24e-9
stem cell differentiation	1.72e-9
regulation of ossification	2.07e-9
negative regulation of DNA binding	2.85e-9
connective tissue development	2.86e-9
osteoblast differentiation	6.12e-9
positive regulation of ossification	7.76e-9
epithelial tube morphogenesis	1.06e-8
odontogenesis of dentin containing tooth	1.06e-8
regulation of DNA binding	1.06e-8
cell cell junction organization	1.27e-8
cell junction assembly	1.62e-8
cardiac muscle tissue development	1.76e-8
embryonic appendage morphogenesis&embryonic limb morphogenesis	1.76e-8
BMP signaling pathway	2.33e-8
cartilage development	3.39e-8
in utero embryonic development	3.61e-8
response to BMP(4)&cellular response to BMP stimulus	3.86e-8
regulation of osteoblast differentiation	5.96e-8
cardiac septum morphogenesis	6.48e-8
regulation of BMP signaling pathway	1.36e-7
gastrulation	2.66e-7
outflow tract morphogenesis	3.68e-7
mesenchyme morphogenesis	5.71e-7
response to mechanical stimulus	6.81e-7
stem cell proliferation	1.09e-6
anterior posterior pattern specification	1.09e-6
ventricular septum development	1.16e-6
epithelial to mesenchymal transition	1.24e-6
endoderm development	1.81e-6
formation of primary germ layer	1.86e-6
ventricular cardiac muscle tissue development	1.89e-6
skeletal system morphogenesis	1.99e-6
actin filament bundle assembly	2.50e-6
embryonic organ morphogenesis	2.73e-6
actin filament bundle organization	2.95e-6

regulation of canonical Wnt signaling pathway	3.03e-6
negative regulation of growth	3.42e-6
palate development	3.42e-6
regulation of Wnt signaling pathway	3.42e-6
embryonic hindlimb morphogenesis	3.64e-6
kidney epithelium development	4.20e-6
ureteric bud development	5.37e-6
regulation of protein localization to nucleus	5.57e-6
mesonephric tubule development&mesonephric epithelium development	5.63e-6
positive regulation of osteoblast differentiation	5.75e-6
segmentation	5.90e-6
chondrocyte differentiation	6.59e-6
mesonephros development	6.59e-6
positive regulation of BMP signaling pathway	6.59e-6
sensory organ morphogenesis	6.83e-6
cardiac ventricle morphogenesis	7.98e-6
regulation of cartilage development	7.98e-6
positive regulation of transmembrane receptor protein serine threonine kinase signaling pathway	8.43e-6
regulation of cellular response to transforming growth factor beta stimulus	8.82e-6
regulation of transforming growth factor beta receptor signaling pathway	8.82e-6
embryonic forelimb morphogenesis	9.51e-6
actomyosin structure organization	9.67e-6
neural crest cell development	1.10e-5
morphogenesis of embryonic epithelium	1.18e-5
hindlimb morphogenesis	1.22e-5
canonical Wnt signaling pathway	1.26e-5
negative regulation of transcription regulatory region DNA binding	1.29e-5
negative regulation of cell development	1.42e-5
adherens junction organization	1.49e-5
cardiocyte differentiation	1.80e-5
regulation of stem cell differentiation	2.02e-5
neural crest cell differentiation	2.08e-5
forelimb morphogenesis	2.53e-5
mesoderm development	2.82e-5
regulation of chondrocyte differentiation	2.82e-5
skin development	4.38e-5
extracellular matrix disassembly	4.45e-5
morphogenesis of a branching epithelium	5.07e-5
transforming growth factor beta receptor signaling pathway	5.24e-5
regulation of cell shape	7.12e-5
morphogenesis of a branching structure	8.59e-5

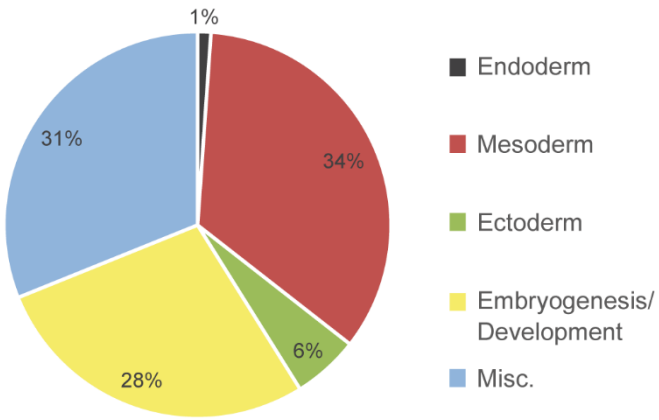

Figure 11: Gene ontology analysis of genes upregulated in NCCIT cells 72 hours after JQ1 Treatment. Modified from [2]
Categorization of biological processes enriched among genes upregulated in NCCIT cells 72 hours after 100 nM JQ1 treatment determined by gene ontology analysis.

Interestingly, in different cancer models (e.g. esophageal squamous cell carcinoma, multiple myeloma) JQ1 treatment additionally resulted in strong downregulation of the proto-oncogene *MYC* [93, 97, 112]. In these studies MYC was described as one of the primary targets of JQ1 treatment and JQ1-mediated cytotoxicity was dependent on MYC downregulation [93]. Since transcription of *MYC* was described to be regulated by BRD4, JQ1-mediated BRD4 inhibition in these cells resulted in downregulation of *MYC* mRNA, further leading to the loss of MYC protein expression. In TGCT cells, however, no downregulation of *MYC* mRNA was observed in response to JQ1 treatment [1]. Surprisingly, *MYC* mRNA levels were even upregulated following JQ1 treatment in seminoma (TCam-2) and EC cells (NCCIT, NT2/D1, 2102EP) [1]. In order to see whether MYC upregulation was similarly observed on protein level in TGCT cells, I analysed whole protein lysates of seminoma (TCam-2) and EC cells (NCCIT, NT2/D1, 2102EP) following JQ1 treatment. I found that MYC protein levels were unaltered in EC lines (NCCIT, NT2/D1, 2102EP) and TCam-2 cells at 100 nM JQ1 (**Fig. 12 A**). At 500 nM JQ1 TCam-2 cells display mild downregulation of MYC protein, while MYC protein levels in EC cells remain unaffected (**Fig. 12 B-C**). Thus, upregulation of *MYC* mRNA does not correlate with upregulation of MYC protein levels in TGCT cells, possibly pointing at post-translational modifications regulating MYC

levels. In summary, those TGCT cells being the most sensitive to JQ1-induced cytotoxicity (NCCIT, NT2/D1) demonstrated no change in MYC expression. Thus, JQ1-associated cytotoxicity in TGCT cells seems to be independent of MYC expression. Also, downregulation of MYC protein in 500 nM treated TCam-2 cells might be a secondary effect of JQ1 treatment, since cytotoxicity of JQ1 in TCam-2 cells is already observed at doses ≥ 250 nM.

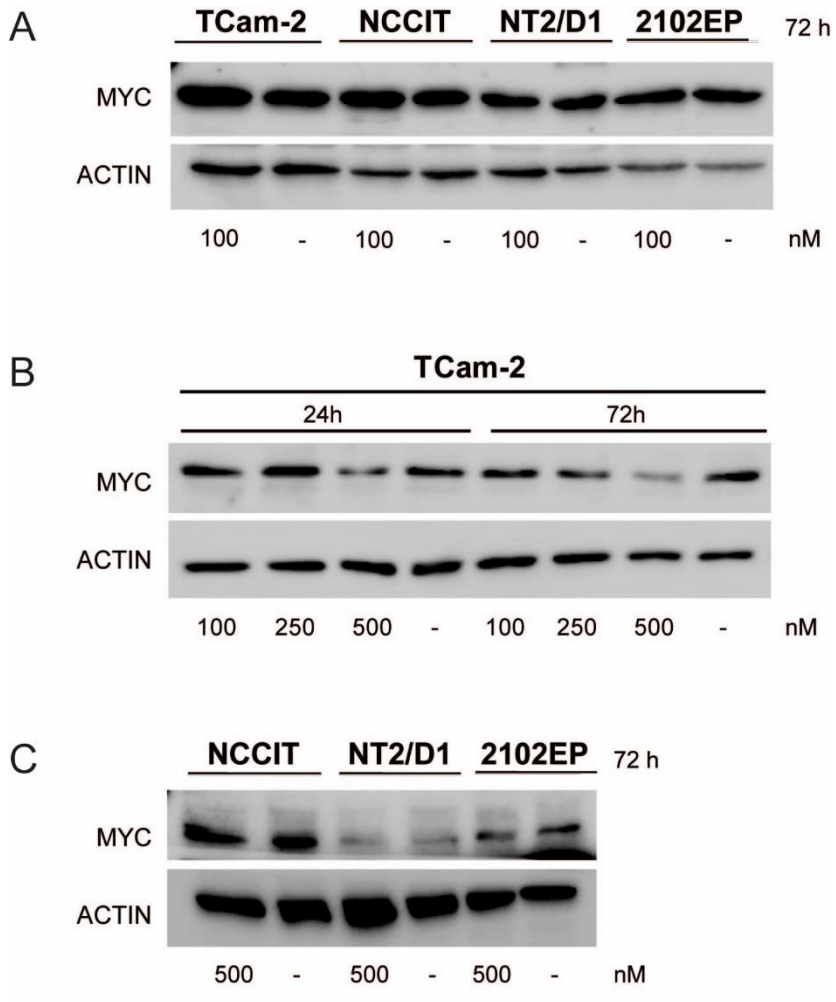

Figure 12: MYC protein levels in JQ1 treated TGCT cell lines. Modified from [2]
(**A-C**) Western blot of MYC protein levels in JQ1-treated TGCT cell lines compared to solvent controls (-). JQ1 concentrations are indicated below in nM. ACTIN was used as loading control. Time of JQ1 treatment is given in hours (h).

3.4. The molecular effects of JQ1 on the testis microenvironment

The effects of JQ1 were additionally tested on somatic control cells (adult fibroblasts and a Sertoli cell line), demonstrating cytotoxicity (G2/M arrest, apoptosis) also in Sertoli cells, while adult fibroblasts remained nearly unaffected (G0/G1 arrest, but no apoptosis) [1, 2]. The JQ1-mediated cytotoxicity of Sertoli cells, however, may indicate the possibility of side effects in the testicular microenvironment when used in patients. I verified JQ1-mediated cytotoxicity in FS1 Sertoli cells additionally by measuring levels of cleaved PARP (**Fig. 13**). In contrast to adult fibroblasts (MPAF), human Sertoli cells (FS1) display strong induction of cleaved PARP levels, indicative for JQ1-mediated cytotoxicity (**Fig. 13**).

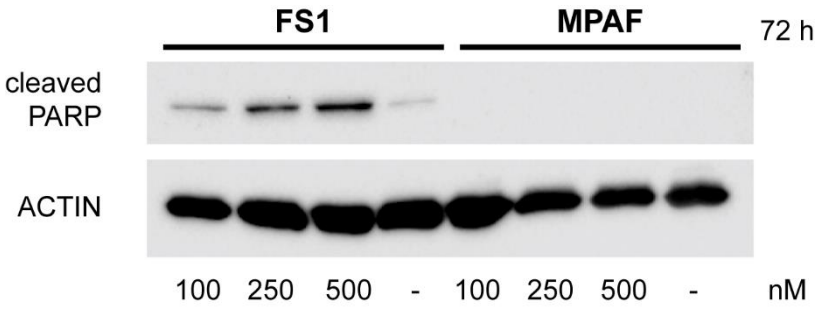

Figure 13: JQ1 induces apoptosis in FS1 Sertoli cells but not fibroblasts. Modified from [2] Western blot of cleaved PARP levels in 100, 250 and 500 nM JQ1-treated FS1 Sertoli cells and adult fibroblasts (MPAF) compared to solvent controls (-). ACTIN was used as loading control. Time of JQ1 treatment is given in hours (h).

To analyse the molecular effects of JQ1 on the testicular microenvironment in more detail, I performed microarray analysis of JQ1 treated Sertoli cells (FS1) after 24 and 72 hours (**Fig. 14 A-B**). After 24 hours, 31 genes (1 upregulated, 30 downregulated) were differentially expressed between JQ1 treated Sertoli cells and solvent controls (**Fig. 14 A**). After 72 hours 33 genes (2 upregulated, 31 downregulated) were differentially expressed (**Fig. 14 B**). In comparison to TCam-2 (24 hours: 242 genes, 72 hours: 212 genes) and NCCIT (24 hours: 225 genes, 72 hours: 512 genes), the number of deregulated genes after JQ1 treatment in FS1 Sertoli cells is much smaller (**Fig. 14** and **15**). Thus, TGCT cells are more susceptible to JQ1-induced gene

deregulations than the somatic control cell line FS1. However, similar to TGCT cells, FS1 cells respond with cell cycle arrest and apoptosis to JQ1 treatment. It remains unclear, which of the deregulated genes is responsible for the cytotoxicity of JQ1 treatment in FS1 Sertoli cells.

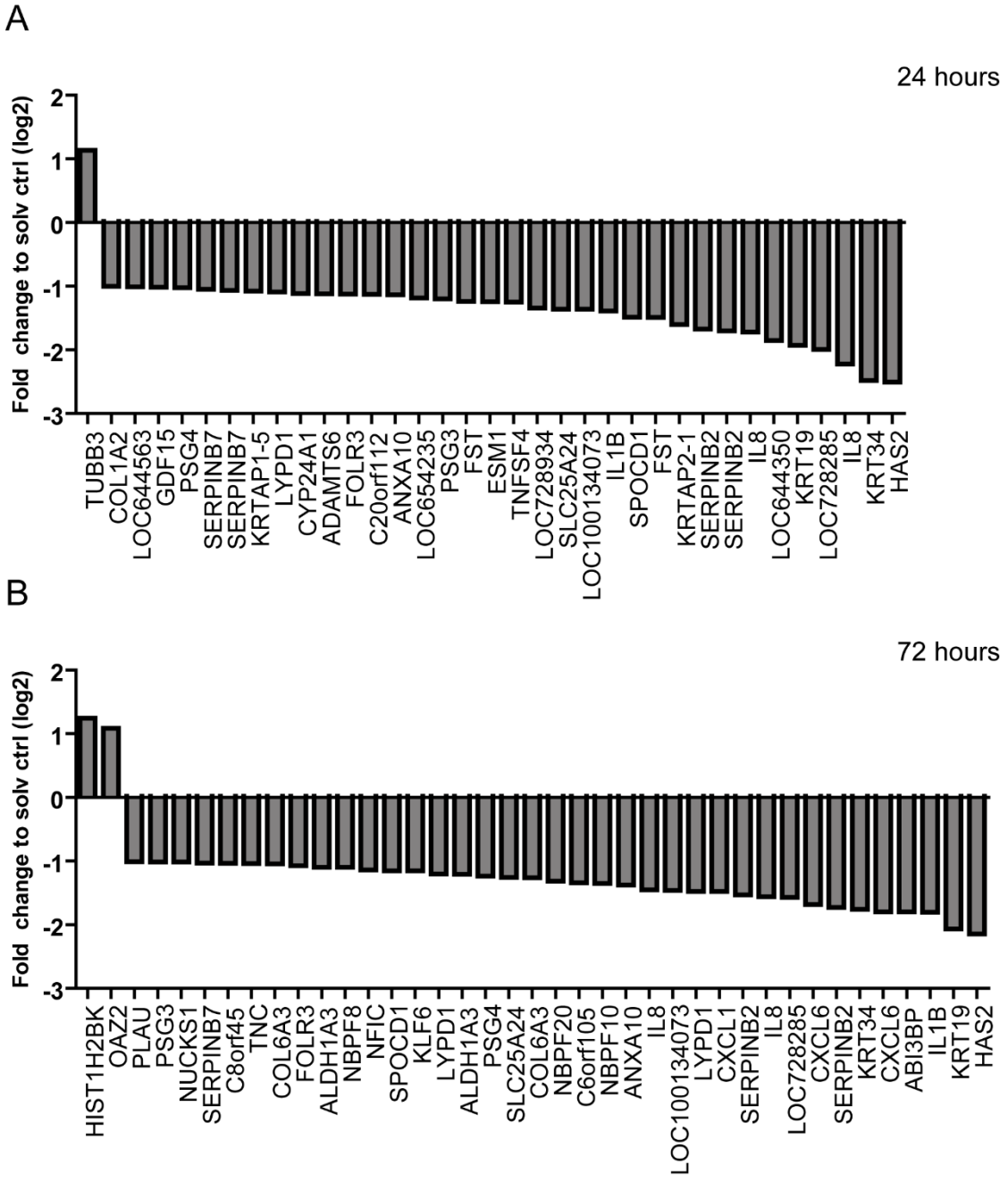

Figure 14: Microarray analysis of 100 nM JQ1 treated Sertoli cells. Modified from [2]
Genes deregulated in FS1 Sertoli cells following 100 nM JQ1 treatment after 24 hours (**A**) and 72 hours (**B**) determined by cDNA microarray analysis. Expression is given as fold change compared to solvent control.

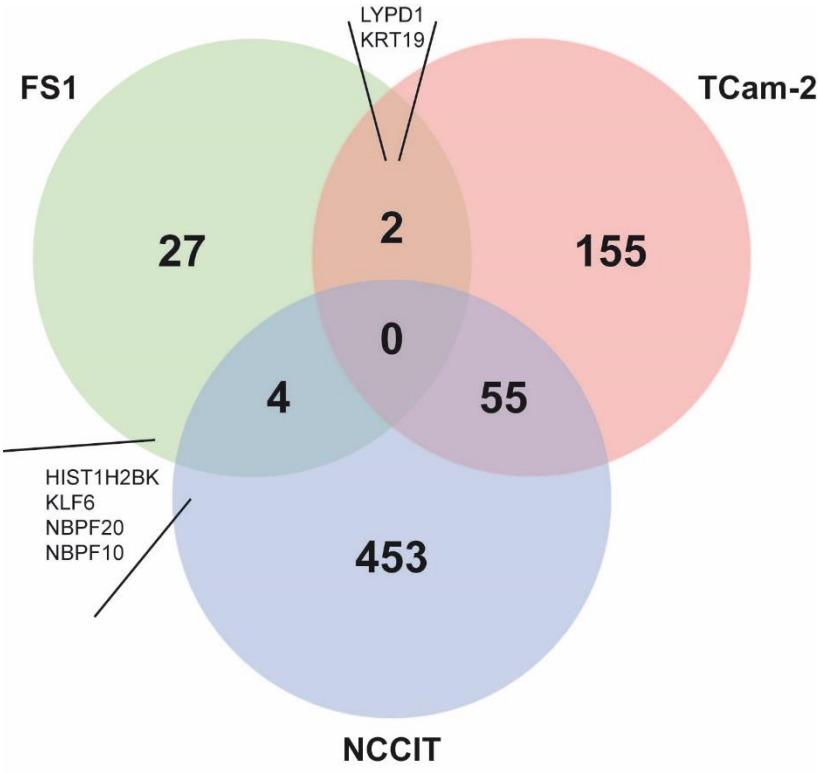

Figure 15: Genes commonly deregulated in TGCT and Sertoli cells
Venn diagram showing genes commonly deregulated in FS1 Sertoli cells, TCam-2 cells and NCCIT cells following 100 nM JQ1 treatment after 72 hours, as determined by cDNA microarray analysis.

Notably, none of the genes deregulated in TGCT cells after JQ1 treatment that have been annotated a role in cytotoxicity (*GADD45B*, *TSC22D1*, *TXNIP*, *RHOB*, *ATF3*, *JUN*, *ID2*) [2] were deregulated in FS1 Sertoli cells after JQ1 treatment. Further, none of the commonly deregulated genes in FS1 Sertoli cells and NCCIT (*HIST1H2BK*, *KLF6*, *NBPF20*, *NBPF10*) or FS1 and TCam-2 (*LYPD1*, *KRT19*) are directly regulating apoptosis or cell cycle arrest (**Fig. 15**). Only *KLF6* was described to induce apoptosis via upregulation of *ATF3* in prostate cancer cells [113]. However, following JQ1 treatment *KLF6* was downregulated in FS1 cells, while being upregulated in NCCIT cells [1, 2]. Thus, a common mechanism of JQ1-mediated cytotoxicity in TGCT and Sertoli cells could not be identified. Although it remains unclear, which of the deregulated genes are responsible for the JQ1-mediated toxicity in FS1 cells, it is evident that BET inhibition can lead to apoptosis and cell cycle arrest in somatic control cells (here: Sertoli cells). I recommend a more detailed analysis of possible side effects and adverse events of JQ1 administration, before commissioning the drug for clinical use.

3.5. Combination therapy with JQ1 and romidepsin in TGCT cell lines

I noted during the analyses that the genes deregulated by JQ1 treatment in TGCT cells were similar to those deregulated by treatment with the HDAC inhibitor romidepsin (induction of *GADD45A*, *GADD45B*, *RHOB*, *ID2*) [1-3]. Since a combination of 100, 250 or 500 nM JQ1 with 5 nM romidepsin also markedly increased apoptosis levels in TCam-2 cells compared to single agent treatment, drug synergy effects for the HDACi+BETi combination were postulated [1, 2].

In order to test, whether a combination of JQ1 and romidepsin will synergistically decrease TGCT cell viability compared to single agent treatment I performed XTT assay on JQ1 and romidepsin treated TCam-2 and NCCIT cells (**Fig. 16**). In contrast to previous experiments where JQ1 was administered every second day due to its relatively short half-life (~1 hour in plasma), in this line of experiments both substances were administered only once before the start of the measurement (timepoint: 0 hours (h)). Under these conditions administration of neither 100 nM nor 250 nM JQ1 showed cytotoxic effects in TCam-2 cells (**Fig. 16 A**). In contrast, 2 nM romidepsin treatment led to a decrease in cell viability of ~ 40% in TCam-2 cells. A combination of 2 nM romidepsin with either 100 or 250 nM JQ1 further reduced cell viability to ~ 30%. This shows that even though a one-time administration of JQ1 alone has no effect on TCam-2 cell viability, the substance can significantly increase cytotoxicity of romidepsin treatment (**Fig. 16 A**). Cytotoxicity levels of high-dose romidepsin treatment (5 nM), however, are not increased by addition of JQ1.

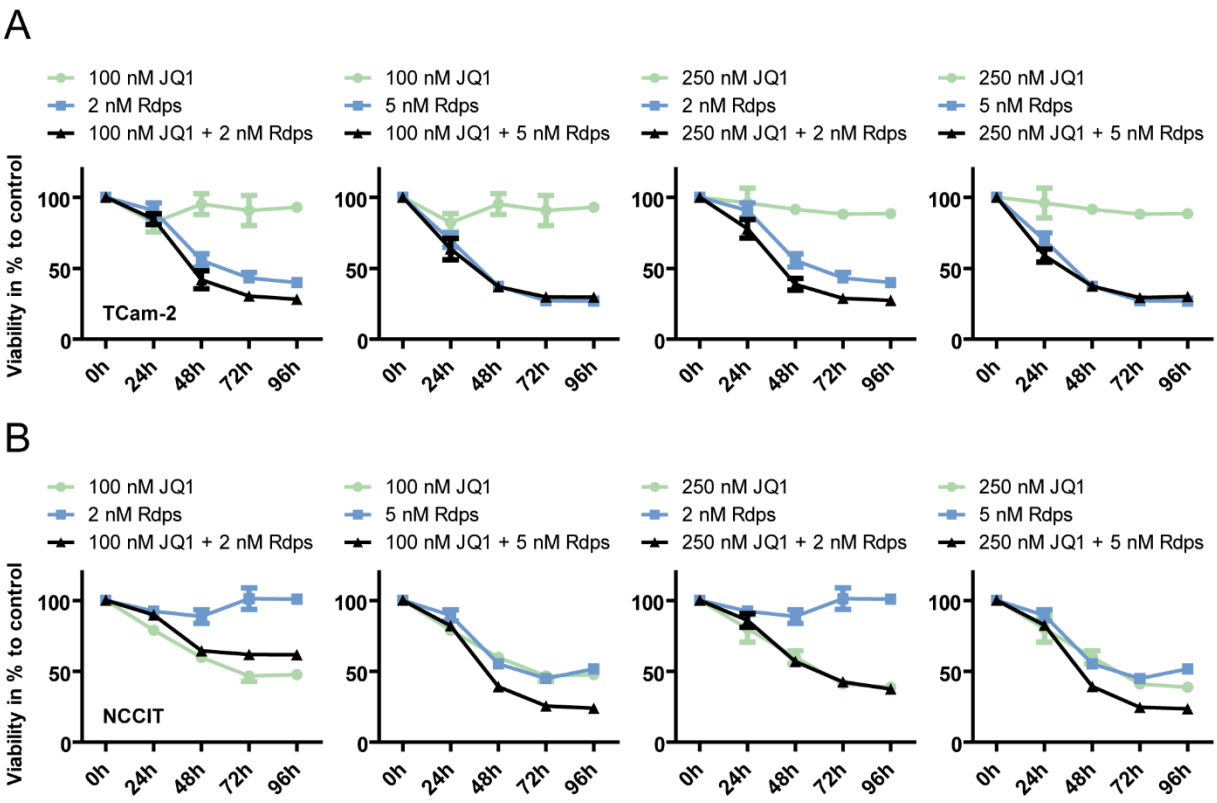

Figure 16: Cell viability of TGCT cells treated with JQ1 and romidepsin. Modified from [2]
Cell viability of TCam-2 (**A**) and NCCIT (**B**) cells treated with JQ1, romidepsin (Rdps) or JQ1 and romidepsin (JQ1 + Rdps) in combination determined by XTT assay. Cell viability is given in % to solvent control.

Similarly, I observed that a one-time administration of 2 nM romidepsin showed no cytotoxic effects in NCCIT cells (**Fig. 16 B**). In contrast, 100 nM or 250 nM JQ1 led to a reduction of cell viability to 40-50% and 5 nM romidepsin treatment led to a reduction of cell viability to 50% (**Fig. 16 B**). While a combination treatment of 100 or 250 nM JQ1 + 2 nM romidepsin had no additional effect on cytotoxicity levels, the combination of 5 nM romidepsin and 100 or 250 nM JQ1 further decreased cell viability to ~ 20% (**Fig. 16 B**). In summary, these data demonstrate that under certain conditions JQ1 and romidepsin may show additive or synergistic effects on cytotoxicity levels of TGCT cells. However, the interplay of both drugs and their exact efficacy vs toxicity (side effects) relationship needs further evaluation using *in vivo* model systems.

3.6. JQ1 treatment of TGCT xenografts

In order to investigate the efficacy of JQ1 treatment (also in combination with romidepsin) *in vivo*, I analysed tumour growth of NCCIT and NT2/D1 xenografts in CD-1 nude mice under drug administration. For this, cell lines were injected into the flank of nude mice and after two weeks of initial tumour growth mice were intraperitoneally (i.p.) injected with drug or solvent control. Tumour growth was continuously monitored. Mice treated with JQ1 (50 mg / kg) presented reduced tumour burden compared to solvent controls (**Fig. 17**). This reduction was significant already after 7 days of treatment in NCCIT (**Fig. 17 A-C**) and only 4 days of treatment in NT2/D1 xenografts (**Fig. 17 D-F**).

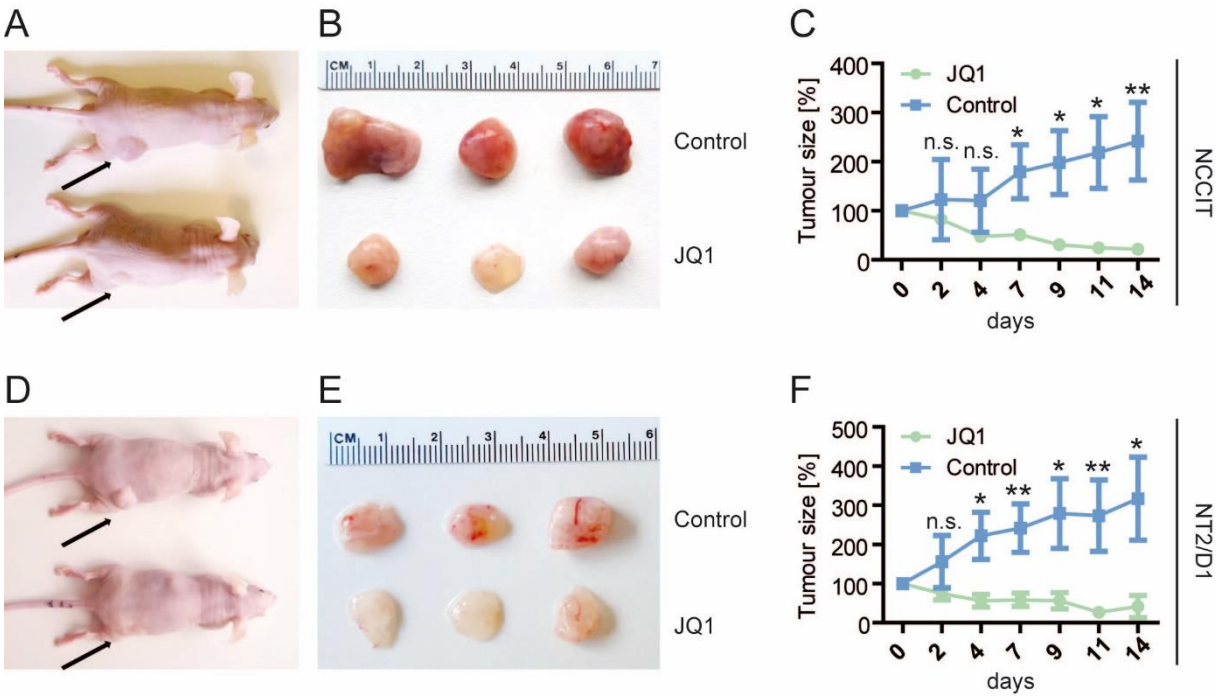

Figure 17: Tumour growth of TGCT xenografts treated with JQ1. Modified from [2]
Tumour size of NCCIT (**A-C**) and NT2/D1 (**D-F**) xenografts treated with JQ1 compared to xenografts treated with solvent control (i.p. injection, 5 days / week for two weeks).

A reduction in tumour growth was also indicated by a significant reduction of Ki67+ tumour cells in NCCIT ($p = 0.026$) and NT2/D1 ($p = 0.0002$) tumours, as determined by immunohistochemical staining (**Fig. 18 A**). Ki67 is a marker of proliferative active cells, thus a relative reduction in the Ki67+ cell population shows the growth-inhibitory

effects of JQ1 in TGCT tumours. I noted further the reduction of blood vessel invagination in JQ1 treated tumours (**Fig. 17**). In order to quantify this difference, NCCIT tumours were additionally stained for the endothelial marker CD31. In line with our observations I measured a significant reduction of CD31+ cells in JQ1 treated tumour samples (p = 0.018) (**Fig. 18 B**). Thus, JQ1 does not only significantly inhibit TGCT tumour growth, but also blood vessel formation within these tumours.

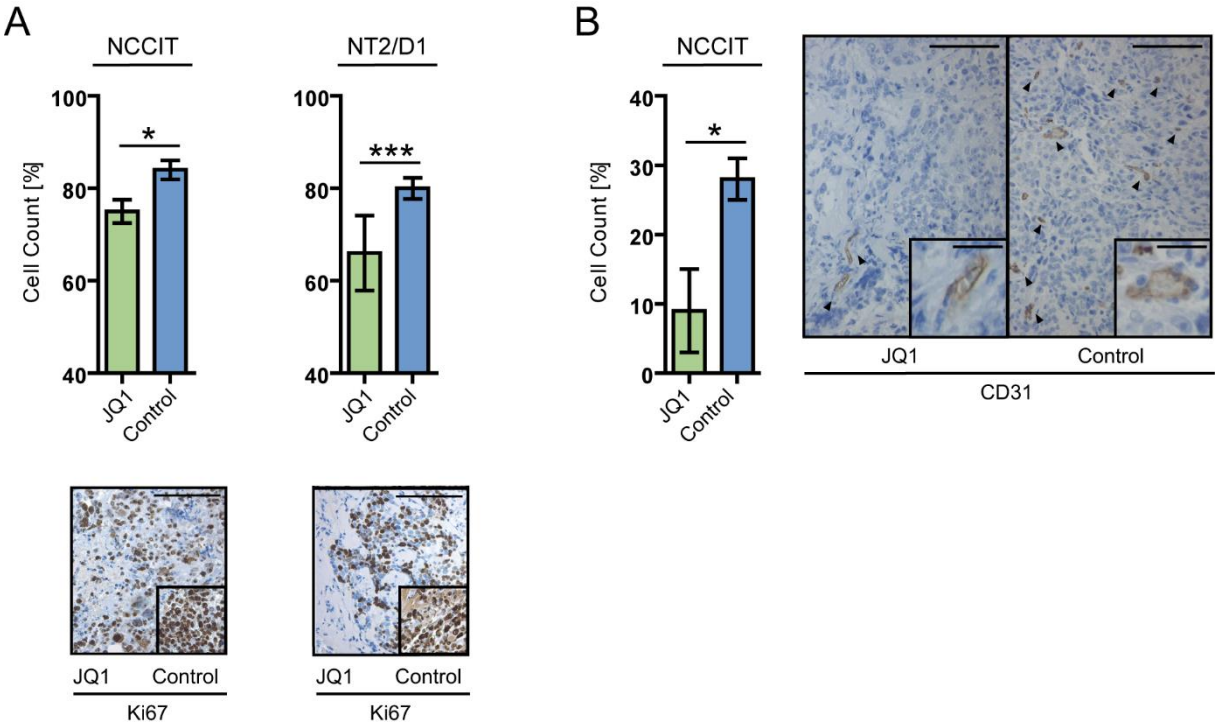

Figure 18: Ki67 and CD31 staining of TGCT xenografts treated with JQ1. Modified from [2]
Ki67 staining of NCCIT and NT2/D1 xenografts treated with JQ1 or solvent control (**A**) and CD31 staining of NCCIT xenografts treated with JQ1 or solvent control (**B**) (i.p. injection, 5 days / week for two weeks). Scale = 100 µm. Errors bars indicate standard deviation from the mean. Significance was calculated by student's t-test.

3.7. Combination therapy with JQ1 and romidepsin in TGCT xenografts

I then proceeded to analyse the efficacy of a combination therapy with JQ1 and romidepsin in NCCIT and NT2/D1 xenografts. For this, cell lines were again injected into the flank of nude mice and after two weeks of tumour growth mice were injected i.p. with drug or solvent control. Similar to JQ1-treated mice, mice treated with JQ1 (50 mg / kg) + romidepsin (0.5 mg / kg) presented reduced tumour burden compared to

solvent controls (**Fig. 19 A-D**). Interestingly, JQ1 + romidepsin was only administered 3 days / week, while JQ1 alone was administered 5 days / week. Thus, fewer applications of combination therapy were sufficient to achieve a similar therapeutic outcome compared to JQ1 alone. The reduction of tumour growth under combination therapy was significant already after 2 days of treatment in NCCIT (**Fig. 19 A-B**) and NT2/D1 xenografts (**Fig. 19 C-D**). In line, the amount of Ki67+ cells was significantly ($p = 0.003$) reduced in NCCIT xenografts (**Fig. 19 E**) and, although not significant, markedly reduced in NT2/D1 xenografts (**Fig. 19 F**). These results indicate that TGCT patients may benefit from a combination therapy with JQ1 and romidepsin, since the combined administration of both substances allows for a less frequent application scheme and lower doses.

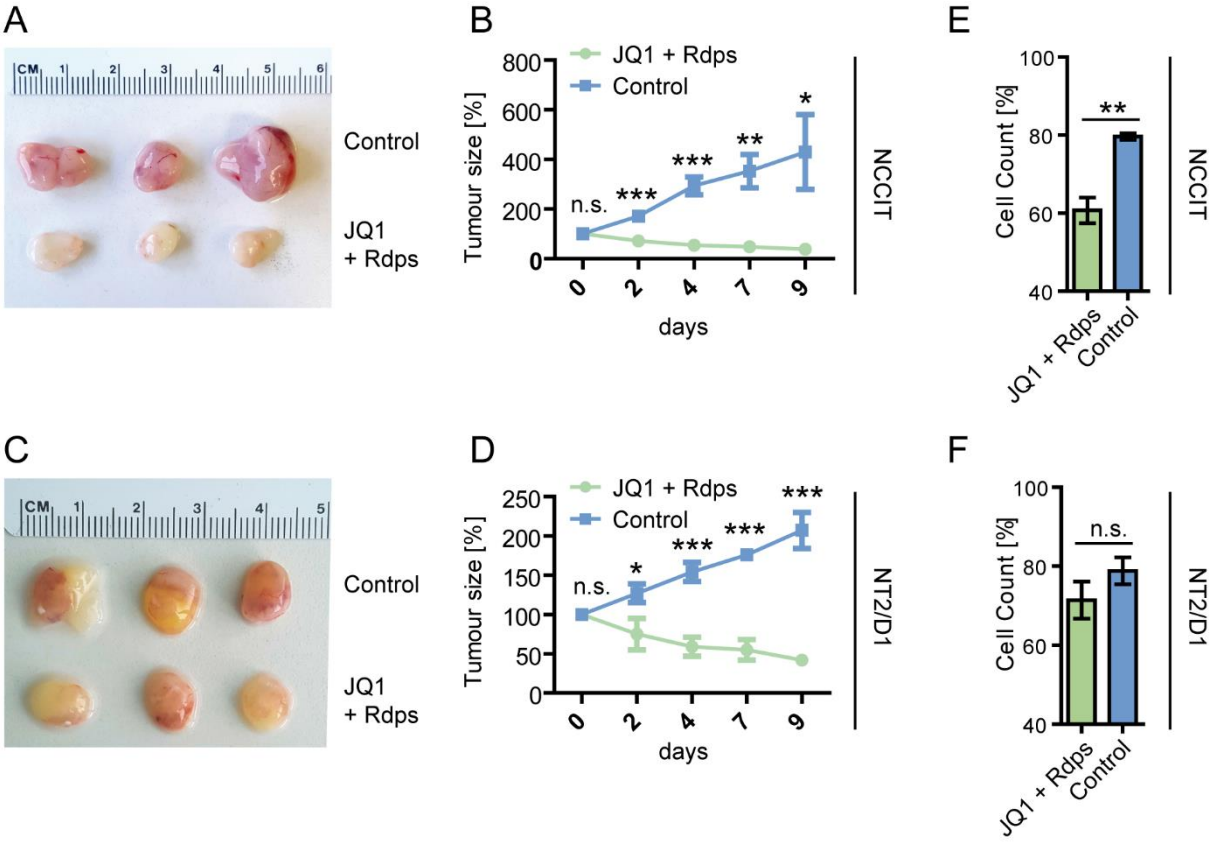

Figure 19: Tumour growth of TGCT xenografts treated with JQ1 + romidepsin. Modified from [2] Tumour size of NCCIT (**A, B**) and NT2/D1 (**C, D**) xenografts treated with JQ1 + romidepsin (JQ1 + Rdps) compared to xenografts treated with solvent control (i.p. injection, 3 days / week for 10 days). Ki67 staining of NCCIT (**E**) and NT2/D1 (**F**) xenografts treated with JQ1 + romidepsin (JQ1 + Rdps) compared to xenografts treated with solvent control. Errors bars indicate standard deviation from the mean. Significance was calculated by student's t-test.

4. Discussion I

Since the development of the first BET inhibitors JQ1 (2011) and I-BET (2010) [114, 115], a multitude of studies have shown the therapeutic effects of these epigenetic compounds in cancer therapy [79, 93, 116-120]. Due to their small-molecule characteristics, both substances show high bioavailability even in difficult-to-penetrate tissues such as brain and testis [79, 114, 121]. Initially, JQ1 was discussed as male contraceptive, due to its inhibitory effect on the testis-specific BET member BRDT [122, 123]. JQ1-mediated inhibition of BRDT led to a reversible contraceptive effect in mice, by completely inhibiting spermatogenesis during course of treatment [122, 123]. However, further studies focussed on the role of JQ1 as cancer therapeutic, probably owing to the fact that JQ1 does not only inhibit the testis-specific BET member BRDT, but also BRD2, BRD3 and BRD4, which are ubiquitously expressed among different tissues of the human body.

Previously, no study had described the effects of JQ1 on testicular cancer, or more precisely, on type II TGCTs. Therefore, I analysed the effects of JQ1 in both TGCT cell lines and TGCT xenografts and compared it to the effects of JQ1 on somatic control cells (fibroblasts and Sertoli cells). JQ1 treatment led to G0/G1 growth arrest and apoptosis in both cisplatin-sensitive, as well as cisplatin-resistant TGCT cell lines (**Fig. 20**) [1]. Cytotoxicity of JQ1 treatment in TGCT cells increased in a time- and dose-dependent manner. In both seminoma and EC cells induction of the DNA damage and stress response genes *GADD45B*, *TSC22D1*, *TXNIP*, *RHOB*, *ATF3*, *JUN* and *ID2* was observed (**Fig. 20**) [1]. Although not formally proven, induction of these genes may relate to the JQ1-mediated cell cycle arrest and apoptosis seen in TGCT cells.

Interestingly, previous studies have shown the transcriptional activation of the oncogene *MYC* via BRD4-mediated pTEFb activation in different cancer types, and further *MYC* downregulation following BRD4 inhibition by JQ1 [112, 124-126]. In some cancer types JQ1-mediated downregulation of *MYC* was even responsible for the cytotoxicity of BET inhibition [93, 112]. However, other studies reported JQ1-mediated cytotoxicity in cancer cells independent of MYC levels [94, 127]. In this study downregulation of the oncogene *MYC* was not observed in TGCT cells on mRNA level. Only on protein level MYC was downregulated in seminoma, but not EC cells. Since seminoma cells, however, were in general less sensitive to JQ1 treatment compared

to EC cells, downregulation of MYC can be excluded as primary cause of JQ1-mediated cytotoxicity in TGCT cells.

One of the main observations of this study was the strong upregulation of the differentiation marker *HAND1* in both seminoma and EC cells following JQ1 treatment and the downregulation of pluripotency-associated genes (such as *UTF1*, *THY1*, *LIN28, ZSCAN10, DPPA4*) (**Fig. 20**) [1, 2]. Interestingly, this effect was even more dramatic in EC cells only, which additionally showed robust downregulation of the key pluripotency markers *NANOG*, *POU5F1*, *GDF3* and *JARID2* [1, 2]. Whereas seminoma cells are restricted in their differentiation potential (a feature termed 'latent pluripotent'), EC cells are capable of differentiating into embryonic and extra-embryonic cell lineages. Therefore, EC cells not only showed upregulation of the differentiation marker *HAND1* following JQ1 treatment, but also many other genes involved in differentiation processes (mainly mesodermal differentiation). This suggests a possible role of BET bromodomain reader proteins in pluripotency regulation, at least for TGCT (in particular EC) cells [79]. In support of this hypothesis, in mouse ESCs expression of the pluripotency factor *NANOG* (which is also highly expressed TGCTs) is maintained and regulated by the JQ1 target protein BRD4 [90, 128]. Also, in both human and mouse ESCs, BRD4 occupies regulatory super-enhancer regions of *POU5F1* and *PRDM14* stem cell genes, which are similarly important for TGCT cell identity and pluripotency [129].

It is tempting to speculate that BRD4 has a similar role in maintaining pluripotency and stem cell identity in EC cells, which share many of the characteristics of ESCs. Also, sensitivity of TGCT cells to JQ1 treatment correlates with the downregulation of pluripotency and induction of differentiation, since pluripotent EC cell lines (such as NCCIT) show higher sensitivity to JQ1 treatment than the nullipotent EC line 2102EP and the latent pluripotent seminoma cell line TCam-2. Together, this suggests a possible link between TGCT sensitivity towards JQ1 treatment and their ability to differentiate.

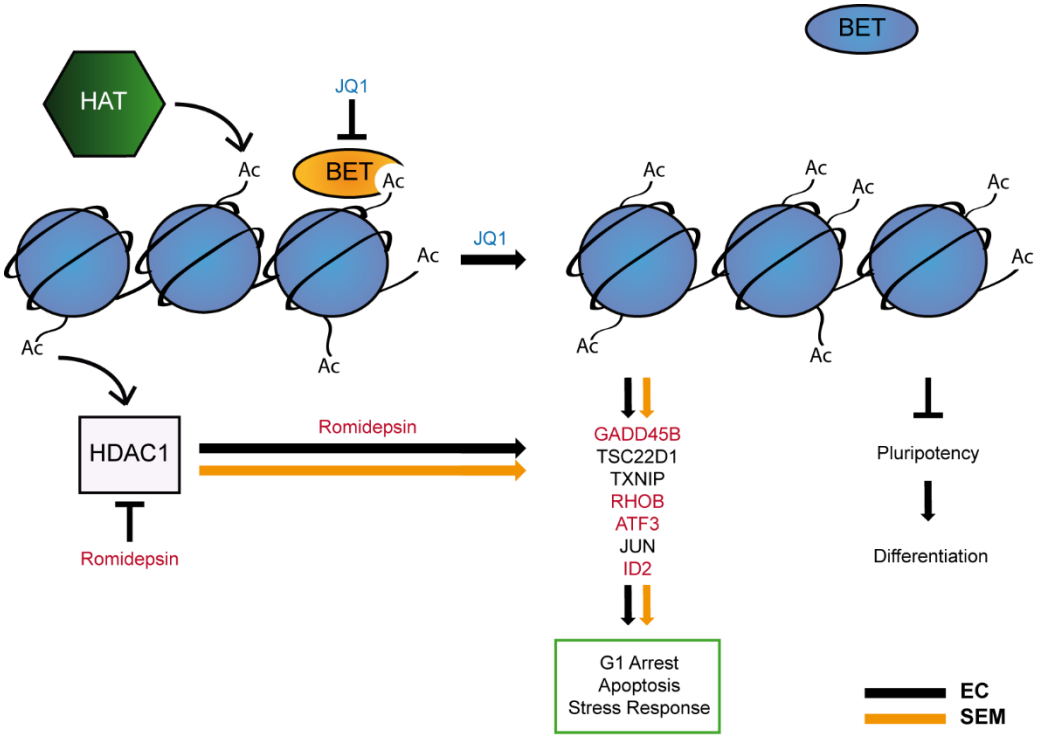

Figure 20: Effects of JQ1 and romidepsin treatment in TGCT cells. Modified from [2].
Schematic showing the molecular effects of romidepsin and JQ1 treatment in seminoma (SEM) and EC cells.

Next to the observed effects of JQ1 treatment on cell stress and pluripotency levels of TGCT cells, *in vivo* xenograft studies showed a reduced blood vessel formation in JQ1 treated tumours (**Fig. 20**). Suppression of angiogenesis in response to JQ1 treatment was similarly reported for models of childhood sarcoma, breast cancer as well as non-cancerous HUVEC (Human umbilical vein endothelial cells) [118, 130, 131]. In these cell types, reduction of blood vessel formation resulted from suppression of VEGF-driven angiogenesis [118, 130, 131]. Downregulation of *VEGFB* was also noted following JQ1 treatment in both seminoma and EC cells [1], thus offering a plausible explanation for the loss of tumour vascularization in TGCT xenografts.

Altogether, the presented data highlight JQ1 as possible therapeutic option for TGCT (ECs in particular). A few studies have additionally reported a synergistic effect of BET inhibition and HDAC inhibition in different cancer models (such as lymphoma, pancreatic ductal adenocarcinoma, breast cancer) [79, 95, 98, 132]. While testing the downstream molecular effects of JQ1 on TGCT cell lines I also noted a strong overlap of differentially expressed genes in TGCT cells following JQ1 and romidepsin

treatment [1]. Further experiments demonstrated an additive effect of JQ1- and romidepsin- mediated cytotoxicity in TGCT cells *in vitro*. The combination (JQ1 + romidepsin) treatment of TGCT xenografts further confirmed these findings, since combination therapy allowed for lower doses and a less-frequent application of both substances compared to single-drug application [2]. It is still not known, however, why HDAC inhibitors and BET inhibitors show synergy effects, since both drugs have a very distinct mode of action: While HDAC inhibition results in histone hyperacetylation and euchromatin formation, BET inhibition prevents the 'reading' of the histone code and may thereby modulate gene transcription [2]. Borbely *et al*. and Mazur *et al.* have identified the stress sensors *USP17* and *CDKN1C* as possible common mediators of BETi and HDACi-induced cytotoxicity, respectively [2, 79, 98, 132]. Thus, the cellular stress response induced by both substances may explain the synergy of combination therapy. In theory, different modes of action may apply for different cancer types. Therefore, future studies would be necessary to evaluate the molecular background of a combination therapy employing BET and HDAC inhibitors in TGCT cells in more detail.

Altogether, I propose JQ1 in combination with romidepsin, as a potential therapeutic option for TGCTs. While JQ1 was one of the first lead compounds presented in the field of BET inhibitors, several next-generation BET inhibitors (such as ABBV-075, BAY1238097, BI 894999) have now been developed, which have already reached clinical trials [79, 133-135]. Especially BI 894999 is a highly potent BET inhibitor, demonstrating an IC50 of 5 and 41 nM for BRD4-BD1 and BRD4-BD2 bromodomains, respectively [133]. In comparison, JQ1 had a considerably higher IC50 of 77 and 22 nM for BRD4-BD1 and BRD4-BD2 bromodomains, respectively [121]. It is structural improvements like these that may positively influence drug specificity and sensitivity levels, and thereby also minimize drug-associated adverse events. Clinical trials need to explore the pharmacokinetic profile of these compounds in more detail. While I believe that the use of these drugs for stage I-II TGCTs is highly unlikely, since standard therapy regimens already result in complete remission in most cases, epigenetic drugs may present an alternative strategy to treat late-stage or cisplatin-resistant TGCTs [79].

Parts of this chapter have been published in:

The bromodomain inhibitor JQ1 triggers growth arrest and apoptosis in testicular germ cell tumours in vitro and in vivo
Jostes S, Nettersheim D, Fellermeyer M, Schneider S, Hafezi F, Honecker F, Schumacher V, Geyer M, Kristiansen G, Schorle H.
J Cell Mol Med. 2016 Dec 27

Parts of this chapter have been discussed in:

Epigenetic drugs and their molecular targets in testicular germ cell tumours
Jostes S, Nettersheim D, Schorle H.
Nature Reviews Urology. 2019 Feb 14

5. Results II

5.1. Introduction

The plasticity of seminoma and embryonal carcinoma cells has been described in various studies [60, 73, 75, 136]. While it was a longstanding belief that seminomas are not able to differentiate and adopt other cell fates, our group was able to show in 2011 that in presence of FGF4, heparin and TGFβ seminomas differentiate into mixed non-seminoma cell fate *in vitro* [73]. Additionally, it was demonstrated that seminoma cells transdifferentiate into an EC-like cell fate after xenotransplantation into the flank of nude mice [75]. Inhibition of BMP signalling is an initial driver of this process and activates NODAL signalling, which initiates the downregulation of SOX17, as well as the upregulation of SOX2 and other stem cell markers [75]. Collectively, these publications show that seminomas and EC fates are plastic, dependent on the surrounding microenvironment and the associated signalling cues. Regarding the described plasticity, it is surprising that seminomas and ECs are so well-discriminated by their exclusive expression of SOX2 (EC) and SOX17 (seminoma). It is generally accepted that the role of SOX2 in EC cells is similar to the role of SOX2 in ESCs, which is being a key determinant of pluripotency and stem cell fate. In seminomas, however, knowledge about the role of SOX17 is lacking. Thus, I was interested in whether SOX17 may have similar function in seminomas as SOX2 in ECs and whether both factors regulate a common set of downstream target genes.

5.2. SOX17 (seminoma) and SOX2 (embryonal carcinoma) partner with OCT4, but not NANOG

In general, SOX factors have weak DNA binding specificity [137]. Higher specificity, however, is achieved by partnering with other factors, such as POU transcription factors [137]. In ESCs SOX17 partners with OCT4 to bind to the compressed motif (CATTGTATGCAAAT-like sequence), thereby driving endodermal genes [70]. By co-immunoprecipitation I confirmed interaction of SOX17 and OCT4 in seminoma cells (TCam-2) (**Fig. 21**), which was previously demonstrated by us [60]. SOX2 partners with the POU transcription factor OCT4 to bind to the canonical motif (CATTGT**C**ATGCAAAT-like sequence) in ESCs, thereby driving pluripotency genes

[70]. This pluripotency circuitry is further supported by SOX2-OCT4 interaction with the stem cell factor NANOG [138]. A similar interaction of SOX2, OCT4 and NANOG was postulated to maintain EC pluripotency. By co-immunoprecipitation I verified interaction of SOX2 with OCT4 in the EC line 2102EP, while I could not determine direct interaction with NANOG protein (**Fig. 21**).

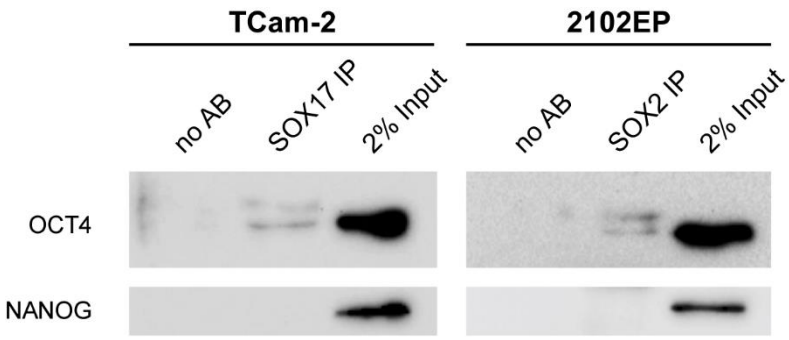

Figure 21: SOX17 and SOX2 interact with OCT4, but not NANOG
Co-immunoprecipitation of OCT4 and NANOG with SOX17 in TCam-2 cells and with SOX2 in 2102EP cells. Immunoprecipitation with no antibody (no AB) served as negative control. 2% Input (= 20 µg protein lysate) served as positive control.

Alike SOX2, SOX17 did not interact with the pluripotency factor NANOG (**Fig. 21**). Collectively, this shows that SOX2 and SOX17 partner with OCT4 and can, as a protein complex, regulate downstream target genes in EC and seminoma cells. However, neither SOX2 nor SOX17 do bind to / partner with NANOG, like it was described for the SOX2-OCT4-NANOG regulatory network in ESCs [138]. Thus far, however, we cannot exclude that NANOG regulates similar genes as SOX2-OCT4 or SOX17-OCT4 by binding to nearby DNA binding motifs without a direct SOX2-NANOG and SOX17-NANOG interaction.

5.3. SOX17 and SOX2 bind to the regulatory regions of pluripotency genes in TGCT cells

In order to determine the role of SOX17 in seminoma cells and compare it to the role of SOX2 in EC cells, I proceeded by analysing genome-wide SOX17 / SOX2 DNA occupancy in TCam-2 and 2102EP cells, respectively. First, I confirmed suitability of

the SOX17 antibody for chromatin immunoprecipiation (ChIP). For this, the SOX17 ChIP sample was loaded on a 12% SDS gel and SOX17 protein was detected by Western blot analysis. I verified presence of SOX17 protein in the SOX17 ChIP sample, as well as in the 2% input control and in TCam-2 whole protein lysate (**Fig. 22 A**) [101]. Expectedly, SOX17 was not detected in whole protein lysate of EC lines 2102EP, NT2/D1 and NCCIT (**Fig. 22 A**). A weak signal for SOX17 protein, however, was detected in the goat-IgG negative control (**Fig. 22 A**), indicating a low unspecific background signal for the IgG ChIP sample.

Next, suitability of the SOX2 antibody for ChIP was confirmed (**Fig. 22 B**) [101]. SOX2 protein could be detected in the SOX2 ChIP sample, as well as in the 2% input control and whole protein lysates of EC lines 2102EP, NT2/D1 and NCCIT (**Fig. 22 B**). As expected, SOX2 protein was absent in the TCam-2 whole protein lysate and the rabbit-IgG negative control. Notably, the antibody used for SOX2 detection in the Western blot was different from the SOX2 antibody used for ChIP-seq. This minimizes the possibility that the ChIP-seq antibody binds to an unspecific product, which is not SOX2. This experiment was performed together with Martin Fellermeyer during his Bachelor Thesis in 2016 [101].

It was previously hypothesized by our group that in seminoma cells SOX17 takes over a similar role as SOX2 in EC cells, which is the maintenance of pluripotency. We hypothesized that SOX17 binds to canonical (SOX2/OCT4) motifs within the regulatory regions of pluripotency genes. This is in contrast to ESCs where SOX17 activates endodermal genes via the compressed (SOX17/OCT4) motif. Therefore, I tested whether SOX17 is enriched at previously described canonical (SOX2/OCT4) binding motifs [3, 99, 100, 102, 139]. I detected enrichment of SOX17 at the canonical (SOX2/OCT4) binding sites within *SOX2*, *NANOG*, *DPPA4*, *LIN28A* and *PRDM14* regulatory regions (**Fig. 23**), strongly suggesting that in seminoma cells SOX17 regulates pluripotency genes via canonical (SOX2/OCT4) binding sites.

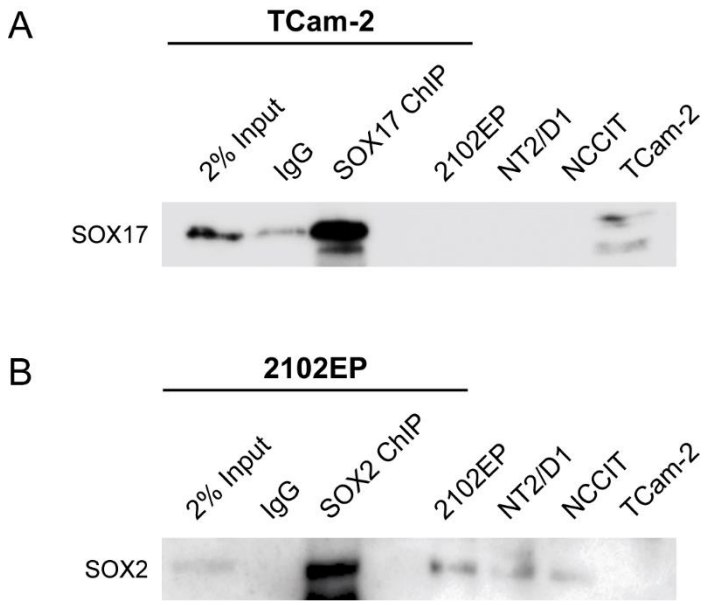

Figure 22: Validation of ChIP-grade antibodies. Modified from [101]

(A) Digested and crosslinked chromatin of TCam-2 cells was immunoprecipitated using a negative control goat IgG antibody or the ChIP-grade SOX17 antibody. 2% Input represents 2% of the TCam-2 chromatin fraction. Protein lysates of 2102EP, NT2/D1 and NCCIT served as negative control. TCam-2 protein lysate served as positive control.

(B) Digested and crosslinked chromatin of 2102EP cells was immunoprecipitated using a negative control rabbit IgG antibody (IgG) or the ChIP-grade SOX2 antibody. 2% Input represents 2% of the 2102EP chromatin fraction. Protein lysates of 2102EP, NT2/D1 and NCCIT served as positive control. TCam-2 protein lysate served as negative control.

SOX17 enrichment was stronger for those genes that are highly expressed in TCam-2 cells (*NANOG*, *LIN28A*, *DPPA4, PRDM14*) (**Fig. 23** and **24**), while there was no enrichment of SOX17 for *LEFTY2* detected (**Fig. 23**). *LEFTY2* is exclusively expressed in EC cells (**Fig. 24**). Additionally, I determined whether SOX17 was enriched at a compressed (SOX17/OCT4) binding site approximately 900 bp upstream of the TSS of *PRDM1* [101] (**Fig. 23**, red label), which is highly expressed in seminoma and TCam-2 cells (**Fig. 24**). Notably, this compressed-like *PRDM1* binding site (CATTGTATGCCATC) was manually assessed by screening for the compressed motif within the *PRDM1* promoter [101]. Indeed, SOX17 was strongly enriched at the compressed motif within the *PRDM1* promoter (**Fig. 23**) This is in line with a previous publication of Irie *et al.*, showing that SOX17 acts upstream of *PRDM1* in maintaining PGC fate [6]. In contrast, previously published SOX17 ChIP-seq data in differentiated

mesoderm, endoderm or mesendoderm-like lineages showed no enrichment of SOX17 within the *PRDM1* promoter region [140]. Only a distal regulatory region -15300 bp upstream of *PRDM1* (-of TSS) was detected, which may not have functional relevance [140]. This suggests that SOX17 binding to the *PRDM1* promoter is a unique feature of seminoma cells or PGCs.

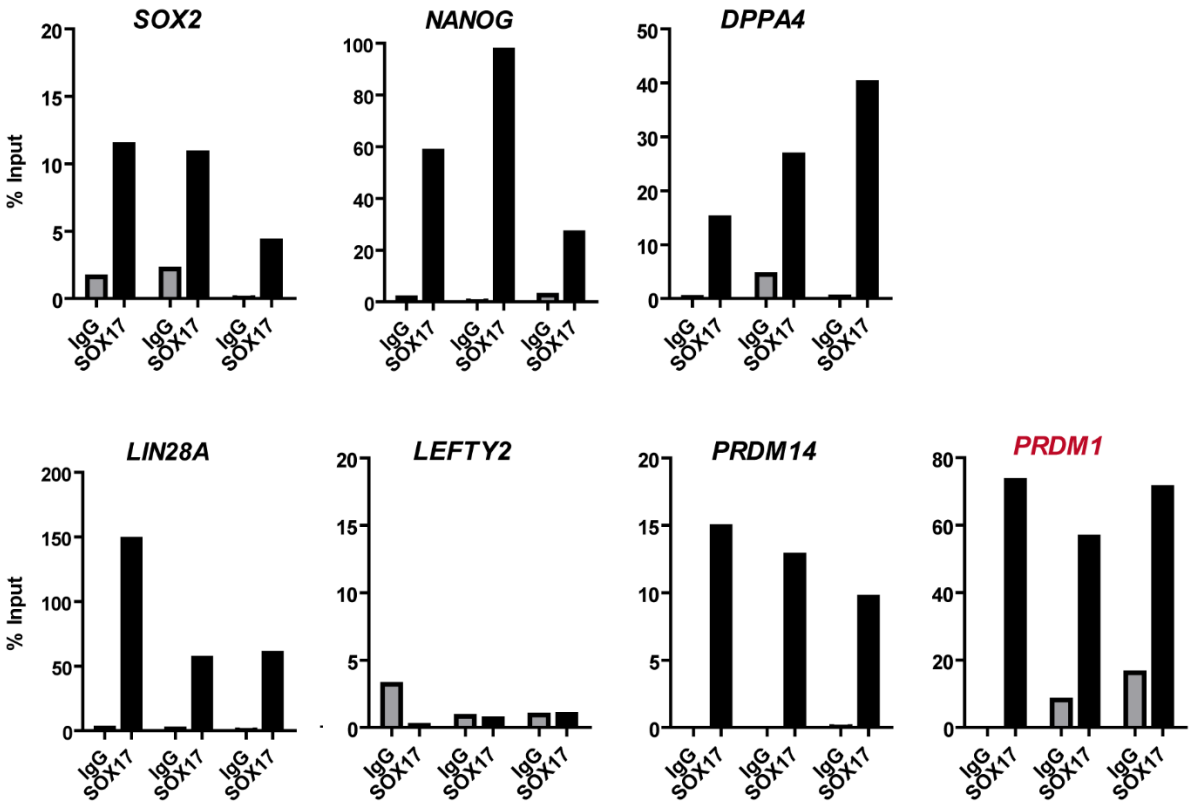

Figure 23: SOX17 binds pluripotency genes in TCam-2 cells
qPCR of known canonical binding motifs in the regulatory regions of *SOX2*, *NANOG*, *DPPA4*, *LIN28A*, *LEFTY2* and *PRDM14*, and a putative compressed binding motif in the regulatory region of *PRDM1* in the SOX17 ChIP. Measurements were performed of three independent experiments. Goat IgG-ChIP served as negative control.

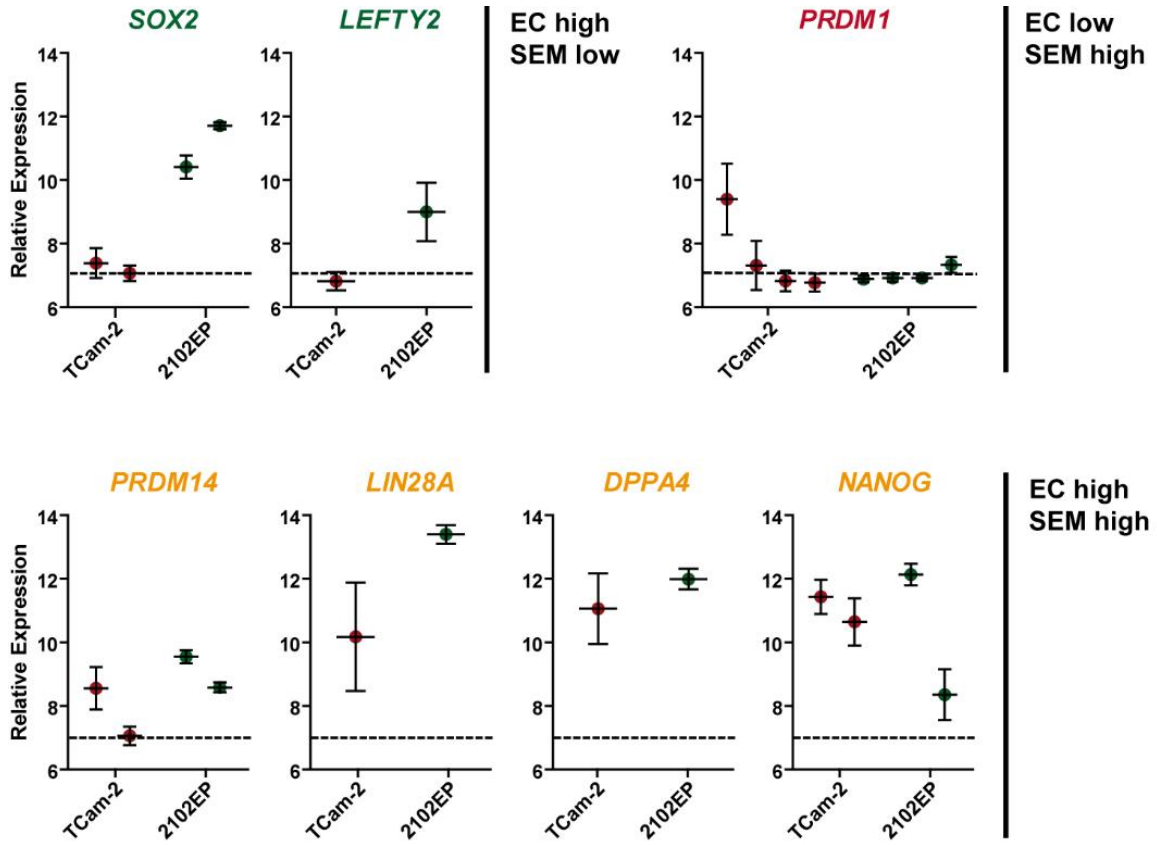

Figure 24: Expression of pluripotency genes in TCam-2 and 2102EP cells
mRNA expression of pluripotency genes in TCam-2 (n=5) and 2102EP (n=5) cells, determined by previously published microarray data [2, 3]. Different datapoints represent different mRNA probes for the respective genes. Genes were categorized according to their expression levels in EC and SEM (seminoma). The dashed line represents the expression threshold.

As control, I then determined enrichment of SOX2 for canonical (SOX2/OCT4) binding motifs (**Fig. 25**). In line with the role of SOX2 as regulator of pluripotency, I detected strong enrichment of SOX2 in the regulatory regions of *SOX2*, *NANOG*, *DPPA4*, *LIN28A, LEFTY2* and *PRDM14* (**Fig. 25**). Notably, all of these genes are also highly expressed in 2102EP cells (**Fig. 24**), suggesting that SOX2 transactivates these genes. Next, I showed that there was no enrichment of SOX2 at the compressed (SOX17/OCT4) binding site within the *PRDM1* regulatory region.

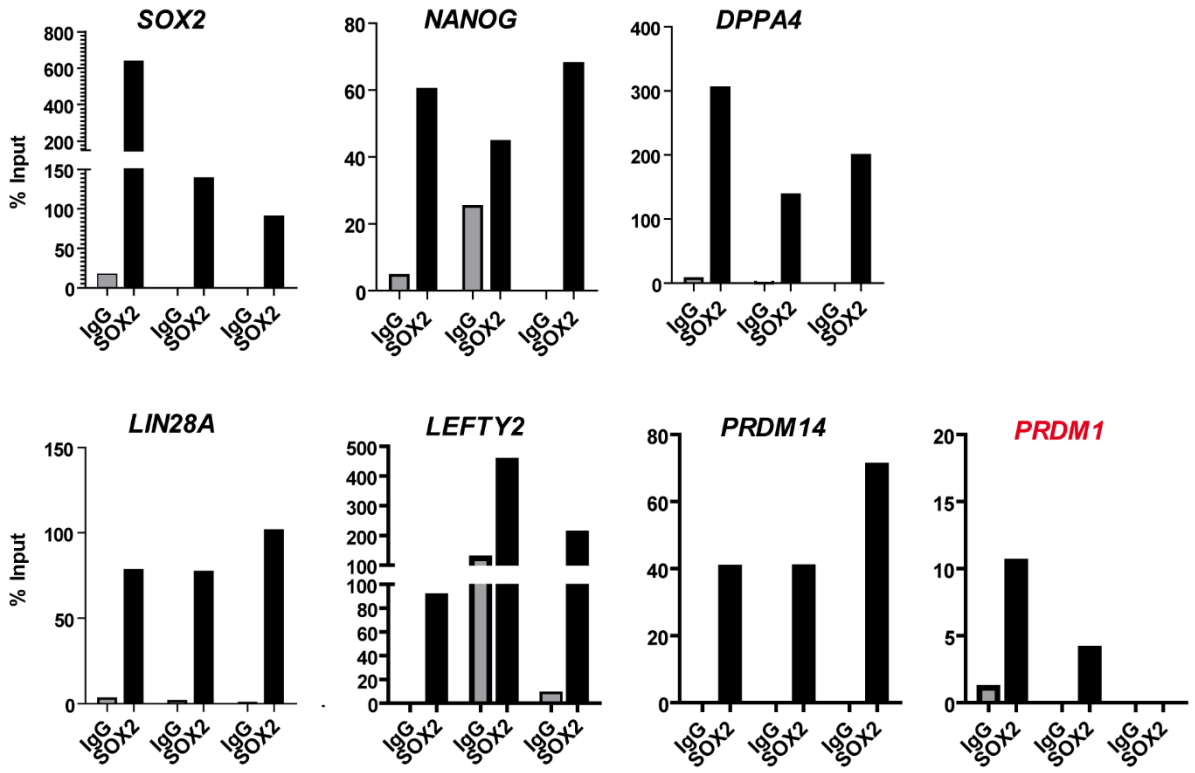

Figure 25: SOX2 binds pluripotency genes in 2102EP cells
qPCR of known canonical binding motifs in the regulatory regions of *SOX2*, *NANOG*, *DPPA4*, *LIN28A*, *LEFTY2* and *PRDM14*, and a putative compressed binding motif in the regulatory region of *PRDM1* in the SOX2 ChIP. Measurements were performed of three independent experiments. Rabbit IgG-ChIP served as negative control.

Together, the data demonstrate that in EC cells SOX2 uses some of the canonical SOX2-OCT4 binding sites described in ESCs. Therefore, in EC cells SOX2 has a similar role like SOX2 in ESCs, which is the maintenance of pluripotency by interacting with OCT4 to regulate downstream target genes. Further, SOX2 seems to regulate its own expression by binding to the canonical motif within the SOX2 regulatory region, thus creating an auto-regulatory feedback loop (**Fig. 25**). Similarly, SOX17 in seminoma cells, at least in part, binds to canonical (SOX2/OCT4) binding motifs. Although weak binding of the SOX17-OCT4 complex to canonical (SOX2/OCT4) motifs was already described in biochemical assays [141], there was no evidence whether this binding may have functional consequences in some cells or simply be a bystander effect. Some of the analysed genes showing SOX17 binding are also highly expressed in these cells (*NANOG*, *LIN28A*, *DPPA4*), making a regulatory function of SOX17 for

these genes in seminoma cells possible. However, it seems that other genes like *PRDM1* are also regulated via SOX17 binding to its compressed motifs in seminoma cells.

5.4. The majority of regions bound by SOX17 in seminoma cells contains the compressed motif and is found near transcriptional start sites

In seminoma cells I could demonstrate that SOX17 binds to canonical (SOX2/OCT4) and compressed (SOX17/OCT4) binding motifs of pluripotency and germ-cell related genes. In 2102EP cells SOX2 binds to canonical SOX2/OCT4 motifs only. In order to analyse genome-wide binding occupancy of SOX17 and SOX2 in TGCT cells I next performed high-throughput ChIP-sequencing (ChIP-seq). For bioinformatic analysis only those peaks were considered significant that were present in the control group (Input or IgG) and in the SOX2/SOX17 IP and that were at least four times higher in the SOX2/SOX17 IP compared to the control group.

Analysis of the SOX17 ChIP-seq data revealed a total of 931 and 904 peaks in the SOX17 vs IgG and SOX17 vs Input dataset, respectively (**8.1**). The subsequent analyses were performed using the SOX17 vs IgG dataset. Analysis of peak count frequency showed that most SOX17 peaks are allocated directly upstream or downstream of the transcription start site (TSS) of genes (**Fig. 26 A**). Further, HOMER Motif analysis identified a total of 375 of 931 peaks (=40.28%) harbouring a SOX17 binding motif and 246 of 931 peaks (=26.24%) harbouring the compressed (SOX17/OCT4) binding motif (**Fig. 26 B-C**). Additionally, 355 of 931 peaks (=38.13%) contain the known SOX2 binding motif and 192 of 931 peaks (=20.62%) the known OCT4 binding motif (**Fig. 26 C**). Interestingly, 101 of 931 peaks (=10.85%) contain the described canonical (SOX2/OCT4) binding motif (**Fig. 26 C**). In line with the qPCR data this indicates that SOX17 binds, and possibly regulates genes via compressed (SOX17/OCT4) (26.24%), but also via canonical (SOX2/OCT4) (20.62%) binding sites. Interestingly, also TFAP2C (also known as AP2γ) and PRDM1 (also known as BLIMP1) motifs were found among top enriched binding motifs in SOX17-bound regions (368 of 931 peaks and 188 of 931 peaks) (**Fig. 26 C**).

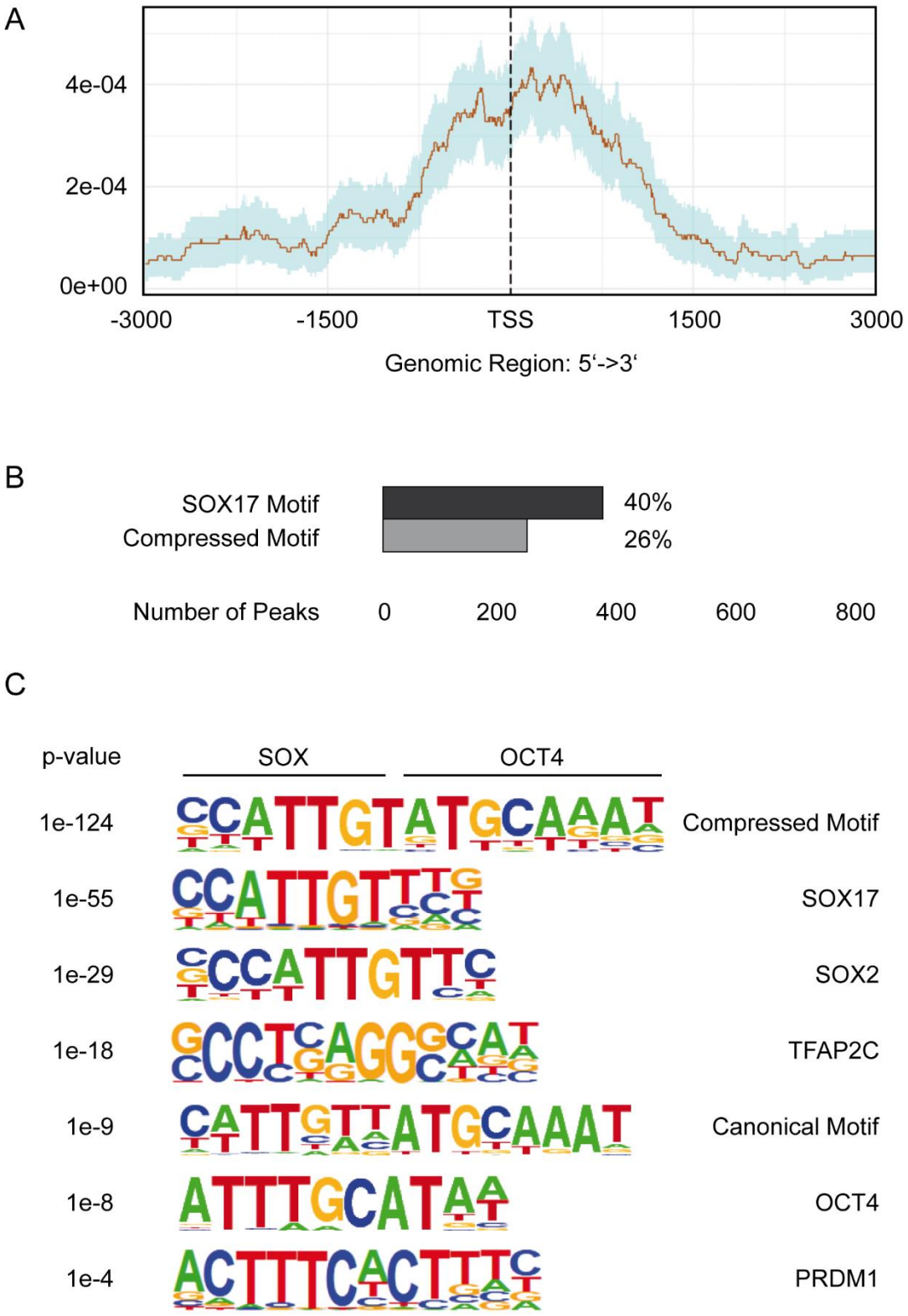

Figure 26: SOX17 occupies canonical and compressed binding sites in seminoma cells

(A) Peak Count Frequency of SOX17 ChIP peaks upstream and downstream of transcription start sites (TSS).

(B) Number and percentage of SOX17 ChIP peaks (SOX17 vs IgG) that harbour the SOX17 binding motif and the compressed SOX17/OCT4 binding motif.

(C) Homer motif analysis of known binding motifs enriched in SOX17 ChIP (SOX17 vs IgG).

Both transcription factors are highly expressed in PGCs and described as key specifiers of germ-cell fate along with SOX17 [8]. Overall, this reflects the germ-cell origin of TCam-2 cells. In PGCs PRDM1 and TFAP2C have been described to suppress somatic differentiation [8]. The fact that PRDM1 and TFAP2C binding sites are detected close to SOX17 peaks may indicate that some of those genes otherwise activated by SOX17 during endodermal differentiation are suppressed by binding of TFAP2C and PRDM1 in germ cell tumours.

In comparison, ChIP-seq data for SOX2 revealed a total of 3314 and 1259 peaks in the SOX2 vs IgG and SOX2 vs Input dataset, respectively (**8.1**). The subsequent analyses were performed using the SOX2 vs IgG control dataset. Analysis of peak count frequency showed that most SOX2 peaks cluster upstream of the transcription start site (TSS) of genes (**Fig. 27 A**). HOMER Motif analysis identified a total of 962 of 3314 peaks (=29,03%) harbouring a SOX2 binding motif and 419 of 3314 peaks (=12,64%) harbouring the canonical SOX2/OCT4 binding motif (**Fig. 27 B-C**). Additionally, 666 of 3314 peaks (=20.10%) contain the known OCT4 binding motif and 560 of 3314 (=16.90%) contain the known KLF4 binding motif (**Fig. 27 C**). This indicates that the genes, which are bound by SOX2 can also be bound and regulated by the pluripotency factors KLF4 and OCT4.

Altogether, these findings demonstrate that in seminoma cells SOX17 binds to canonical (SOX2/OCT4) motifs, similar to SOX2 in ECs. This way, both SOX17 (in seminoma) and SOX2 (in EC) can mediate the regulation of an overlapping set of downstream target genes, such as pluripotency genes *NANOG*, *DPPA4*, *LIN28A a*nd *PRDM14*. Surprisingly, however, many SOX17 peaks detected in TCam-2 cells also contain the compressed (SOX17/OCT4) motif. SOX17 binding to this motif is known to activate genes responsible for endodermal cell-fate decisions in ESCs. Further analysis will show whether the compressed (SOX17/OCT4) motifs bound by SOX17 in seminoma cells map to the regulatory regions of endodermal genes and whether this binding leads to an activation or a suppression of genes.

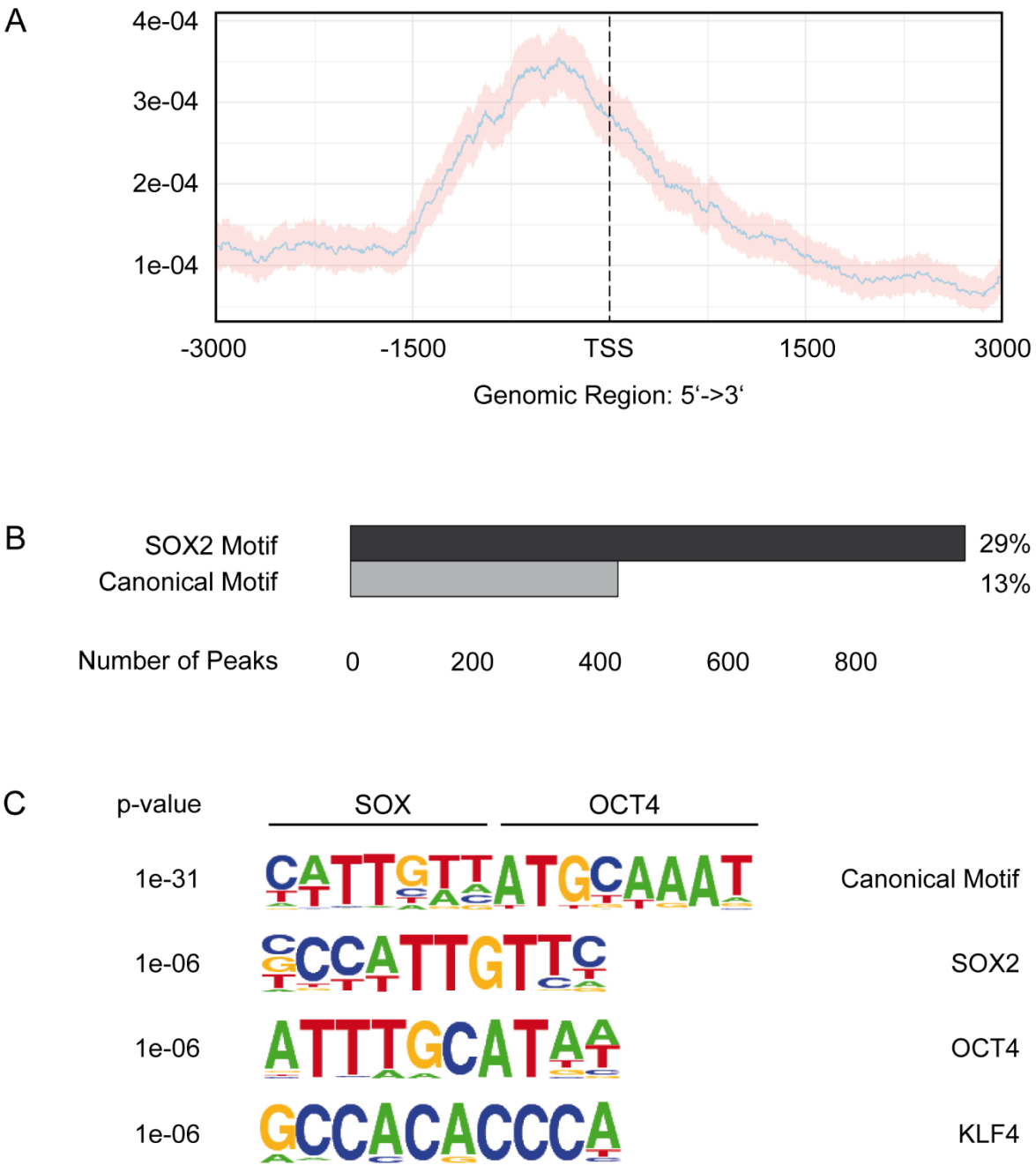

Figure 27: SOX2 occupies canonical binding sites in EC cells

(A) Peak Count Frequency of SOX2 ChIP peaks upstream and downstream of transcription start sites (TSS).

(B) Number and percentage of SOX2 ChIP peaks (SOX2 vs IgG) that harbour the SOX2 binding motif and the canonical SOX2/OCT4 binding motif.

(C) Homer motif analysis of known binding motifs enriched in SOX2 ChIP (SOX2 vs IgG).

5.5. In seminoma cells SOX17 binds to the regulatory regions of neuro-ectodermal genes, as well as pluripotency and germ-cell related genes

In order to see whether the SOX17 peaks obtained in TCam-2 correlate with pluripotency gene signatures or endodermal genes I performed gene set enrichment analysis (GSEA) using the Molecular Signature Database (MSigDB). Here, individual SOX17 peaks were first annotated to the genes with the nearest TSS. GSEA was then performed for the two ChIP-seq datasets SOX17 vs IgG and SOX17 vs Input. I detected a strong overlap of SOX17 peaks with neuronal signatures and genes associated with embryonic development or differentiation (**Table 7-8**, green labels). In line with the previous ChIP-qPCR data, however, the SOX17 peaks additionally show significant enrichment for stem cell-associated signatures, although less pronounced (**Table 7-8**, blue labels). In comparison, the same analysis on SOX2 datasets (SOX2 vs IgG, SOX2 vs Input) showed robust enrichment for different stem cell-associated and pluripotency-associated signatures (**Table 9-10,** blue labels), while enrichment for neuronal signatures was minor (**Table 9-10**, green labels).

Table 7: MSigDB GSEA of SOX17 targets in TCam-2 (normalized to IgG background)

TERM	logP
AACTTT_UNKNOWN	-27.36
GO_TISSUE_DEVELOPMENT	-26.47
GO_REGULATION_OF_MULTICELLULAR_ORGANISMAL_DEVELOPMENT	-22.92
GO_REGULATION_OF_NERVOUS_SYSTEM_DEVELOPMENT	-22.17
CTTTGT_V$LEF1_Q2	-20.95
GO_REGULATION_OF_CELL_DEVELOPMENT	-18.93
GO_EPITHELIUM_DEVELOPMENT	-18.46
V$HNF3B_01	-17.95
GGGAGGRR_V$MAZ_Q6	-17.71
GO_REGULATION_OF_NEURON_DIFFERENTIATION	-17.59
BENPORATH_SOX2_TARGETS	-17.53
AAAYWAACM_V$HFH4_01	-17.52
BENPORATH_OCT4_TARGETS	-17.25
GO_REGULATION_OF_NEURON_PROJECTION_DEVELOPMENT	-17.06
GO_TUBE_DEVELOPMENT	-17.05
TGGTGCT,MIR-29A,MIR-29B,MIR-29C	-17.01
GO_POSITIVE_REGULATION_OF_DEVELOPMENTAL_PROCESS	-16.77
GO_REGULATION_OF_CELL_PROJECTION_ORGANIZATION	-16.30
GO_NEUROGENESIS	-16.20
GO_REGULATION_OF_CELL_DIFFERENTIATION	-16.13

Table 8: MSigDB GSEA of SOX17 targets in TCam-2 (normalized to 2% input)

TERM	logP
AACTTT_UNKNOWN	-39.35
GOZGIT_ESR1_TARGETS_DN	-24.50
TTGTTT_V$FOXO4_01	-24.27
NIKOLSKY_BREAST_CANCER_8Q12_Q22_AMPLICON	-18.28
chr8q21	-16.82
YNGTTNNNATT_UNKNOWN	-16.12
V$S8_01	-15.70
V$IPF1_Q4	-15.55
CTTTGT_V$LEF1_Q2	-15.54
V$OCT1_04	-15.07
V$FOXO4_01	-14.92
CTTTGA_V$LEF1_Q2	-14.86
GO_NEUROGENESIS	-14.54
PLASARI_TGFB1_TARGETS_10HR_DN	-14.34
YTATTTTNR_V$MEF2_02	-14.11
AAAYWAACM_V$HFH4_01	-13.93
ACEVEDO_LIVER_CANCER_WITH_H3K27ME3_UP	-13.89
WGTTNNNNNAAA_UNKNOWN	-13.86
V$OCT1_07	-13.62
TGACATY_UNKNOWN	-13.20

Table 9: MSigDB GSEA of SOX2 targets in 2102EP (normalized to IgG background)

TERM ID	logP
Chr19p13	-75.26
Chr12q24	-36.97
PILON_KLF1_TARGETS_DN	-29.89
BENPORATH_ES_1	-28.60
BENPORATH_NANOG_TARGETS	-28.50
LASTOWSKA_NEUROBLASTOMA_COPY_NUMBER_DN	-22.14
GCCATNTTG_V$YY1_Q6	-21.10
BENPORATH_SOX2_TARGETS	-21.46
NIKOLSKY_BREAST_CANCER_17Q21_Q25_AMPLICON	-21.20
CTTTGT_V$LEF1_Q2	-21.14
KORKOLA_CORRELATED_WITH_POU5F1	-20.87
RAO_BOUND_BY_SALL4	-20.68
BHATTACHARYA_EMBRYONIC_STEM_CELL	-20.61
BENPORATH_NOS_TARGETS	-19.59
Chr20q11	-18.15
Chr12p13	-18.01
LASTOWSKA_NEUROBLASTOMA_COPY_NUMBER_UP	-17.83
BENPORATH_OCT4_TARGETS	-17.34
MARTENS_BOUND_BY_PML_RARA_FUSION	-17.30
BLUM_RESPONSE_TO_SALIRASIB_DN	-16.73

Table 10: MSigDB GSEA of SOX2 targets in 2102EP (normalized to 2% input)

TERM ID	logP
CTTTGT_V$LEF1_Q2	-19.84
BENPORATH_ES_1	-18.86
TTGTTT_V$FOXO4_01	-18.70
DACOSTA_UV_RESPONSE_VIA_ERCC3_DN	-18.61
AACTTT_UNKNOWN	-18.07
chr1p31	-15.79
GO_NEGATIVE_REGULATION_OF_NITROGEN_COMPOUND_METABOLIC_PROCESS	-15.28
chr3q26	-14.32
V$CDPCR3HD_01	-13.93
RAO_BOUND_BY_SALL4	-13.76
TAATTA_V$CHX10_01	-13.30
GO_NEUROGENESIS	-12.98
V$OCT1_04	-12.21
DACOSTA_UV_RESPONSE_VIA_ERCC3_COMMON_DN	-12.07
CTTTGTA,MIR-524	-12.04
WGTTNNNNNAAA_UNKNOWN	-12.00
V$HFH3_01	-11.75
GO_REGULATION_OF_NEURON_DIFFERENTIATION	-11.74
GO_REGULATION_OF_NERVOUS_SYSTEM_DEVELOPMENT	-11.54
V$POU3F2_02	-11.32

In order to see whether these genes are not only bound, but also expressed (and therefore transactivated by SOX17 and SOX2) in TCam-2 and 2102EP cells I performed a meta-analysis of previously published gene expression datasets from TCam-2 and 2102EP cells [1-3] and compared it to the SOX17 vs IgG and SOX2 vs IgG datasets, respectively. In TCam-2 cells pluripotency genes are bound by SOX17 (*NANOG, TFAP2C, POU5F1, LIN28B, ZIC3, KLF4, TRIM71, ZIC4*) (**Fig. 28**, highlighted in red). Of these only *NANOG* (peak score: 10.3) and *TFAP2C* (peak score: 6.44) are strongly enriched for SOX17 binding. With a peak score < 5 the remainder do not seem to be primary targets of SOX17 binding (**Table 11**). In contrast, 19 genes showed a SOX17 peak score > 10 and a gene expression > 8: *TUBB*, *AACS*, *BCL11B*, *ZHX2*, *COL23A1*, *CD9*, *BEND7*, *PSEN2*, *DCTD*, *NCBP2*, *GBAS*, *UBTD2*, *PSAP*, *ADAMTS1*, *RNF130*, *SLC39A10*, *NANOG*, *ZNF281*, *HABP4* (**Fig. 28**). The majority of these genes is linked to neuro-ectodermal development (*ZHX2*, *COL23A1*, *CD9*, *BEND7*, *PSEN2*, *GBAS*, *UBTD2*, *PSAP*, *ADAMTS1* and *ZNF281*). This suggests a role of SOX17 in regulating somatic genes (in addition to pluripotency genes) in TCam-2 cells, which is in line with the presented MiSigDB GSEA (compare **Table 7-8**). Next

to somatic genes, however, the pluripotency factor *NANOG* was also among genes bound by SOX17 and highly expressed in TCam-2 cells (**Fig. 28**, **Table 11**). Notably, *NANOG* seemed to be regulated by SOX17 via different binding sites including the canonical motif described before (260 bp upstream of TSS, **Fig. 23**) and the binding site identified in the SOX17 vs IgG dataset (4143 bp upstream of TSS, **Fig. 28**). Interestingly, both regions were also enriched for SOX2 binding in 2102EP cells, as well as one more region upstream (9264 bp) and three more regions downstream (1871 bp, 7801 bp, 37403 bp) of the *NANOG* TSS (**8.1**, SOX2 vs IgG dataset). This highlights *NANOG* as a common target gene of SOX2 and SOX17 in TGCT cells. In a previous publication, it was shown that siRNA-mediated knockdown of *NANOG* in TCam-2 cells induces mRNA expression of extraembryonic endoderm- and trophectoderm-associated differentiation markers (*GATA2, GATA4, GATA6*), but no changes in cell morphology were observed [142]. It was assumed that upregulation of *POU5F1 (OCT4)* and *SOX17* expression seen after *NANOG* knockdown prevented differentiation of TCam-2 cells [142]. Collectively, this shows a role of NANOG in supporting the pluripotency network of seminoma cells downstream of SOX17.

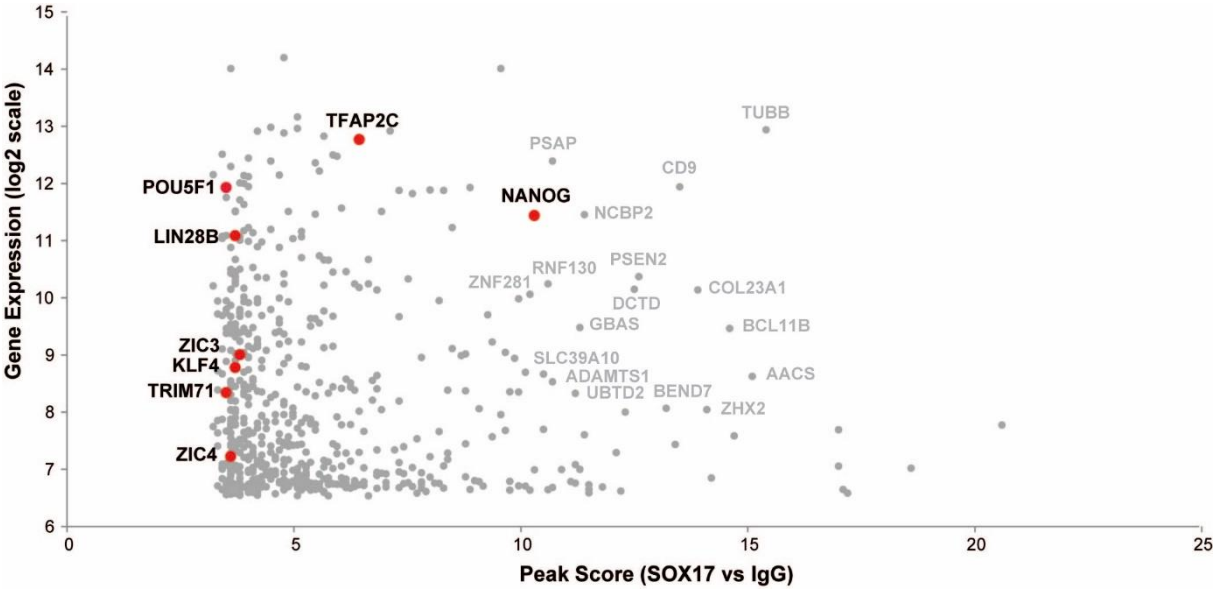

Figure 28: Scatterplot of TCam-2 gene expression data with SOX17 ChIP-seq peaks
Scatterplot of TCam-2 gene expression data (y-axis) and SOX17 ChIP-seq (SOX17 vs IgG) data (x-axis). Pluripotency genes are highlighted in red.

Table 11: Top 20 SOX17 (vs IgG)-peaks with gene expression > 8 in TCam-2

Gene Name	Peak Score	Gene Expression
TUBB	15.4	12.9
AACS	15.1	8.6
BCL11B	14.6	9.5
ZHX2	14.1	8.0
COL23A1	13.9	10.1
CD9	13.5	11.9
BEND7	13.2	8.1
PSEN2	12.6	10.4
DCTD	12.5	10.1
NCBP2	11.4	11.5
GBAS	11.3	9.5
UBTD2	11.2	8.3
PSAP	10.7	12.4
ADAMTS1	10.7	8.5
RNF130	10.6	10.2
SLC39A10	10.5	8.7
NANOG	10.3	11.4
ZNF281	10.2	10.1
HABP4	10.1	8.7
NFIB	9.95	10.0

Altogether I found opposing functions of SOX17 in regulating genes involved with pluripotency, but also differentiation in seminoma cells. In contrast, in ECs there is a clear correlation between the expression of pluripotency-associated genes (*GDF3, DPPA3, TRIM71, DPPA5, SALL4, PRDM14* and *NANOG*) and SOX2 binding (**Fig. 29**, **Table 12**). This finding confirms the role of SOX2 as a positive regulator of pluripotency in EC cells and nicely aligns with the previously generated GSEA (compare **Table 9-10**) and ChIP-qPCR data (compare **Fig. 25**). 21 genes showed a SOX2 peak score > 15 and a gene expression > 8: *LASP1*, *ETV6*, *LOC643770*, *NANOG*, *KPNA2*, *SLC2A3*, *DPP9*, *NDUFS7*, *COMMD7*, *RCC2*, *FAM60A*, *RAC1*, *EIF5A*, *VDAC1*, *UBE2D2*, *HMGN4*, *SLC2A14*, *BCAS4*, *DNAJB6*, *NACC1* and *ABT1* (**Fig. 29**). Most of these genes have a role in self-renewal of stem cells or cancer stem cells and therefore may be associated with cancer malignancy [143-149].

These data show that in EC cells SOX2 binds and activates different regulators of pluripotency (i.e. *NANOG*), similar to the role of SOX2 in ESCs. Interestingly, SOX17 may support pluripotency of seminoma cells also in part via transactivation of

pluripotency-associated genes, such as *NANOG*. The functional consequences of SOX17 for binding to genes with roles in neuronal differentiation and embryonic development, however, remain unclear. So far, a mechanism by which SOX17 acts as a repressor of genes has not been described. Therefore, SOX17 most likely binds and transactivates these genes.

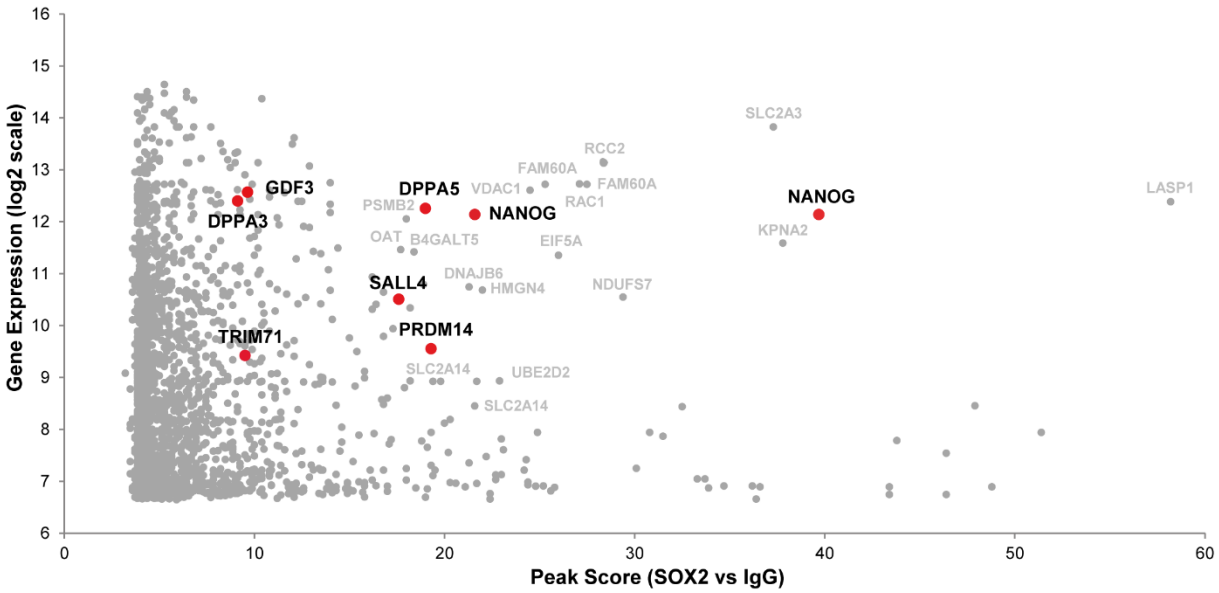

Figure 29: Scatterplot of 2102EP gene expression data with SOX2 ChIP-seq peaks
Scatterplot of 2102EP gene expression data (y-axis) and SOX2 ChIP-seq (SOX2 vs IgG) data (x-axis). Pluripotency genes are highlighted in red.

Table 12: Top 20 SOX2 (vs IgG)-peaks with gene expression > 8 in 2102EP

Gene Name	Peak Score	Gene Expression
LASP1	58.2	12.4
ETV6	47.9	8.5
NANOG	39.7	12.1
KPNA2	37.8	11.6
SLC2A3	37.3	13.9
DPP9	32.5	8.4
NDUFS7	30.8	10.9
COMMD7	29.4	10.5
RCC2	28.4	13.1
FAM60A	27.5	12.7
RAC1	27.1	12.7
EIF5A	26	11.3
FAM60A	25.3	12.7
VDAC1	24.5	12.6

UBE2D2	22.9	8.9
HMGN4	22	10.7
SLC2A14	21.7	8.9
NANOG	21.6	12.1
BCAS4	21.6	8.4
DNAJB6	21.3	10.7

5.6. In seminoma cells SOX17 regulates *TFAP2C* and *PRDM1* expression

The question remains, why seminoma cells keep a state of latent pluripotency, if the majority of genes bound by SOX17 has roles in neuronal differentiation and embryonic development. Similar to seminoma cells, human PGCs express TFAP2C, PRDM1 and SOX17 at high levels, which form a tripartite transcription factor network governing PGC cell fate [1] (**Fig. 1**). Importantly, TFAP2C and PRDM1 have roles in the suppression of somatic differentiation in PGCs [6]. I here showed that in seminoma cells SOX17 activates *PRDM1* and *TFAP2C* expression (**Fig. 23** and **28**). Although *PRDM1* was not detected as SOX17 target in the SOX17 vs IgG dataset, it was detected in the SOX17 vs Input dataset (**8.1**) and further binding of SOX17 to the compressed motif within the *PRDM1* regulatory region was demonstrated by qPCR (**Fig. 23**). A closer look at the SOX17 ChIP-seq profiles at *PRDM1*, *TFAP2C* and *SOX17* regulatory regions confirms that SOX17 binds and putatively regulates this transcription factor network, including the activation of its own expression (**Fig. 30 A-B**). Although SOX17 was not calculated as SOX17 ChIP-seq target in the bioinformatics analysis (maybe due to the stringent settings of the analysis), the ChIP-seq profile indicates that SOX17 may indeed regulate its own expression (**Fig. 30 A**). Although SOX17 additionally binds somatic genes (linked to in neuro-ectodermal development) in seminoma cells, these findings indicate a regulatory role of SOX17 for maintaining latent pluripotency via activation of *PRDM1* and *TFAP2C* expression, thereby in turn suppressing somatic differentiation. A meta-analysis of our SOX17 ChIP-seq data with PRDM1 and TFAP2C ChIP-seq (i.e. in human fetal testis) data could help to confirm this hypothesis.

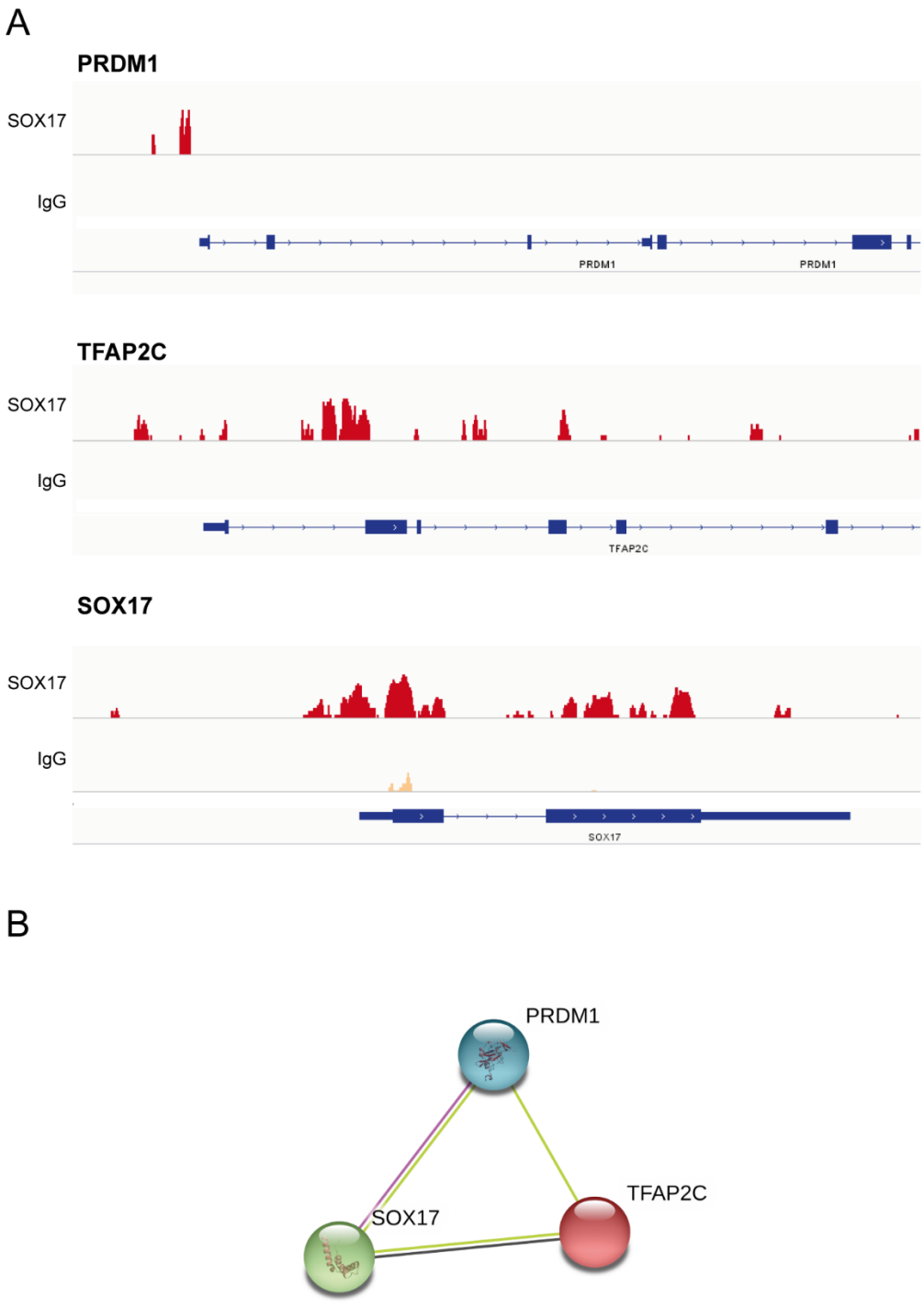

Figure 30: SOX17 regulates the SOX17-PRDM1-TFAP2C network in seminoma

(A) SOX17 ChIP-seq profiles at *PRDM1*, *TFAP2C* and *SOX17* genetic loci (log2 scale). IgG ChIP-seq profiles are given as negative control.

(B) STRING analysis demonstrating interaction of SOX17, PRDM1 and TFAP2C.

5.7. SOX17 maintains latent pluripotency of seminoma cells

Since seminomas always show high expression of both SOX17 and OCT4, an essential role of these two transcription factors for maintaining seminoma cell fate was suggested. So far, I could demonstrate that SOX17 binds to somatic (i.e. neuroectodermal) genes, but also to pluripotency genes in seminoma cells via the compressed (SOX17/OCT4) and the canonical (SOX2/OCT4) binding sites. I have hypothesized that the transactivation of *PRDM1* and *TFAP2C* expression by SOX17 may be essential to suppress the somatic differentiation program in seminoma cells otherwise activated by SOX17. Now, functional analysis needs to demonstrate whether a loss of SOX17 results in suppression of *TFAP2C* and *PRDM1* expression, as well as an overall loss of pluripotency and induction of differentiation.

Therefore, I continued by analysing the effects of SOX17 depletion in seminoma cells. For this, TCam-2 cells were transfected with two different single guide RNAs (gRNAs) homologous to the second exon of the *SOX17* gene locus. CRISPR/Cas9-mediated gene editing using both gRNAs should result in a deletion of approximately 130 bp (**Fig. 31**). TCam-2 cells contain six copies of chromosome 8 [59], where *SOX17* is encoded. Therefore CRISPR/Cas9-mediated gene editing results in a mixture of cells displaying deletions in 0-6 alleles of *SOX17.*

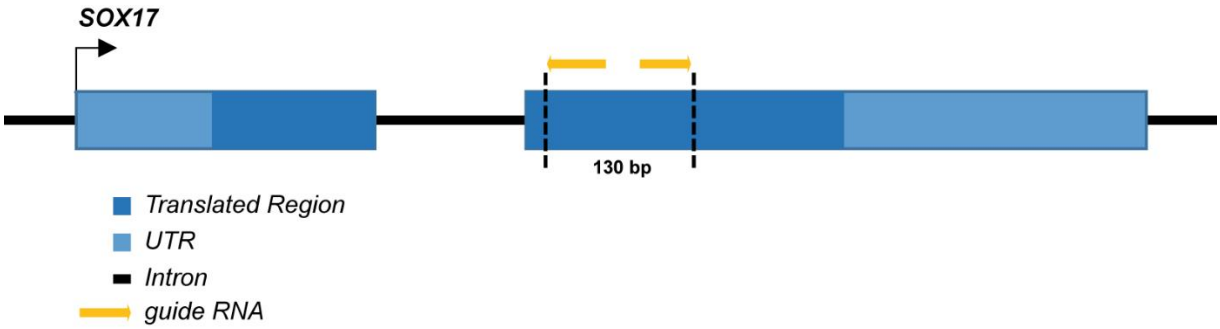

Figure 31: CRISPR/Cas9 mediated gene editing of *SOX17* gene locus
Two gRNAs were designed, directed against the second exon of the human *SOX17* gene (yellow arrows). CRISPR/Cas9-mediated gene editing using both gRNAs should result in a final deletion of approximately 130 bp.

Within 72 hours following transfection of TCam-2 cells with the CRISPR/Cas9 constructs qRT-PCR demonstrated significant reduction of *SOX17* expression, suggesting successful gene editing at least in some cells (**Fig. 32**). Additionally, I was able to demonstrate significant downregulation of the pluripotency markers *NANOG*, *TFAP2C*, *POU5F1*, *PRDM14, ALPL* and *PRDM1* (**Fig. 32**). All of these genes were shown to be bound by SOX17 according to our ChIP analysis. The fact that downregulation of SOX17 results in downregulation of these genes shows that SOX17 transactivates these genes. Furthermore, these analyses show that downregulation or loss of SOX17 ultimately results in a loss of the latent pluripotent state in seminoma cells, possibly allowing for cellular differentiation. Notably, since differentiated cells lose their capacity to self-renew and divide the derivation of single cell clones was prohibited and the following analyses were performed on the TCam-2 Δ SOX17 bulk population only.

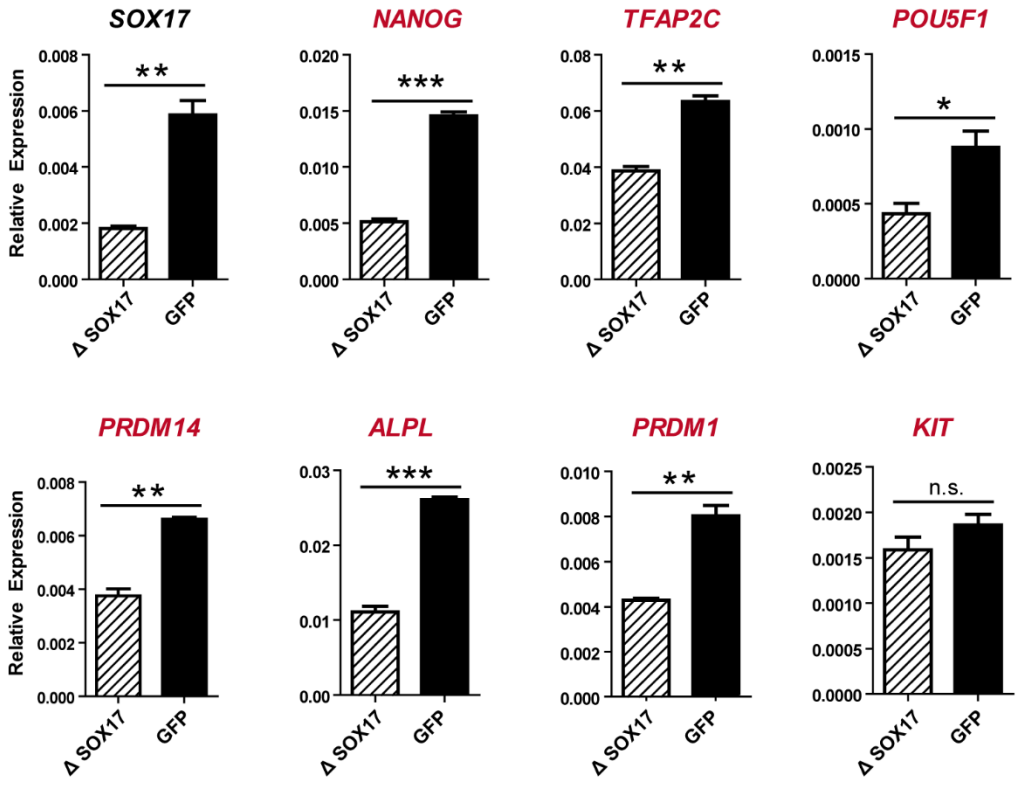

Figure 32: Expression of pluripotency and germ cell markers after depletion of SOX17 in TCam-2 cells

qRT-PCR of ChIP-validated targets of SOX17-mediated transcription (red) in TCam-2 Δ SOX17 bulk population and GFP-transfected TCam-2 as control (72 hours following transfection). Expression is normalized against *GAPDH* as housekeeping gene.

While reduction of *SOX17* and its downstream target genes *NANOG*, *TFAP2C*, *POU5F1*, *PRDM14, ALPL* and *PRDM1* was clearly evident on mRNA level, protein levels of TFAP2C, OCT4, LIN28A and NANOG in the TCam-2 Δ SOX17 bulk population were not affected (**Fig. 33**). However, due to the heterogeneity of the TCam-2 Δ SOX17 bulk population and the presence of SOX17 wildtype cells within this population, Western blot analysis of the whole protein lysate may not have been sensitive enough to detect the effects of SOX17 depletion in individual single cells. Also, mRNA and protein levels can deviate from one another, due to the prolonged half-life of proteins compared to mRNA.

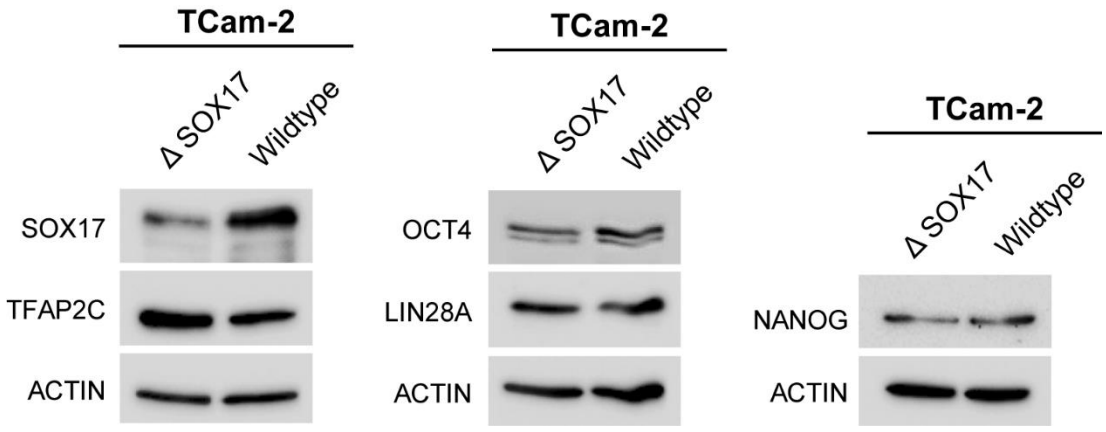

Figure 33: Depletion of SOX17 in TCam-2 cells
Western blot showing levels of SOX17, TFAP2C, OCT4, LIN28A and NANOG protein 72 hours following CRISPR/Cas9 mediated gene editing of *SOX17* gene locus in the TCam-2 Δ SOX17 bulk population (Δ SOX17). The wildtype control represents TCam-2 cells that were transiently transfected with a GFP-coding plasmid. ACTIN was used as loading control.

The analysis of TCam-2 cell morphology 10-15 days following gene editing of *SOX17,* however, revealed signs of cell differentiation, such as the formation of polynucleated cells and an enlarged cytoplasm within these differentiated cell colonies (**Fig. 34**). Differentiated areas were negative for the pluripotency marker alkaline phosphatase (AP), while cells resembling TCam-2 wildtype cells stained positive for AP activity (**Fig. 35**). In comparison, TCam-2 control cells that were transfected with a GFP-coding plasmid remained 100% positive for AP activity (**Fig. 35**). This confirms that the

reduction or loss of SOX17 in TCam-2 cells leads to the downregulation of pluripotency resulting in induction of differentiation.

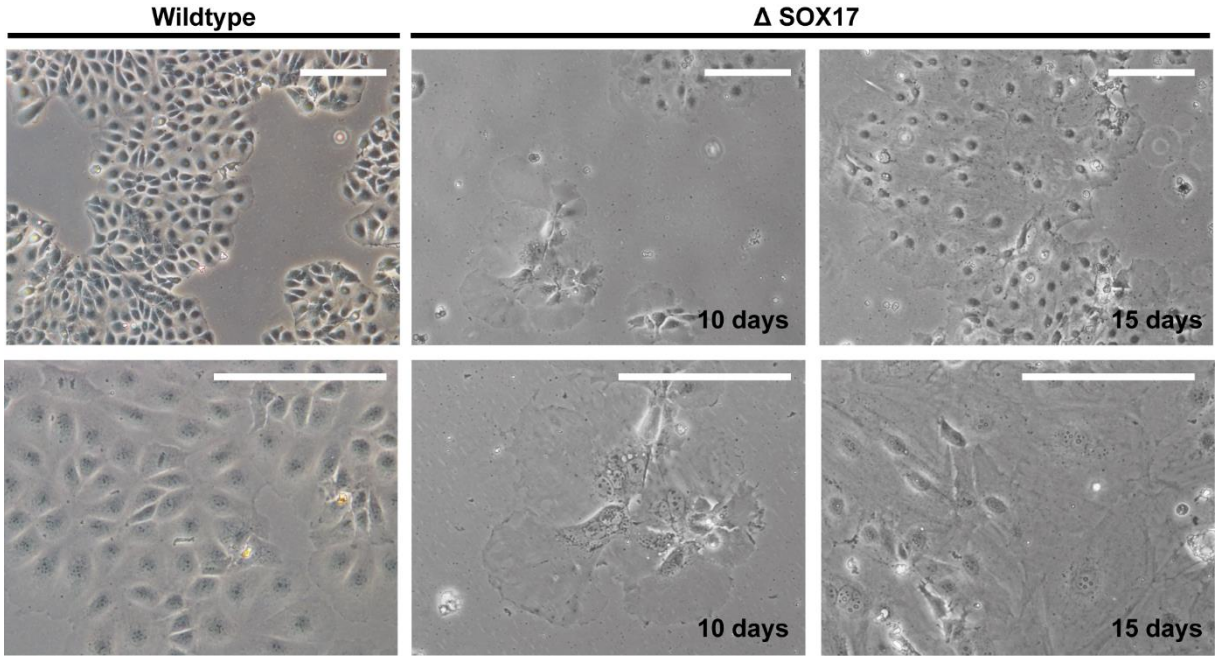

Figure 34: Morphology of TCam-2 Δ SOX17 bulk
Morphology of TCam-2 cells 10 and 15 days following CRISPR/Cas9 mediated gene editing of *SOX17* gene locus (right) compared to wildtype TCam-2 control cells (left). Scalebar = 250 µm.

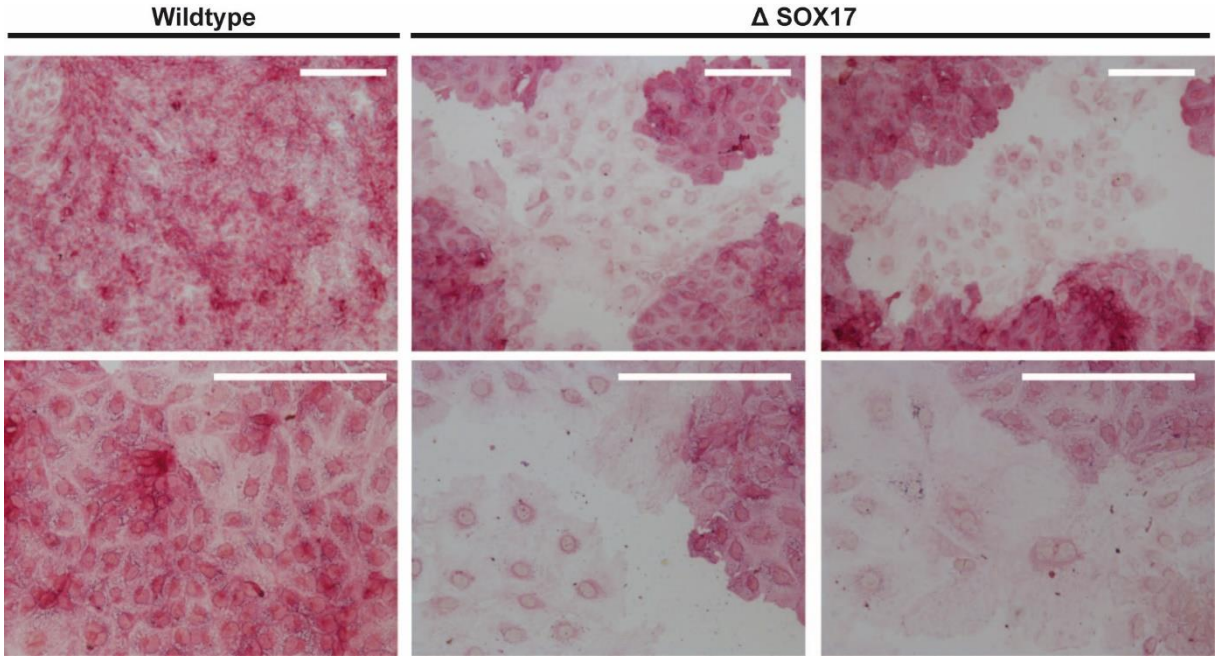

Figure 35: Alkaline phosphatase activity of TCam-2 Δ SOX17 bulk
AP activity of TCam-2 cells following CRISPR/Cas9 mediated gene editing of *SOX17* gene locus (right) compared to TCam-2 (GFP-transfected) control cells (left). Scalebar = 250 µm.

However, since the analysis of the whole protein lysate by Western blot was not sensitive enough to detect loss of TFAP2C and OCT4 on protein level in the TCam-2 Δ SOX17 bulk population, I additionally performed immunofluorescence staining on individual cells that stained either weakly or completely negative for SOX17 protein (**Fig. 36**). As expected, those cells that showed only weak staining for SOX17 protein also showed reduced levels of OCT4 and TFAP2C protein. This correlates with the ChIP-seq and qRT-PCR data and again confirms TFAP2C and OCT4 as direct targets of SOX17-mediated transcriptional activation in TCam-2 cells and shows that depletion of SOX17 results in loss of pluripotency and germ-cell-identity in TCam-2. Since morphological alterations already suggested induction of differentiation of TCam-2 cells (**Fig. 34**), I addressed the question whether the cells differentiate into random cell fates or if the induced differentiation is restricted to a specific cell fate.

Due to the resemblance to multinucleated trophoblast giant cells I analysed expression of trophectodermal markers (*GATA3, HAND1, αHCG, CDX2, EOMES*) (**Fig. 37**), as well as additional germ-cell related markers (*SPRY4*, *NANOS3*) (**Fig. 37**) in the TCam-2 Δ SOX17 bulk population. Notably, in humans HAND1 is expressed in the trophectoderm layer, where it regulates formation of the amniotic membrane [150]. GATA3 is expressed within the stem cell compartment of the placenta [151]. Human chorionic gonadotropin (αHCG) is a hormone involved in trophoblast differentiation and fusion [152]. qRT-PCR demonstrated a loss in germ-cell related markers and significant induction of *GATA3*, *HAND1*, as well as upregulation of *αHCG* (**Fig. 37**). Upregulation of *GATA3* was additionally confirmed by immunofluorescence staining (**Fig. 37**).

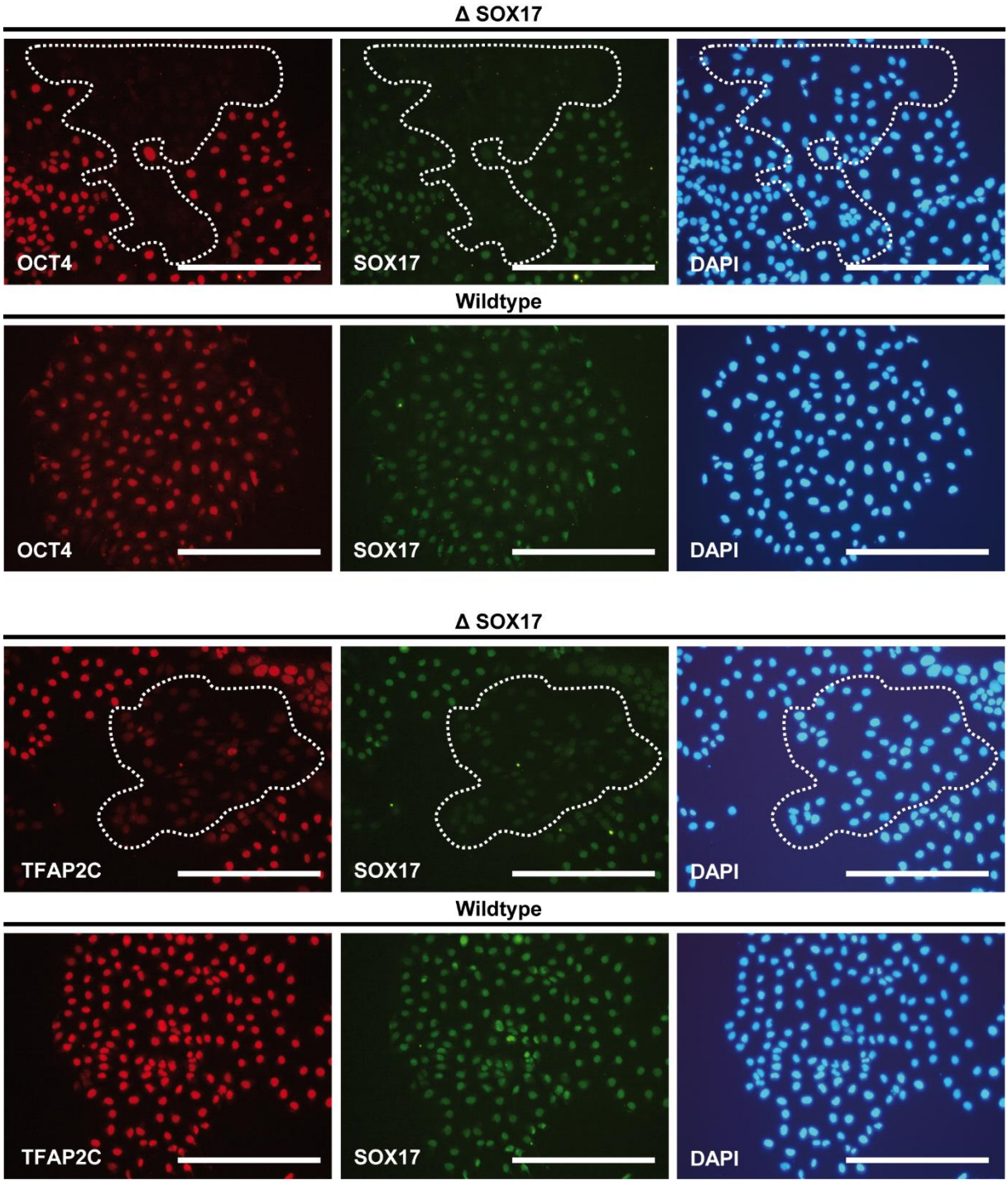

Figure 36: SOX17, OCT4 and TFAP2C protein expression in TCam-2 Δ SOX17 bulk
Immunofluorescence showing expression of SOX17, TFAP2C and OCT4 protein following CRISPR/Cas9-mediated gene editing of *SOX17* gene locus. The wildtype control represents TCam-2 cells that were transiently transfected with a GFP-coding plasmid. Scalebar = 250 µm.

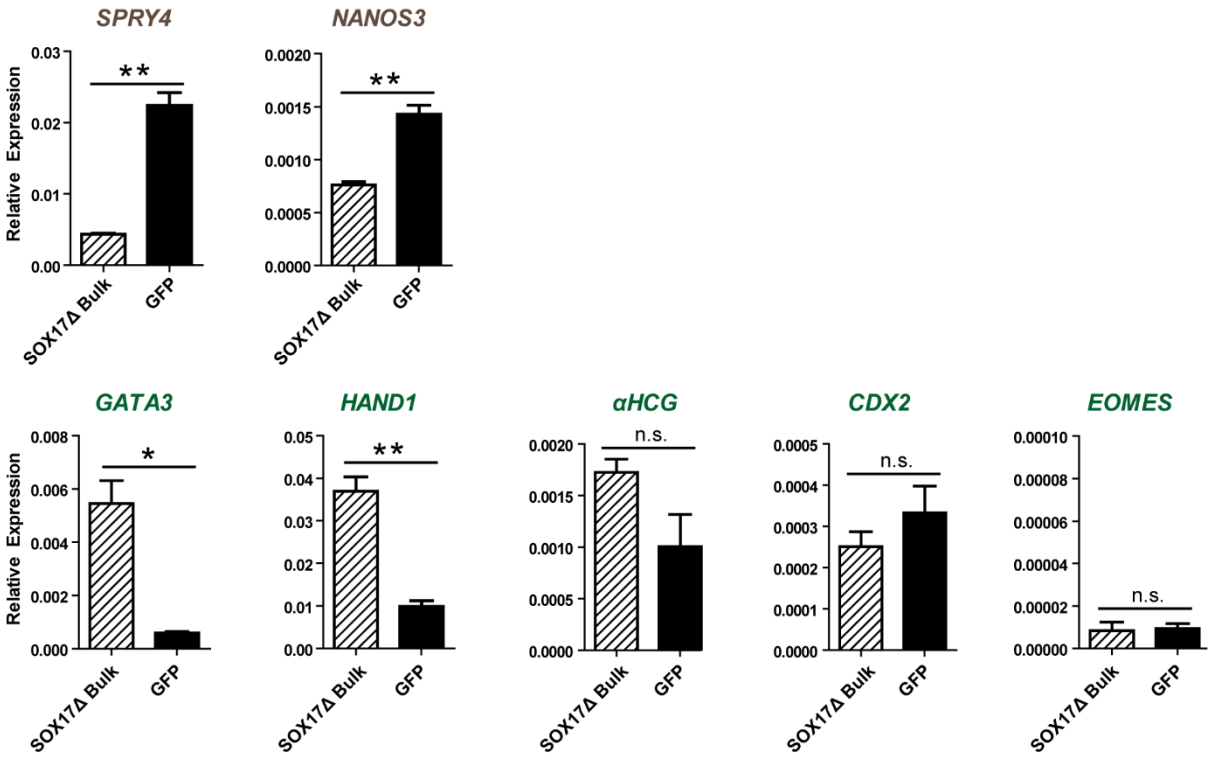

Figure 37: Expression of germ cell markers and trophoblast differentiation markers after depletion of SOX17 in TCam-2 cells
qRT-PCR of germ cell related markers (brown) and markers of extra-embryonic lineages (green) in TCam-2 Δ SOX17 bulk and GFP-transfected TCam-2 as control. Expression is normalized against *GAPDH* as housekeeping gene.

Altogether this indicates that reduction or loss of SOX17 in TCam-2 cells forces the cells to initiate differentiation to a trophectodermal cell fate. Interestingly, GATA3 protein was only detected in TCam-2 cells that were low, but not completely devoid of SOX17 protein (**Fig. 38**). Thus, it seems like different levels of SOX17 lead to formation of different cell types, meaning only a reduction but not a complete loss of SOX17 will lead to a GATA3+ cell population. Collectively, this shows that SOX17 is essential to maintain the latent pluripotency of seminoma cells and to prevent cellular differentiation. The analysis of additional markers specific for embryonic (mesoderm, endoderm, ectoderm) lineages, as well as for different extra-embryonic cell types of the placenta may help to fully understand the plasticity and differentiation potential of TCam-2 cells after reduction or complete loss of SOX17.

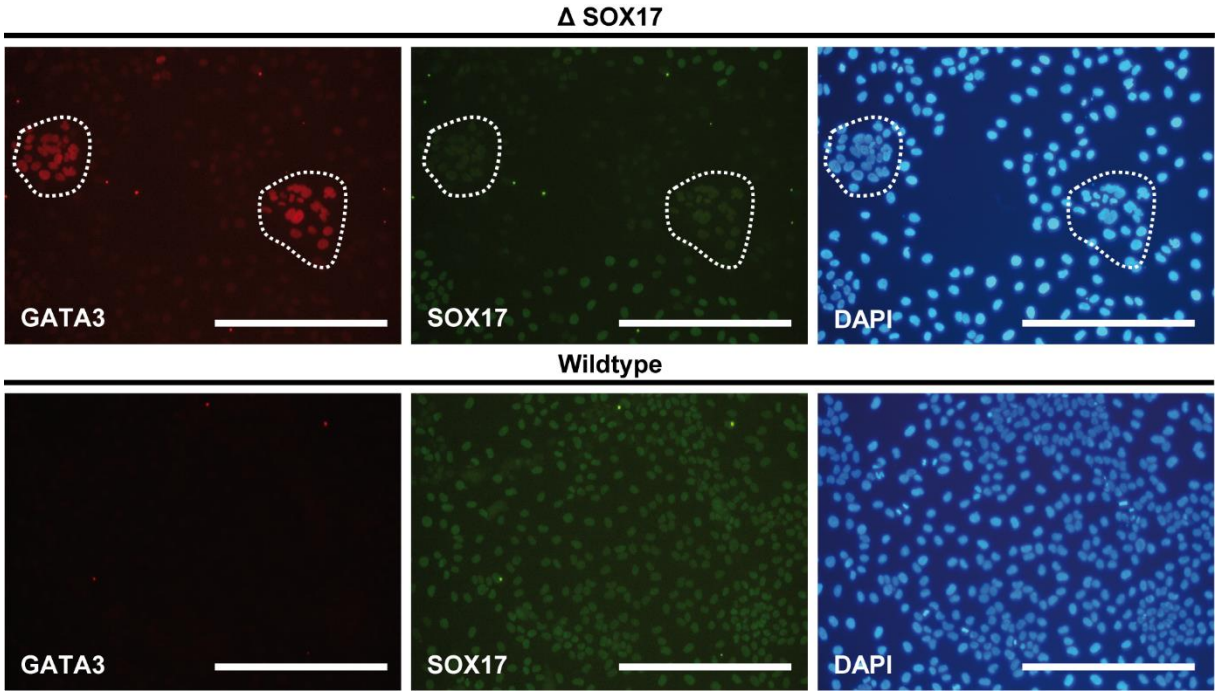

Figure 38: SOX17 and GATA3 protein expression in TCam-2 Δ SOX17 bulk population
Immunofluorescence showing expression of SOX17 and GATA3 protein following CRISPR/Cas9 mediated gene editing of *SOX17* gene locus. The wildtype control represents TCam-2 cells that were transiently transfected with a GFP-coding plasmid. Scalebar = 250 µm.

5.8. In TGCT cells *NANOG* is a common downstream target of SOX2 and SOX17

So far, analyses have shown that both SOX2 and SOX17 are key determinants of TGCT cell fate by activating expression of pluripotency genes and preventing differentiation (either directly or via downstream factors, such as PRDM1 and TFAP2C). By comparing SOX2- and SOX17 regulated genes (meaning those genes that are bound by SOX2 in EC and SOX17 in seminoma cells), I calculated a common overlap of 56 genes (**Fig. 39 A**). Expectedly, *NANOG* was found as a common downstream target gene of SOX2 in EC and SOX17 in seminoma cells (**Fig. 39 A**). Furthermore, GSEA of these 56 genes revealed that 13 of these genes (*CDC42EP4, ID1, SGK1, PSEN2, KRT18, PDPN, NANOG, FRAT2, AP3B1, SERINC3, NIF3L1, HN1, ALKBH7*) are additional NANOG targets in ESCs (gene set: 'BENPORATH_NANOG_TARGETS') [153]. These findings again highlight NANOG as a supporting factor in maintaining TGCT cell fate (and pluripotency). Although SOX2

and SOX17 do not physically interact with NANOG in EC and seminoma cells, respectively, NANOG regulates some of the same target genes.

Together with other known factors and regulators of pluripotency (TRIM71, LIN28B, KLF4, TFAP2C, ALPL) [67, 154-157] that are also bound by SOX2 in EC and SOX17 in seminoma cells, NANOG forms a regulatory network supporting TGCT pluripotency (**Fig. 39 B**). Collectively, these results suggest that in seminoma cells SOX17 is able to take over the role of SOX2 in regulating a set of target genes with roles in pluripotency maintenance (via the canonical motif). The binding of SOX17 (and not SOX2) to compressed motifs within regulatory regions of somatic genes, however, illustrates that both transcription factors are not completely redundant to one another in regulating TGCT cell fate.

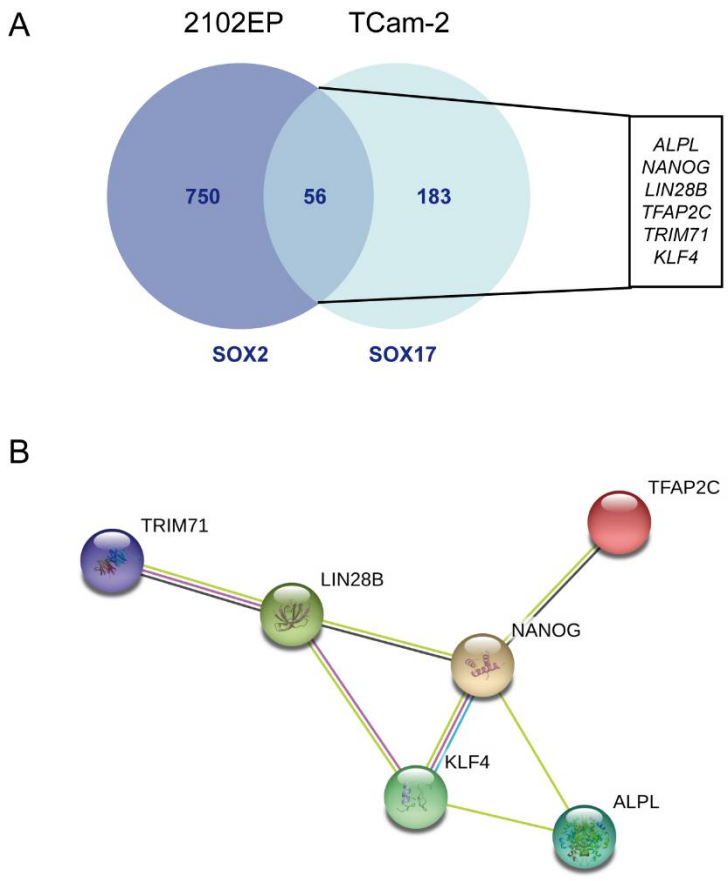

Figure 39: SOX2 and SOX17 regulate a common set of pluripotency genes

(A) Venn diagram depicting common overlap of SOX2- and SOX17-regulated genes in TGCT cells

(B) STRING diagram shows interaction of pluripotency regulators that are regulated by SOX2 in 2102EP and SOX17 in TCam-2 cells.

5.9. The Role of SOX2 and SOX17 in TGCT plasticity

As previously described, we already showed that seminoma cells differentiate into an EC-like phenotype after xenotransplantation into the flank of nude mice [75]. During this transition SOX17 is downregulated and SOX2 is upregulated. However, so far no transition of EC cells to seminoma-like cells was ever demonstrated. We asked whether a transition of EC to seminoma could be induced by overexpression of SOX17. Therefore, I used the dCas9 CRISPR synergistic activator system (SAM) to induce expression of SOX17 in the EC cell line NCCIT. Lentiviral transduction with 100, 200 and 500 µl SOX17 SAM virus led to a dose-dependent induction of SOX17 protein (**Fig. 40 A**). SOX17 overexpression following transduction with 500 µl virus was further confirmed by qRT-PCR (**Fig. 40 B**). However, this did not lead to morphological changes in NCCIT cells (**Fig. 40 C**). Also, protein levels of OCT4 did not change following overexpression of SOX17 (**Fig. 40 A**).

I continued to analyse the downstream effects of SOX17 overexpression on selected markers by qRT-PCR. Although there was significant overexpression of *SOX17* detected after transduction with 500 µl SOX17 SAM virus (**Fig. 40 B**), there was no significant change in the expression levels of the pluripotency and germ cell-associated genes *POU5F1, KIT, TFAP2C* and *PRDM14*, which were all identified as targets of SOX17 in seminoma cells (**Fig. 41, 8.1**). Here, it is necessary to note that *POU5F1*, *TFAP2C* and *PRDM14* are already highly expressed in EC cells, therefore no further induction may be expected. In contrast, however, *PRDM1* and *KIT* are markers of seminomas (**Fig. 24**). This may explain, why a significant induction of *PRDM1* and mild, but not significant induction of *KIT* were observed (**Fig. 41**).

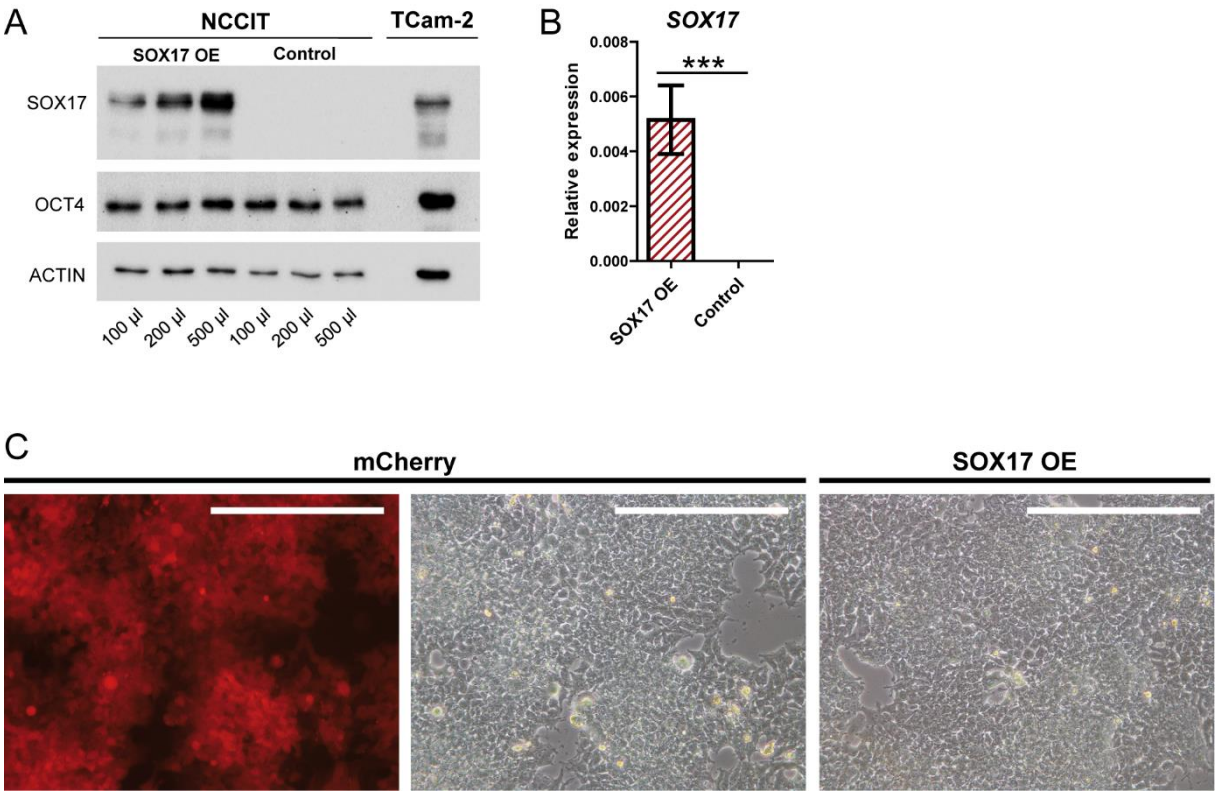

Figure 40: SOX17 overexpression in NCCIT Cells

(A) Western Blot of SOX17 and OCT4 protein levels in NCCIT cells after transduction with 100, 200 and 500 µl SOX17 SAM virus (SOX17 OE). As negative control, NCCIT cells were transduced with mCherry virus. TCam-2 protein lysate served as positive control. ACTIN was used as loading control.

(B) qRT-PCR demonstrating SOX17 overexpression in NCCIT cells after transduction with 500 µl SOX17 SAM virus (SOX17 OE). As negative control, NCCIT cells were transduced with mCherry virus. Expression levels were normalized to *GAPDH* as housekeeping gene.

(C) Morphology of NCCIT cells 72 hours after transduction with 500 µl mCherry virus (left) or SOX17 overexpression (SOX17 OE) SAM construct (right). Scalebar = 250 µm.

But does the overexpression of SOX17 and downstream effectors (i.e. *PRDM1*) lead to a transition into a seminoma-like cell fate? Since no morphological changes were seen (**Fig. 40 C**) and so far only *PRDM1* upregulation was detected, it seems like the overexpression of SOX17 alone is not sufficient to force an EC to seminoma transition, at least in the NCCIT cell line. Also, *SOX2* was still expressed at high levels (**Fig. 41**) Importantly, SOX2 expression is absent in PGCs, TCam-2 and seminoma cells. In presence of both SOX2 and SOX17 the two factors might compete for OCT4 binding. Thus, in order to achieve a conversion of EC to seminoma cells it may be necessary to additionally knockout / knockdown or inhibit SOX2.

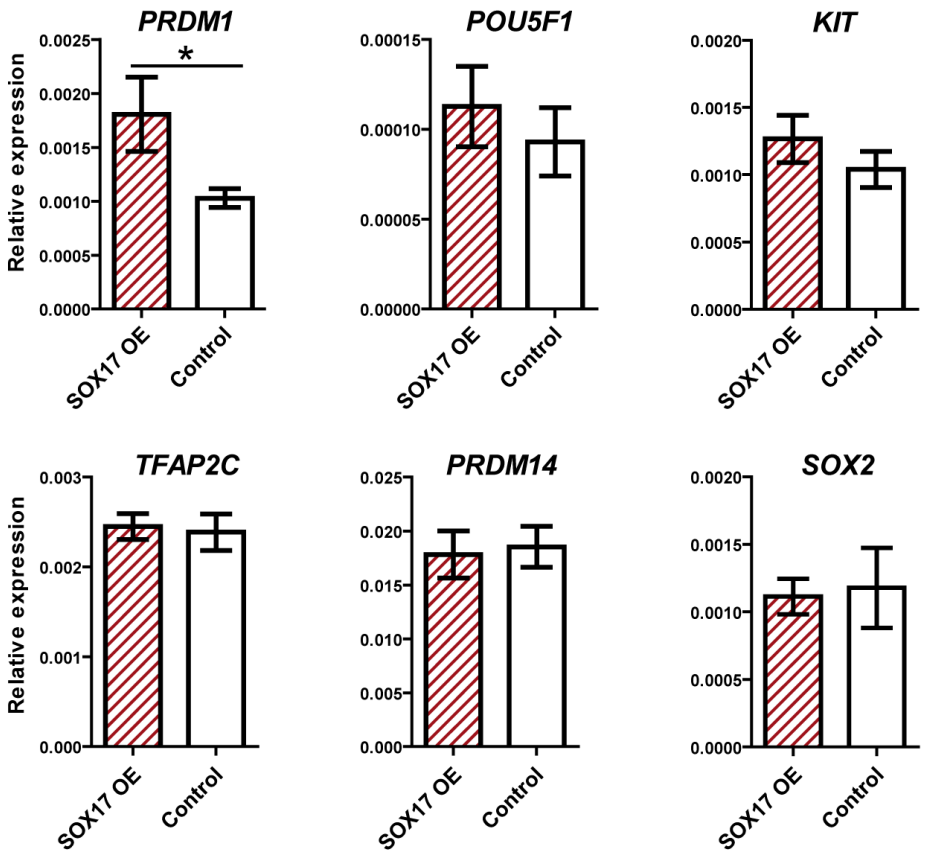

Figure 41: The effects of SOX17 overexpression in EC cells on the expression of SOX17 target genes

qRT-PCR of selected genes in NCCIT cells after transduction with 500 µl SOX17 SAM virus (SOX17 OE). As negative control, NCCIT cells were transduced with mCherry virus. Expression levels were normalized to *GAPDH* as housekeeping gene.

6. Discussion II

Here, I showed that SOX2, which is highly expressed in EC cells, partners with OCT4 to bind to canonical (SOX2/OCT4) binding sites on the DNA. This way, SOX2 regulates important players of pluripotency in ECs, such as *SOX2, NANOG, DPPA4, LIN28A, SALL4, TRIM71, GDF3* and *PRDM14*. I therefore conclude that SOX2 in EC cells has a similar role as SOX2 in ESCs, which is to maintain pluripotency and to prevent differentiation. Although NANOG does not directly interact with SOX2 and OCT4 in ECs to regulate downstream target genes, I believe that it has a supporting role in pluripotency maintenance downstream of SOX2.

In seminoma cells we find a high expression of SOX17. In this cell type SOX17 partners with OCT4 to bind to both compressed (SOX17/OCT4) and canonical (SOX2/OCT4) binding sites on the DNA. Gene set enrichment analysis has shown that the majority of SOX17-bound genes in seminoma cells are having roles in neuronal differentiation (such as *ZHX2*, *COL23A1*, *CD9*, *BEND7*, *PSEN2*, *GBAS*, *UBTD2*, *PSAP*, *ADAMTS1* and *ZNF281*). This is surprising, since seminoma cells maintain a latent pluripotent state and do not spontaneously differentiate into embryonic (and / or neuronal) lineages like ECs, evident by the expression of i.e. LIN28, PRDM14, TFAP2C, OCT4 and NANOG. Only in presence of TGFβ, EGF and FGF4 it was demonstrated that TCam-2 cells differentiate into mixed non-seminoma lineages (then showing features of choriocarcinomas, teratomas and yolk-sac tumours) [73]. But what prevents the differentiation of seminoma cells into neuronal lineages? Most importantly, I could show that SOX17, in seminoma cells, also binds and regulates markers of pluripotency, such as *NANOG, DPPA4, LIN28A, PRDM14, POU5F1* and *TRIM71.* Therefore SOX17 directly contributes to the expression of the seminoma pluripotency cluster and in this respect replaces SOX2 in EC cells. Additionally, SOX17 induces expression of the PGC specifiers PRDM1 and TFAP2C. Both factors are known to suppress somatic differentiation in PGCs [8]. Thus, PRDM1 and TFAP2C may similarly suppress (neuronal) differentiation in seminoma cells. In line with this hypothesis, I could demonstrate that many of those regions bound by SOX17 in seminoma cells (i.e. neuronal genes) harbour additionally binding motifs of PRDM1 and TFAP2C. So, in seminoma cells SOX17, PRDM1 and TFAP2C could cooperate to maintain TGCT cell fate and prevent somatic differentiation.

In line, loss of SOX17 in seminoma cells resulted in loss of *TFAP2C* and *PRDM1* expression, resulting in differentiation into trophectodermal-like lineages. Therefore, it seems plausible that SOX17 has a regulatory function for maintaining pluripotency in seminoma cells, in part via activation of *PRDM1* and *TFAP2C* expression, but also by directly activating expression of germ-cell and pluripotency-associated target genes, such as *NANOG, DPPA4* and *LIN28A* (**Fig. 42**). It would be interesting to see, whether expression of TFAP2C or PRDM1 protein could rescue the effects of loss of SOX17 in seminoma cells and prevent differentiation.

Interestingly, we have shown in a different study that the cancer-testis antigen PRAME is also repressing differentiation of seminoma cells (**Fig. 42**) [136]. PRAME is highly expressed in seminoma and TCam-2 cells and absent in ECs [136]. PRAME knockdown in seminoma cells led to a downregulation of pluripotency and germ-cell-related markers and induction of genes associated with endodermal or mesodermal differentiation [136]. Also, during seminoma to EC transition downregulation of SOX17 was first followed by downregulation of PRAME, which suggested that PRAME acts downstream of SOX17 [75, 136]. However, here PRAME was not identified as a direct target of SOX17-mediated transcription. Nonetheless, our previous analyses indicate that PRAME also represses somatic differentiation in seminoma cells, without being a direct transcriptional target of SOX17 (**Fig. 42**).

While we had already postulated a role for SOX17 in maintaining pluripotency of seminoma cells, I could now additionally show that loss of SOX17 induces differentiation of these cells into extra-embryonic lineages. In a previous study by Irie *et al*. it was demonstrated that siRNA-mediated knockdown of SOX17 in TCam-2 cells leads to a loss of pluripotency- and germ cell- related markers [6]. However, the authors did not investigate the long-term effects of SOX17 knockdown in TCam-2 cells. Here, the differentiation of seminoma cells into extra-embryonic cell types after SOX17 loss resembles the differentiation of seminoma cells seen after treatment with TGFβ, EGF and FGF4 into mixed non-seminoma [73], although this differentiation was not accompanied by a loss in SOX17 expression [73].

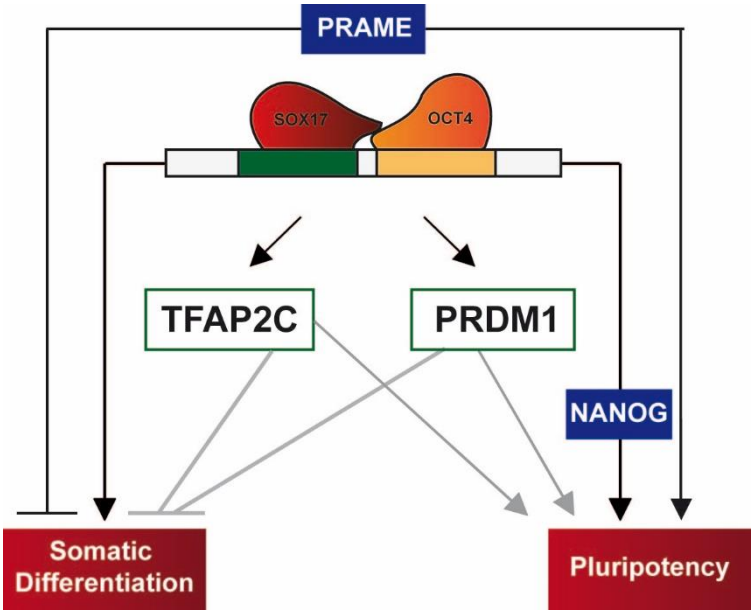

Figure 42: Transcription factor network maintaining seminoma pluripotency
SOX17 and OCT4 interact and bind to the DNA, thereby activating expression of somatic genes and genes associated with pluripotency, including *NANOG*. Also, SOX17 regulates *TFAP2C* and *PRDM1* expression, which in turn are able to suppress somatic differentiation and maintain pluripotency. PRAME may additionally support the pluripotency network of seminoma cells by repressing somatic differentiation.

Nonetheless, it seems interesting that seminoma cells respond to different signalling cues (i.e. treatment with TGFβ, EGF and FGF4) or dysregulations (i.e. loss of SOX17) with the differentiation into extraembryonic lineages that resemble mixed non-seminoma / choriocarcinoma. Especially the multinucleated cell types within these differentiated colonies are reminiscent of syncytial trophoblastic cells. Such trophoblast-like foci are sometimes seen within patient seminoma samples [158], thus the data presented here could serve to explain the development of these foci. In light of the presented data, I speculate that distinct signalling cues or cytokines present within the tumour microenvironment could favour a downregulation of SOX17 levels in seminomas, thereby inducing seminoma differentiation into extra-embryonic cell tyes.

In conclusion, seminomas may only keep their cell identity by expressing SOX17 (and its partner OCT4). Due to the resemblance of seminoma cells to GCNIS and PGCs, seminomas are considered the default pathway of GCNIS progression. Inhibition of BMP signalling, however, can result in a seminoma to EC transition, accompanied by

downregulation of SOX17 and upregulation of SOX2 [75]. In turn, the overexpression of SOX17 alone did not lead to a shift in EC cell identity towards a seminoma phenotype, nor did it alter *SOX2* levels. This is despite the fact that OCT4 has a much higher affinity for the SOX17 DNA complex, at least on compressed motifs (binding energy: −3.86 ± 0.74 kcal/mol), than for the SOX2 DNA complex at canonical motifs (binding energy: 8.09 ± 0.73 kcal/mol) [71]. One theory in favour of a preferred SOX2-OCT4 binding to canonical motifs in ECs would be that the DNA is more accessible at regions containing the canonical motif, while DNA accessibility is restricted at regions containing compressed motifs (i.e. by DNA methylation). Additional ATAC-seq on EC and seminoma chromatin could therefore help to investigate this hypothesis.

Interestingly, although *SOX2* levels were not altered upon overexpression of SOX17 in ECs, we find a mutual exclusive expression of SOX2 and SOX17 in TGCT subtypes. Several hypotheses try to explain this phenomenon: In TCam-2 cells Kushwaha *et al.* proposed that SOX2 repression is mediated by histone methylation (H3K27me3) via the polycomb repressive complex [159]. In colorectal cancer expression of *SOX2* is suppressed by the SOX17 target miR-371-5p [160]. However, I could not identify miR-371-5p as a SOX17 target in TCam-2 cells. Also, it seems like SOX17 induction alone is not sufficient to alter *SOX2* levels in EC cells *in vitro*. In the future, it would be interesting to investigate the mechanism by which SOX17 is repressed during TCam-2 to EC conversion (after xenotransplantation into the flank of nude mice) in more detail, in order to understand whether a similar conversion was also possible from EC to seminoma. Also, it would be interesting to see how SOX2 knockout / knockdown affects the outcome of SOX17 overexpression in EC cells.

7. Bibliography

[1]**Jostes S**. Master Thesis, Sina Jostes 2014, University of Bonn.

[2]**Jostes S, Nettersheim D, Fellermeyer M, Schneider S, Hafezi F, Honecker F, et al.** The bromodomain inhibitor JQ1 triggers growth arrest and apoptosis in testicular germ cell tumours in vitro and in vivo. *J Cell Mol Med* 2016; 21; 1300–14.

[3]**Nettersheim D, Jostes S, Fabry M, Honecker F, Schumacher V, Kirfel J, et al.** A signaling cascade including ARID1A, GADD45B and DUSP1 induces apoptosis and affects the cell cycle of germ cell cancers after romidepsin treatment. *Oncotarget* 2016; 5.

[4]**Sasaki K, Nakamura T, Okamoto I, Yabuta Y, Iwatani C, Tsuchiya H, et al.** The Germ Cell Fate of Cynomolgus Monkeys Is Specified in the Nascent Amnion. *Dev Cell* 2016; 39; 169–85.

[5]**Kojima Y, Sasaki K, Yokobayashi S, Sakai Y, Nakamura T, Yabuta Y, et al.** Evolutionarily Distinctive Transcriptional and Signaling Programs Drive Human Germ Cell Lineage Specification from Pluripotent Stem Cells. *Cell Stem Cell* 2017; 21; 517–532.e5.

[6]**Irie N, Weinberger L, Tang WWC, Kobayashi T, Viukov S, Manor YS, et al.** SOX17 Is a Critical Specifier of Human Primordial Germ Cell Fate. *Cell* 2015; 160.

[7]**Sasaki K, Yokobayashi S, Nakamura T, Okamoto I, Yabuta Y, Kurimoto K, et al.** Robust In Vitro Induction of Human Germ Cell Fate from Pluripotent Stem Cells. *Cell Stem Cell* 2015; 17; 178–94.

[8]**Jostes S, Schorle H**. Signals and transcription factors for specification of human germ cells. *Stem Cell Investig* 2018; 5; 13.

[9]**Meyenn von F, Reik W**. Forget the Parents: Epigenetic Reprogramming in Human Germ Cells. *Cell* 2015; 161; 1248–51.

[10]**Nettersheim D, Jostes S, Schneider S, Schorle H**. Elucidating human male germ cell development by studying germ cell cancer. *Reproduction* 2016; 152; R101–13.

[11]**Stukenborg J-B, Kjartansdóttir KR, Reda A, Colon E, Albersmeier JP, Söder O**. Male germ cell development in humans. *Horm Res Paediatr* 2013; 81; 2–12.

[12]**Neto FTL, Bach PV, Najari BB, Li PS, Goldstein M**. Spermatogenesis in humans and its affecting factors. *Seminars in Cell &Amp; Developmental Biology* 2016; 59; 10–26.

[13]**Bao J, Bedford MT**. Epigenetic regulation of the histone-to-protamine transition during spermiogenesis. *Reproduction* 2016; 151; R55–70.

[14]**Sullivan R, Mieusset R**. The human epididymis: its function in sperm maturation. *Hum Reprod Update* 2016; 22; 574–87.

[15]**Amann RP**. The cycle of the seminiferous epithelium in humans: a need to revisit? *J Androl* 2008; 29; 469–87.

[16]**Manecksha RP, Fitzpatrick JM**. Epidemiology of testicular cancer. *BJU Int* 2009; 104; 1329–33.

[17]**Looijenga LHJ, Stoop H, Biermann K**. Testicular cancer: biology and biomarkers. *Virchows Archiv : an International Journal of Pathology* 2014; 464.

[18]**Oosterhuis JW, Stoop H, Honecker F, Looijenga LHJ**. Why human extragonadal germ cell tumours occur in the midline of the body: old concepts, new perspectives. *International Journal of Andrology* 2007; 30.

[19]**Nohynek GJ, Borgert CJ, Dietrich D, Rozman KK**. Endocrine disruption: fact or urban legend? *Toxicol Lett* 2013; 223; 295–305.

[20]**Shanmugalingam T, Soultati A, Chowdhury S, Rudman S, Van Hemelrijck M**. Global incidence and outcome of testicular cancer. *Clin Epidemiol* 2013; 5; 417–27.

[21]**Oosterhuis JW, Looijenga LHJ**. Testicular germ-cell tumours in a broader perspective. *Nature Reviews Cancer* 2005; 5.

[22]**Metcalfe PD, Farivar-Mohseni H, Farhat W, McLorie G, Khoury A, Bägli DJ**. Pediatric testicular tumors: contemporary incidence and efficacy of testicular preserving surgery. *J Urol* 2003; 170; 2412.

[23]**Wei Y, Wu S, Lin T, He D, Li X, Liu J, et al.** Testicular yolk sac tumors in children: a review of 61 patients over 19 years. *World J Surg Oncol* 2014; 12; 400.

[24]**Nistal M, Paniagua R, González-Peramato P, Reyes-Múgica M**. Perspectives in Pediatric Pathology, Chapter 25. Testicular and Paratesticular Tumors in the Pediatric Age Group. *Pediatr Dev Pathol* 2016; 19; 471–92.

[25]**Ye Y-L, Sun X-Z, Zheng F-F, Bian J, Huang Y-P, Zhang X-Q, et al.** Clinical analysis of management of pediatric testicular germ cell tumors. *Urology* 2012; 79; 892–7.

[26]**Wetherell D, Weerakoon M, Williams D, Beharry BK, Sliwinski A, Ow D, et al.** Mature and Immature Teratoma: A Review of Pathological Characteristics and Treatment Options. *Med Surg Urol* 2014.

[27]**Palmer RD, Foster NA, Vowler SL, Roberts I, Thornton CM, Hale JP, et al.** Malignant germ cell tumours of childhood: new associations of genomic imbalance. *British Journal of Cancer* 2007; 96; 667–76.

[28]**Mosbech CH, Rechnitzer C, Brok JS, Meyts ER-D, Hoei-Hansen CE**. Recent advances in understanding the etiology and pathogenesis of pediatric germ cell tumors. *J Pediatr Hematol Oncol* 2014; 36; 263–70.

[29]**Hayes-Lattin B, Nichols CR**. Testicular cancer: a prototypic tumor of young adults. *Semin Oncol* 2009; 36; 432–8.

[30]**Sheikine Y, Genega E, Melamed J, Lee P, Reuter VE, Ye H**. Molecular genetics of testicular germ cell tumors. *Am J Cancer Res* 2012; 2; 153–67.

[31]**Berney DM, Looijenga LHJ, Idrees M, Oosterhuis JW, Meyts ER-D, Ulbright TM, et al.** Germ cell neoplasia in situ (GCNIS): evolution of the current nomenclature for testicular pre-invasive germ cell malignancy. *Histopathology* 2016; 69; 7–10.

[32]**Hoei-Hansen CE, Meyts ER-D, Daugaard G, Skakkebaek NE**. Carcinoma in situ testis, the progenitor of testicular germ cell tumours: a clinical review. *Ann Oncol* 2005; 16; 863–8.

[33]**de Jong J, Stoop H, Gillis AJM, van Gurp RJHLM, van de Geijn G-JM, de Boer M, et al.** Differential expression of SOX17 and SOX2 in germ cells and stem cells has biological and clinical implications. *The Journal of Pathology* 2008; 215; 21–30.

[34]**Nonaka D**. Differential expression of SOX2 and SOX17 in testicular germ cell tumors. *American Journal of Clinical Pathology* 2009; 131; 731–6.

[35]**Hart AH, Hartley L, Parker K, Ibrahim M, Looijenga LHJ, Pauchnik M, et al.** The pluripotency homeobox gene NANOG is expressed in human germ cell tumors. *Cancer* 2005; 104; 2092–8.

[36]**Mikuz G**. [Spermatocytic seminoma. A tumor with many faces]. *Pathologe* 2014; 35; 232–7.

[37]**Looijenga LHJ, Hersmus R, Gillis AJM, Pfundt R, Stoop HJ, Van Gurp RJHLM, et al.** Genomic and expression profiling of human spermatocytic seminomas: primary spermatocyte as tumorigenic precursor and DMRT1 as candidate chromosome 9 gene. *Cancer Research* 2006; 66; 290–302.

[38]**Mizuno Y, Gotoh A, Kamidono S, Kitazawa S**. [Establishment and characterization of a new human testicular germ cell tumor cell line (TCam-2)]. *Nippon Hinyokika Gakkai Zasshi* 1993; 84; 1211–8.

[39]**Kinugawa K, Hyodo F, Matsuki T, Jo Y, Furukawa Y, Ueki A, et al.** Establishment and characterization of a new human testicular seminoma cell line, JKT-1. *Int J Urol* 1998; 5; 282–7.

[40]**Mokashi A, Megiel C, Looijenga LHJ**. Establishment and characterization of a new human extragonadal germ cell line, SEM-1, and its comparison with TCam-2 and JKT-1. *Urology* 2013; 81.

[41]**Vogelzang NJ, Bronson D, Savino D, Vessella RL, Fraley EF**. A human embryonal-yolk sac carcinoma model system in athymic mice. *Cancer* 1985; 55; 2584–93.

[42]**Houldsworth J, Reuter V, Bosl GJ, Chaganti RS**. Aberrant expression of cyclin D2 is an early event in human male germ cell tumorigenesis. *Cell Growth Differ* 1997; 8; 293–9.

[43]**Bronson DL, Andrews PW, Vessella RL, Fraley EE**. In vitro differentiation of human embryonal carcinoma cells. *Teratocarcinoma Stem Cells* 1983; 597–605.

[44]**Andrews PW, Goodfellow PN, Shevinsky LH, Bronson DL, Knowles BB**. Cell-surface antigens of a clonal human embryonal carcinoma cell line: morphological and antigenic differentiation in culture. *International Journal of Cancer* 1982; 29; 523–31.

[45]**Bronson DL, Andrews PW, Solter D, Cervenka J, Lange PH, Fraley EE**. Cell line derived from a metastasis of a human testicular germ cell tumor. *Cancer Research* 1980; 40; 2500–6.

[46]**Pera MF, Lafita MJB, Mills J**. Cultured stem-cells from human testicular teratomas: the nature of human embryonal carcinoma, and its comparison with two types of yolk-sac carcinoma. *International Journal of Cancer* 1987; 40; 334–43.

[47]**Casper J, Schnaidt U, Fonatsch C**. Cell lines of human germinal cancer. *International Journal of Andrology* 1987; 10; 105–13.

[48]**Damjanov I, Horvat B, Gibas Z**. Retinoic acid-induced differentiation of the developmentally pluripotent human germ cell tumor-derived cell line, NCCIT. *Lab Invest* 1993; 68; 220–32.

[49]**Sekiya S, Kawata M, Iwasawa H, Inaba N, Sugita M, Suzuki N, et al.** Characterization of human embryonal carcinoma cell lines derived from testicular germ-cell tumors. *Differentiation* 1985; 29; 259–67.

[50]**Hogan B, Fellous M, Avner P, Jacob F**. Isolation of a human teratoma cell line which expresses F9 antigen. *Nature* 1977; 270; 515–8.

[51]**Andrews PW, Damjanov I, Simon D, Banting GS, Carlin C, Dracopoli NC, et al.** Pluripotent embryonal carcinoma clones derived from the human teratocarcinoma cell line Tera-2. Differentiation in vivo and in vitro. *Lab Invest* 1984; 50; 147–62.

[52]**Wang N, Trend B, Bronson DL, Fraley EE**. Nonrandom abnormalities in chromosome 1 in human testicular cancers. *Cancer Research* 1980; 40; 796–802.

[53]**Pattillo RA, Gey GO**. The establishment of a cell line of human hormone-synthesizing trophoblastic cells in vitro. *Cancer Research* 1968; 28; 1231–6.

[54]**Hochberg A, Rachmilewitz J, Eldar-Geva T, Salant T, Schneider T, de Groot N**. Differentiation of choriocarcinoma cell line (JAr). *Cancer Research* 1992; 52; 3713–7.

[55]**Kohler PO, Bridson WE**. Isolation of hormone-producing clonal lines of human choriocarcinoma. *The Journal of Clinical Endocrinology and Metabolism* 1971; 32; 683–7.

[56]**Eckert D, Nettersheim D, Heukamp LC, Kitazawa S, Biermann K, Schorle H.** TCam-2 but not JKT-1 cells resemble seminoma in cell culture. *Cell and Tissue Research* 2008; 331.

[57]**De Jong J, Stoop H, Gillis AJM, Van Gurp RJHLM, Van Drunen E, Beverloo HB, et al.** JKT-1 is not a human seminoma cell line. *International Journal of Andrology* 2007; 30; 350–65.

[58]**Olie RA, Boersma AW, Dekker MC, Nooter K, Looijenga LH, Oosterhuis JW**. Apoptosis of human seminoma cells upon disruption of their microenvironment. *British Journal of Cancer* 1996; 73.

[59]**De Jong J, Stoop H, Gillis AJM, Hersmus R, Van Gurp RJHLM, Van De Geijn GJM, et al.** Further characterization of the first seminoma cell line TCam-2. *Genes Chromosomes and Cancer* 2008; 47.

[60]**Nettersheim D, Heimsoeth A, Jostes S, Schneider S, Fellermeyer M, Hofmann A, et al.** SOX2 is essential for *in vivo* reprogramming of seminoma-like TCam-2 cells to an embryonal carcinoma-like fate. *Oncotarget* 2016; 7; 47095.

[61]**Simões PD, Ramos T**. Human pluripotent embryonal carcinoma NTERA2 cl.D1 cells maintain their typical morphology in an angiomyogenic medium. *J Negat Results Biomed* 2007; 6; 5.

[62]**Baldassarre G, Boccia A, Bruni P, Sandomenico C, Barone MV, Pepe S, et al.** Retinoic acid induces neuronal differentiation of embryonal carcinoma cells by reducing proteasome-dependent proteolysis of the cyclin-dependent inhibitor p27. *Cell Growth Differ* 2000; 11; 517–26.

[63]**Mavilio F, Simeone A, Boncinelli E, Andrews PW**. Activation of four homeobox gene clusters in human embryonal carcinoma cells induced to differentiate by retinoic acid. *Differentiation* 1988; 37; 73–9.

[64]**Josephson R, Ording CJ, Liu Y, Shin S, Lakshmipathy U, Toumadje A, et al.** Qualification of embryonal carcinoma 2102Ep as a reference for human embryonic stem cell research. *Stem Cells* 2007; 25.

[65]**Duran C, Talley PJ, Walsh J, Pigott C, Morton IE, Andrews PW**. Hybrids of pluripotent and nullipotent human embryonal carcinoma cells: partial retention of a pluripotent phenotype. *International Journal of Cancer* 2001; 93; 324–32.

[66]**Abdelalim EM, Emara MM, Kolatkar PR**. The SOX transcription factors as key players in pluripotent stem cells. *Stem Cells and Development* 2014; 23; 2687–99.

[67]**Liu X, Huang J, Chen T, Wang Y, Xin S, Li J, et al.** Yamanaka factors critically regulate the developmental signaling network in mouse embryonic stem cells. *Cell Research* 2008; 18; 1177–89.

[68]**Ying L, Mills JA, French DL, Gadue P**. OCT4 Coordinates with WNT Signaling to Pre-pattern Chromatin at the SOX17 Locus during Human ES Cell Differentiation into Definitive Endoderm. *Stem Cell Reports* 2015; 5; 490–8.

[69]**Aksoy I, Jauch R, Chen J, Dyla M, Divakar U, Bogu GK, et al.** Oct4 switches partnering from Sox2 to Sox17 to reinterpret the enhancer code and specify endoderm. *The EMBO Journal* 2013; 32.

[70]**Tapia N, Maccarthy C, Esch D, Marthaler AG, Tiemann U, Araúzo-bravo MJ, et al.** Dissecting the role of distinct OCT4-SOX2 heterodimer configurations in pluripotency. *Nature Publishing Group* 2015; DOI: 10.1038/srep13533.

[71]**Merino F, Ng CKL, Veerapandian V, Schöler HR, Jauch R, Cojocaru V**. Structural Basis for the SOX-Dependent Genomic Redistribution of OCT4 in Stem Cell Differentiation. *Cell* 2014; 22.

[72]**Jauch R, Aksoy I, Hutchins AP, Ng CKL, Tian XF, Chen J, et al.** Conversion of Sox17 into a Pluripotency Reprogramming Factor by Reengineering Its Association with Oct4 on DNA. *Stem Cells* 2011; DOI: 10.1002/stem.639.

[73]**Nettersheim D, Gillis AJ, Looijenga LH, Schorle H**. TGF-β1, EGF and FGF4 synergistically induce differentiation of the seminoma cell line TCam-2 into a cell type resembling mixed non-seminoma. *International Journal of Andrology* 2011; 34.

[74]**Ancelin K, Lange UC, Hajkova P, Schneider R, Bannister AJ, Kouzarides T, et al.** Blimp1 associates with Prmt5 and directs histone arginine methylation in mouse germ cells. *Nat Cell Biol* 2006; 8; 623–30.

[75]**Nettersheim D, Jostes S, Sharma R, Schneider S, Hofmann A, Ferreira HJ, et al.** BMP Inhibition in Seminomas Initiates Acquisition of Pluripotency via NODAL Signaling Resulting in Reprogramming to an Embryonal Carcinoma. *PLoS Genetics* 2015; 11; e1005415.

[76]**Nettersheim D, Schorle H**. The plasticity of germ cell cancers and its dependence on the cellular microenvironment. *J Cell Mol Med* 2017; 21; 1463–7.

[77]**Oldenburg J, Nuver J, Heidenreich A, Schmoll H-J, Bokemeyer C, Horwich A, et al.** Testicular seminoma and non-seminoma: ESMO Clinical Practice Guidelines for diagnosis, treatment and follow-up. *Ann Oncol* 2013; 24 Suppl 6; vi125–32.

[78]**Albers P, Albrecht W, Algaba F, Bokemeyer C, Cohn-Cedermark G, Fizazi K, et al.** EAU guidelines on testicular cancer: 2011 update. *Eur Urol* 2011; 60; 304–19.

[79]**Jostes S, Nettersheim D, Schorle H**. Epigenetic drugs and their molecular targets in testicular germ cell tumours. *Nat Rev Urol* 2019; DOI: 10.1038/s41585-019-0154-x.

[80]**Waddington CH**. Genetic assimilation of the bithorax phenotype. *International Journal of Organic Evolution* 1956; 10; 1-13

[81]**Eberharter A, Becker PB**. Histone acetylation: a switch between repressive and permissive chromatin. Second in review series on chromatin dynamics. *EMBO Rep* 2002; 3; 224–9.

[82]**Li Y, Seto E**. HDACs and HDAC Inhibitors in Cancer Development and Therapy. *Cold Spring Harb Perspect Med* 2016; 6; a026831.

[83]**Eckschlager T, Plch J, Stiborova M, Hrabeta J**. Histone Deacetylase Inhibitors as Anticancer Drugs. *Int J Mol Sci* 2017; 18; 1414.

[84]**Florence B, Faller DV**. You bet-cha: a novel family of transcriptional regulators. *Frontiers in Bioscience : a Journal and Virtual Library* 2001; 6.

[85]**Prinjha RK, Dittmann A, Giotopoulos G, Bantscheff M, Chan W-I, Robson SC, et al.** Inhibition of BET recruitment to chromatin as an effective treatment for MLL-fusion leukaemia. *Nature* 2011; 478.

[86]**French CA, Ramirez CL, Kolmakova J, Hickman TT, Cameron MJ, Thyne ME, et al.** BRD-NUT oncoproteins: a family of closely related nuclear proteins that block epithelial differentiation and maintain the growth of carcinoma cells. *Oncogene* 2007; 27; 2237–42.

[87]**Ryan SL, Schwalbe EC, Cole M, Lu Y, Lusher ME, Megahed H, et al.** MYC family amplification and clinical risk-factors interact to predict an extremely poor prognosis in childhood medulloblastoma. *Acta Neuropathol* 2011; 123; 501–13.

[88]**Lee HY, Cha J, Kim SK, Park JH, Song KH, Kim P, et al.** c-MYC Drives Breast Cancer Metastasis to the Brain, but Promotes Synthetic Lethality with TRAIL. *Mol Cancer Res* 2018; molcanres.0630.2018.

[89]**Zimmerman MW, Liu Y, He S, Durbin AD, Abraham BJ, Easton J, et al.** MYC Drives a Subset of High-Risk Pediatric Neuroblastomas and Is Activated through Mechanisms Including Enhancer Hijacking and Focal Enhancer Amplification. *Cancer Discov* 2017; 8; 320–35.

[90]**Horne GA, Stewart HJS, Dickson J, Knapp S, Ramsahoye B, Chevassut T**. Nanog Requires BRD4 to Maintain Murine Embryonic Stem Cell Pluripotency and Is Suppressed by Bromodomain Inhibitor JQ1 Together with Lefty1. *Stem Cells and Development* 2015; 24.

[91]**Wu T, Pinto HB**. The BET Family Member BRD4 Interacts with OCT4 and Regulates Pluripotency Gene Expression. *Stem Cell Reports* 2015; 4.

[92]**Doroshow DB, Eder JP, LoRusso PM**. BET inhibitors: a novel epigenetic approach. *Ann Oncol* 2017; 28; 1776–87.

[93]**Delmore JE, Issa GC, Lemieux ME, Rahl PB, Shi J, Jacobs HM, et al.** BET bromodomain inhibition as a therapeutic strategy to target c-Myc. *Cell* 2011; 146.

[94]**Baker EK, Taylor S, Gupte A, Sharp PP, Walia M, Walsh NC, et al.** BET inhibitors induce apoptosis through a MYC independent mechanism and synergise with CDK inhibitors to kill osteosarcoma cells. *Sci Rep* 2015; 5; 10120.

[95]**Bhadury J, Nilsson LM, Muralidharan SV, Green LC, Li Z, Gesner EM, et al.** BET and HDAC inhibitors induce similar genes and biological effects and synergize to kill in Myc-induced murine lymphoma. *Proceedings of the National Academy of Sciences of the United States of America* 2014; 111.

[96]**Henssen A, Thor T, Odersky A, Heukamp L, El- N, Beckers A, et al.** BET bromodomain protein inhibition is a therapeutic option for medulloblastoma. *Oncotarget* 2013; 4.

[97]**Lovén J, Hoke HA, Lin CY, Lau A, Orlando DA, Vakoc CR, et al.** Selective inhibition of tumor oncogenes by disruption of super-enhancers. *Cell* 2013; 153.

[98]**Borbely G, Haldosen L-A, Dahlman-Wright K, Zhao C**. Induction of USP17 by combining BET and HDAC inhibitors in breast cancer cells. *Oncotarget* 2015; 6.

[99]**Chakravarthy H, Boer B, Desler M, Mallanna SK, McKeithan TW, Rizzino A**. Identification of DPPA4 and other genes as putative Sox2:Oct-3/4 target genes using a combination of in silico analysis and transcription-based assays. *J Cell Physiol* 2008; 216; 651–62.

[100]**Cimadamore F, Amador-Arjona A, Chen C, Huang C-T, Terskikh AV**. SOX2-LIN28/let-7 pathway regulates proliferation and neurogenesis in neural precursors. *Proceedings of the National Academy of Sciences* 2013; 110; E3017–26.

[101]**Fellermeyer M**. Bachelor Thesis, Martin Fellermeyer 2016, University of Bonn

[102]**Chew J-L, Loh Y-H, Zhang W, Chen X, Tam W-L, Yeap L-S, et al.** Reciprocal transcriptional regulation of Pou5f1 and Sox2 via the Oct4/Sox2 complex in embryonic stem cells. *Molecular and Cellular Biology* 2005; 25; 6031–46.

[103]**Heinz S, Benner C, Spann N, Bertolino E, Lin YC, Laslo P, et al.** Simple combinations of lineage-determining transcription factors prime cis-regulatory elements required for macrophage and B cell identities. *Molecular Cell* 2010; 38; 576–89.

[104]**Oliveros JC**. Venny. An interactive tool for comparing lists with Venn's diagrams. 2007.

[105]**Konermann S, Brigham MD, Trevino AE, Joung J, Abudayyeh OO, Barcena C, et al.** Genome-scale transcriptional activation by an engineered CRISPR-Cas9 complex. *Nature* 2014; 517; 583–8.

[106]**Voutsadakis IA**. The chemosensitivity of testicular germ cell tumors. *Cell Oncol (Dordr)* 2014; 37; 79–94.

[107]**Yin F, Lan R, Zhang X, Zhu L, Chen F, et al.** LSD1 Regulates Pluripotency of Embryonic Stem/Carcinoma Cells through Histone Deacetylase 1-Mediated Deacetylation of Histone H4 at Lysine 16. *Molecular and Cellular Biology* 2013; 34; 158.

[108]**Albany C, Hever-Jardine MP, Herrmann von KM, Yim CY, Tam J, Warzecha JM, et al.** Refractory testicular germ cell tumors are highly sensitive to the second generation DNA methylation inhibitor guadecitabine. *Oncotarget* 2016; 8; 2949–59.

[109]**Eckert D, Biermann K, Nettersheim D, Gillis AJM, Steger K, Jäck H-M, et al.** Expression of BLIMP1/PRMT5 and concurrent histone H2A/H4 arginine 3 dimethylation in fetal germ cells, CIS/IGCNU and germ cell tumors. *BMC Developmental Biology* 2008; 8; 106.

[110]**Wang L, Wolgemuth DJ**. BET Protein BRDT Complexes With HDAC1, PRMT5, and TRIM28 and Functions in Transcriptional Repression During Spermatogenesis. *Journal of Cellular Biochemistry* 2015; 117; 1429–38.

[111]**Chaitanya GV, Steven AJ, Babu PP**. PARP-1 cleavage fragments: signatures of cell-death proteases in neurodegeneration. *Cell Commun Signal* 2010; 8; 31.

[112]**Wang J, Liu Z, Wang Z, Wang S, Chen Z, Li Z, et al.** Targeting c-Myc: JQ1 as a promising option for c-Myc-amplified esophageal squamous cell carcinoma. *Cancer Letters* 2018; 419; 64–74.

[113]**Huang X, Li X**. KLF6 induces apoptosis in prostate cancer cells through up-regulation of ATF3. *Journal of Biological Chemistry* 2008; 283; 29795–801.

[114]**Mirguet O, Gosmini R, Toum J, Clément CA, Barnathan M, Brusq J-M, et al.** Discovery of epigenetic regulator I-BET762: lead optimization to afford a clinical candidate inhibitor of the BET bromodomains. *J Med Chem* 2013; 56; 7501–15.

[115]**Filippakopoulos P, Picaud S, Mangos M, Keates T, Lambert JP, Barsyte-Lovejoy D, et al.** Histone recognition and large-scale structural analysis of the human bromodomain family. *Cell* 2012; 149.

[116]**Jung M, Philpott M, Schulze J, Badock V, Eberspächer U, Moosmayer D, et al.** Affinity map of bromodomain protein 4 (BRD4) interactions with the histone H4 tail and the small molecule inhibitor JQ1. *The Journal of Biological Chemistry* 2014; 289.

[117]**Feng Q, Zhang Z, Shea MJ, Creighton CJ, Coarfa C, Hilsenbeck SG, et al.** An epigenomic approach to therapy for tamoxifen-resistant breast cancer. *Cell Research* 2014; 24; 809–19.

[118]**Bid HK, Phelps DA, Xaio L, Guttridge DC, Lin J, London C, et al.** The Bromodomain BET Inhibitor JQ1 Suppresses Tumor Angiogenesis in Models of Childhood Sarcoma. *Mol Cancer Ther* 2016; 15; 1018–28.

[119]**Leal AS, Williams CR, Royce DB, Pioli PA, Sporn MB, Liby KT**. Bromodomain inhibitors, JQ1 and I-BET 762, as potential therapies for pancreatic cancer. *Cancer Letters* 2017; 394; 76–87.

[120]**Leal AS, Carapellucci S, Zydeck K, Sporn MB, Liby KT**. Chemoprevention of Preclinical Breast and Lung Cancer with the Bromodomain Inhibitor I-BET 762. *Cancer Prev Res (Phila)* 2017; 11; 143–56.

[121]**Filippakopoulos P, Qi J, Picaud S, Shen Y, Smith WB, Morse EM, et al.** Selective inhibition of BET bromodomains. *Nature* 2011; 468.

[122]**Matzuk MM, McKeown MR, Filippakopoulos P, Li Q, Ma L, Agno JE, et al.** Small-molecule inhibition of BRDT for male contraception. *Cell* 2012; 150.

[123]**Zengerle M, Chan K-H, Ciulli A**. Selective Small Molecule Induced Degradation of the BET Bromodomain Protein BRD4. *ACS Chemical Biology* 2015; 10; 1770–7.

[124]**Fowler T, Ghatak P, Price DH, Conaway R, Conaway J, Chiang C-M, et al.** Regulation of MYC expression and differential JQ1 sensitivity in cancer cells. *PloS One* 2014; 9; e87003.

[125]**Shi X, Mihaylova VT, Kuruvilla L, Chen F, Viviano S, Baldassarre M, et al.** Loss of TRIM33 causes resistance to BET bromodomain inhibitors through MYC- and TGF-β-dependent mechanisms. *Proceedings of the National Academy of Sciences* 2016; 113; E4558.

[126]**Biswal BK, Beyrouthy MJ, Hever-Jardine MP, Armstrong D, Tomlinson CR, Christensen BC, et al.** Acute hypersensitivity of pluripotent testicular cancer-derived embryonal carcinoma to low-dose 5-aza deoxycytidine is associated with global DNA Damage-associated p53 activation, anti-pluripotency and DNA demethylation. *PloS One* 2012; 7; e53003.

[127]**Ambrosini G, Sawle AD, Musi E, Schwartz GK**. BRD4-targeted therapy induces Myc-independent cytotoxicity in Gnaq/11-mutatant uveal melanoma cells. *Oncotarget* 2015; 6; 33397–409.

[128]**Liu W, Stein P, Cheng X, Yang W, Shao N-Y, Morrisey EE, et al.** BRD4 regulates Nanog expression in mouse embryonic stem cells and preimplantation embryos. *Cell Death and Differentiation* 2014; 21; 1950–60.

[129]**Di Micco R, Low V, Ntziachristos P, Yuen SK, Lovell CD, Dolgalev I, et al.** Control of embryonic stem cell identity by BRD4-dependent transcriptional elongation of super-enhancer-associated pluripotency genes. *Cell Reports* 2014; 9; 234–47.

[130]**Huang M, Qiu Q, Xiao Y, Zeng S, Zhan M, Shi M, et al.** BET Bromodomain Suppression Inhibits VEGF-induced Angiogenesis and Vascular Permeability by Blocking VEGFR2-mediated Activation of PAK1 and eNOS. *Sci Rep* 2016; 6; 23770.

[131]**da Motta LL, Ledaki I, Purshouse K, Haider S, De Bastiani MA, Baban D, et al.** The BET inhibitor JQ1 selectively impairs tumour response to hypoxia and downregulates CA9 and angiogenesis in triple negative breast cancer. *Oncogene* 2016; 36; 122–32.

[132]**Mazur PK, Herner A, Mello SS, Wirth M, Hausmann S, Sánchez-rivera FJ, et al.** Combined inhibition of BET family proteins and histone deacetylases as a potential

epigenetics-based therapy for pancreatic ductal adenocarcinoma. *Nature Medicine* 2015.

[133]**Gerlach D, Tontsch-Grunt U, Baum A, Popow J, Scharn D, Hofmann MH, et al.** The novel BET bromodomain inhibitor BI 894999 represses super-enhancer-associated transcription and synergizes with CDK9 inhibition in AML. *Oncogene* 2018; 37; 2687–701.

[134]**Bernasconi E, Gaudio E, Lejeune P, Tarantelli C, Cascione L, Kwee I, et al.** Preclinical evaluation of the BET bromodomain inhibitor BAY 1238097 for the treatment of lymphoma. *Br J Haematol* 2017; 178; 936–48.

[135]**McDaniel KF, Soltwedel T, Fidanze SD, Hasvold LA, Liu D, Mantei RA, et al.** Discovery of N-(4-(2,4-Difluorophenoxy)-3-(6-methyl-7-oxo-6,7-dihydro-1H-pyrrolo[2,3-c]pyridin-4-yl)phenyl)ethanesulfonamide (ABBV-075/Mivebresib), a Potent and Orally Available Bromodomain and Extraterminal Domain (BET) Family Bromodomain Inhibitor. *J Med Chem* 2017; 60; 8369–84.

[136]**Nettersheim D, Arndt I, Sharma R, Riesenberg S, Jostes S, Schneider S, et al.** The cancer/testis-antigen PRAME supports the pluripotency network and represses somatic and germ cell differentiation programs in seminomas. *British Journal of Cancer* 2016; 115; 454–64.

[137]**Bernard P, Harley VR**. Acquisition of SOX transcription factor specificity through protein-protein interaction, modulation of Wnt signalling and post-translational modification. *Int J Biochem Cell Biol* 2009; 42; 400–10.

[138]**Boyer LA, Lee TI, Cole MF, Johnstone SE, Levine SS, Zucker JP, et al.** Core transcriptional regulatory circuitry in human embryonic stem cells. *Cell* 2005; 122; 947–56.

[139]**Sharov AA, Masui S, Sharova LV, Piao Y, Aiba K, Matoba R, et al.** Identification of Pou5f1, Sox2, and Nanog downstream target genes with statistical confidence by applying a novel algorithm to time course microarray and genome-wide chromatin immunoprecipitation data. *BMC Genomics* 2008; 9; 269.

[140]**Tsankov AM, Gu H, Akopian V, Ziller MJ, Donaghey J, Amit I, et al.** Transcription factor binding dynamics during human ES cell differentiation. *Nature* 2015; 518; 344–9.

[141]**Ng CKL, Li NX, Chee S, Prabhakar S, Kolatkar PR, Jauch R**. Deciphering the Sox-Oct partner code by quantitative cooperativity measurements 2012; 40.

[142]**Nettersheim D, Gillis A, Biermann K, Looijenga LHJ, Schorle H**. The seminoma cell line TCam-2 is sensitive to HDAC inhibitor depsipeptide but tolerates various other chemotherapeutic drugs and loss of NANOG expression. *Genes Chromosomes and Cancer* 2011; 50.

[143]**Zhou J, Dong D, Cheng R, Wang Y, Jiang S, Zhu Y, et al.** Aberrant expression of KPNA2 is associated with a poor prognosis and contributes to OCT4 nuclear transportation in bladder cancer. *Oncotarget* 2016; 7; 72767–76.

[144]**Li X-L, Jia L-L, Shi M-M, Li X, Li Z-H, Li H-F, et al.** Downregulation of KPNA2 in non-small-cell lung cancer is associated with Oct4 expression. *J Transl Med* 2013; 11; 232.

[145]**Huang L, Zhou Y, Cao X-P, Lin J-X, Zhang L, Huang S-T, et al.** KPNA2 is a potential diagnostic serum biomarker for epithelial ovarian cancer and correlates with poor prognosis. *Tumour Biol* 2017; 39; 1010428317706289.

[146]**Alshareeda AT, Negm OH, Green AR, Nolan CC, Tighe P, Albarakati N, et al.** KPNA2 is a nuclear export protein that contributes to aberrant localisation of key proteins and poor prognosis of breast cancer. *British Journal of Cancer* 2015; 112; 1929–37.

[147]**Yoon C, Cho S-J, Chang KK, Ryeom SW, Yoon SS**. Role of Rac1 Pathway in Epithelial-to-Mesenchymal Transition and Cancer Stem-like Cell Phenotypes in Gastric Adenocarcinoma. *Mol Cancer Res* 2017; 15; 1106–16.

[148]**Streubel G, Fitzpatrick DJ, Oliviero G, Scelfo A, Moran B, Das S, et al.** Fam60a defines a variant Sin3a-Hdac complex in embryonic stem cells required for self-renewal. *The EMBO Journal* 2017; 36; 2216–32.

[149]**Fang X, Yoon J-G, Li L, Yu W, Shao J, Hua D, et al.** The SOX2 response program in glioblastoma multiforme: an integrated ChIP-seq, expression microarray, and microRNA analysis. *BMC Genomics* 2011; 12; 11.

[150]**Knöfler M, Meinhardt G, Bauer S, Loregger T, Vasicek R, Bloor DJ, et al.** Human Hand1 basic helix-loop-helix (bHLH) protein: extra-embryonic expression pattern, interaction partners and identification of its transcriptional repressor domains. *Biochem J* 2002; 361; 641–51.

[151]**Mirkovic J, Elias K, Drapkin R, Barletta JA, Quade B, Hirsch MS**. GATA3 expression in gestational trophoblastic tissues and tumours. *Histopathology* 2015; 67; 636–44.

[152]**Cocquebert M, Berndt S, Segond N, Guibourdenche J, Murthi P, Aldaz-Carroll L, et al.** Comparative expression of hCG β-genes in human trophoblast from early and late first-trimester placentas. *Am J Physiol Endocrinol Metab* 2012; 303; E950–8.

[153]**Ben-Porath I, Thomson MW, Carey VJ, Ge R, Bell GW, Regev A, et al.** An embryonic stem cell-like gene expression signature in poorly differentiated aggressive human tumors. *Nature Genetics* 2008; 40; 499–507.

[154]**Meyts ER-D, Nielsen JE, Skakkebaek NE, Almstrup K**. Diagnostic markers for germ cell neoplasms: from placental-like alkaline phosphatase to micro-RNAs. *Folia Histochem Cytobiol* 2015; 53; 177–88.

[155]**Pastor WA, Liu W, Ho J, Kim R, Hunt TJ, Lukianchikov A, et al.** TFAP2C regulates transcription in human naive pluripotency by opening enhancers. *Nat Cell Biol* 2018; 20; 553–64.

[156]**Zhou J, Ng SB, Chng WJ**. LIN28/LIN28B: An emerging oncogenic driver in cancer stem cells. Int J Biochem Cell Biol. 2013; 45; 973-8.

[157]**Hayashi Y, Sami S, Takahashi K, Tanabe K, Narita M, Srivastava D, et al.** The let-7/LIN-41 Pathway Regulates Reprogramming to Human Induced Pluripotent Stem Cells by Controlling Expression of Prodifferentiation Genes. *Cell Stem Cell* 2014; 14; 40.

[158]**Manivel JC, Niehans G, Wick MR, Dehner LP**. Intermediate trophoblast in germ cell neoplasms. *Am J Surg Pathol* 1987; 11; 693–701.

[159]**Kushwaha R, Jagadish N, Kustagi M, Mendiratta G, Seandel M, Soni R, et al.** Mechanism and Role of SOX2 Repression in Seminoma: Relevance to Human Germline Specification. *Stem Cell Reports* 2016; 6; 772–83.

[160]**Li Y, Lv Z, He G, Wang J, Zhang X, Lu G, et al.** The SOX17/miR-371-5p/SOX2 axis inhibits EMT, stem cell properties and metastasis in colorectal cancer. *Oncotarget* 2015; 6; 9099–112.

8. Appendix

8.1. Top 500 ChIP-seq Peaks of SOX2 and SOX17 ChIP in TGCT Cells

SOX2 vs IgG	
Peak Score	**Annotated Gene**
150.2	*LINC00324*
86.5	*MIR4521*
75.6	*LOC105374988*
73.9	*RNVU1-6*
67.2	*LINC01962*
58.2	*LASP1*
51.8	*MIR5188*
51.4	*HIST1H4H*
49.6	*LINC01012*
48.8	*PRSS16*
47.9	*ETV6*
46.4	*BICD1*
46.4	*LOC643770*
43.8	*KCTD2*
43.4	*PRSS16*
43.4	*OR4D9*
43.0	*LINC01623*
42.0	*MIR4638*
41.5	*NLGN1-AS1*
41.4	*LINC01962*
40.6	*LOC105374988*
39.7	*NANOG*
37.8	*KPNA2*
37.3	*SLC2A3*
36.6	*PRSS16*
36.4	*HES7*
36.2	*OR1F1*
34.7	*OR1F1*
34.6	*LINC01012*
34.2	*LINC01012*
33.9	*TRIM7*
33.7	*ZFP64*
33.5	*MIR3162*
33.3	*MDM4*
32.5	*DPP9*
31.7	*MIR3162*
31.5	*CHST14*
30.8	*HIST1H4H*
30.8	*NDUFS7*
30.6	*CASP16P*
30.3	*MIR5188*
30.1	*WWTR1*
29.9	*KIAA1551*
29.4	*COMMD7*
29.4	*LINC00324*
29.2	*LINC00533*
29.2	*LINC01556*
28.4	*RCC2*
27.6	*KIAA1551*
27.5	*MIR3162*
27.5	*FAM60A*
27.2	*KIAA1551*
27.2	*LINC00339*
27.1	*RAC1*

SOX2 vs Input	
Peak Score	**Annotated Gene**
58.0	*MIR4521*
45.4	*PRSS16*
41.8	*PRSS16*
41.5	*NLGN1-AS1*
40.9	*LINC01012*
38.6	*RNVU1-6*
37.3	*LINC01962*
35.3	*LINC01623*
34.7	*LOC105374988*
34.1	*OR4D9*
33.8	*LOC105374988*
32.6	*LINC01962*
30.5	*MIR4638*
30.3	*LOC105374988*
28.9	*ETV6*
27.5	*MIR3162*
25.8	*MIR3162*
25.4	*HFE2*
25.4	*WWTR1*
25.3	*KCTD2*
25.3	*CASP16P*
23.5	*LINC00324*
22.4	*HIST1H4H*
22.4	*LINC00533*
22.2	*OR1F1*
21.8	*NDUFS7*
21.5	*RNY1*
21.3	*DNAJB6*
21.3	*ZNF184*
21.2	*HIST1H4H*
20.9	*SLC45A1*
20.4	*OR6S1*
19.8	*CFAP126*
19.7	*ABT1*
19.1	*OR1F1*
19.0	*BTN3A2*
19.0	*RCC2*
19.0	*RN7SL2*
18.9	*MARCKS*
17.9	*ZFP64*
17.9	*LASP1*
17.7	*HIST1H4H*
17.7	*PRDM14*
17.7	*DPP9*
17.5	*LOC101929011*
17.2	*CCDC129*
17.0	*HM13-AS1*
16.8	*DPPA5*
16.3	*SNX16*
16.2	*LINC00443*
16.1	*HIST1H4H*
15.9	*LINC01556*
15.8	*MPPED2*
15.7	*LOC100996654*

SOX17 vs IgG	
Peak Score	**Annotated Gene**
20.6	*TBX3*
18.6	*TRPS1*
17.6	*MIR5692A1*
17.2	*DAPL1*
17.1	*SPOCD1*
17.0	*EPHB1*
17.0	*SCARNA3*
15.8	*KIAA1456*
15.7	*LINC01716*
15.4	*TUBB*
15.1	*AACS*
15.1	*UTS2B*
14.7	*PPFIBP2*
14.6	*BCL11B*
14.3	*LINC01991*
14.2	*CRYGB*
14.2	*LOC284581*
14.1	*ZHX2*
13.9	*COL23A1*
13.5	*CD9*
13.4	*LOC729732*
13.2	*BEND7*
12.8	*ZNF853*
12.6	*PSEN2*
12.5	*DCTD*
12.4	*MIR4454*
12.3	*PIF1*
12.2	*GPR37L1*
12.1	*SSUH2*
12.1	*BDNF*
11.9	*LINC00483*
11.9	*MIR4318*
11.8	*SRGAP3-AS3*
11.8	*MC2R*
11.7	*LINC02104*
11.6	*DDX11-AS1*
11.5	*SERPIND1*
11.5	*TPRG1*
11.5	*C4orf51*
11.4	*NCBP2*
11.4	*CACHD1*
11.3	*TMEM132B*
11.3	*GBAS*
11.2	*ZAP70*
11.2	*SLC6A6*
11.2	*UBTD2*
11.1	*MIR1915*
11.1	*LOC102724532*
11.1	*SPRY4-IT1*
11.0	*MIR3116-2*
10.9	*FAM49A*
10.8	*EPB41L4A-AS2*
10.7	*ADAMTS1*
10.7	*PSAP*

SOX17 vs Input	
Peak Score	**Annotated Gene**
15.7	*KIAA1456*
14.7	*SPOCD1*
13.2	*BEND7*
13.1	*LOC105369739*
13.0	*SLC6A6*
12.9	*MIR4318*
12.9	*TUBB*
12.6	*COL23A1*
12.4	*MC2R*
12.2	*C1orf100*
12.0	*PTPN5*
11.6	*EIF2S2*
11.4	*XXYLT1*
11.4	*PIF1*
11.4	*CD9*
11.3	*CACHD1*
11.3	*PRKAR2B*
11.0	*NUAK1*
10.9	*LINC00251*
10.7	*SSUH2*
10.5	*LOC729732*
10.3	*PER4*
10.2	*UTS2B*
10.1	*HABP4*
9.95	*ASIC2*
9.95	*SNX16*
9.76	*MIR5692A1*
9.66	*MIR3116-2*
9.56	*GBAS*
9.37	*LOC441155*
8.98	*LINC02104*
8.88	*PSAP*
8.78	*GSTA3*
8.69	*ZSCAN2*
8.59	*LOC102724804*
8.59	*GC*
8.59	*ZAP70*
8.49	*RSPO3*
8.39	*ZFAT-AS1*
8.39	*NXPH1*
8.39	*CFAP44-AS1*
8.39	*PPFIBP2*
8.30	*MIR3139*
8.20	*BDNF*
8.20	*LOC101928988*
8.10	*RIPK2*
8.10	*CLRN1*
8.10	*FRAT1*
8.00	*LINC02095*
8.00	*OTUD4*
7.91	*ZNF724*
7.91	*PDZD8*
7.91	*FRAS1*
7.81	*COL17A1*

26.0	*EIF5A*	15.7	*MIR4643*	10.7	*TMPRSS11E*	7.81	*MIMT1*
25.8	*PLVAP*	15.2	*OR6S1*	10.6	*PYDC2*	7.81	*CYP7A1*
25.6	*OR6S1*	15.2	*MIR3162*	10.6	*RNF130*	7.71	*IER2*
25.3	*FAM60A*	15.2	*PRSS16*	10.5	*GSTA3*	7.71	*CARS*
25.2	*OR1F1*	15.2	*MIR3143*	10.5	*SLC39A10*	7.61	*PRKD1*
24.9	*HIST1H4H*	15.0	*EIF5A*	10.4	*CCZ1B*	7.52	*LINC01005*
24.8	*MLLT1*	15.0	*MIR5188*	10.3	*NANOG*	7.52	*C8orf34-AS1*
24.7	*CTC1*	14.9	*LINC01012*	10.3	*LYST*	7.52	*ATL2*
24.5	*VDAC1*	14.9	*TRIM55*	10.2	*LOC102724579*	7.42	*ZBTB7C*
24.4	*ALOXE3*	14.8	*MIS18BP1*	10.2	*ZNF281*	7.32	*KHDRBS3*
24.4	*LOC100049716*	14.8	*HCG16*	10.2	*MIR646*	7.32	*LOC101927881*
24.3	*HM13-AS1*	14.8	*MIR4634*	10.1	*LOC105369739*	7.22	*YWHAZ*
24.3	*AMN1*	14.6	*LINC02016*	10.1	*HABP4*	7.22	*LINC01381*
24.2	*ZNF184*	14.4	*VN1R10P*	10.1	*MIR548I1*	7.12	*ZNF281*
23.8	*HCG16*	14.3	*DOT1L*	9.95	*LOC101929341*	7.12	*LOC101928304*
23.5	*LINC00533*	14.3	*MDM4*	9.95	*SNX16*	7.12	*ESRRB*
23.5	*LINC01623*	14.3	*ZYG11A*	9.95	*NFIB*	7.03	*AGBL4-IT1*
23.1	*SCAMP4*	14.1	*KIAA1551*	9.95	*CCDC179*	7.03	*MIR548XHG*
23.0	*DOT1L*	14.0	*RBMS3-AS1*	9.95	*ARTN*	7.03	*SUSD3*
23.0	*MPZL1*	14.0	*ZNF184*	9.86	*COL17A1*	7.03	*CNTN4-AS1*
22.9	*UBE2D2*	13.8	*LINC01623*	9.76	*IER2*	6.93	*SMG8*
22.9	*LINC01012*	13.8	*ARHGEF3*	9.76	*PTPN5*	6.93	*LINC00862*
22.7	*SLC45A1*	13.8	*SOX5*	9.76	*MIR141*	6.93	*SIAE*
22.7	*GNGT2*	13.5	*USP7*	9.66	*NARS2*	6.83	*DAPL1*
22.4	*OR2V2*	13.5	*CCNH*	9.66	*LOC101928988*	6.73	*KIT*
22.4	*HES7*	13.4	*ZBED9*	9.66	*EIF2S2*	6.73	*PRDM1*
22.2	*RNY1*	13.2	*ZNF184*	9.56	*TFDP2*	6.73	*ALDH3B2*
22.1	*LINC01556*	13.1	*LINC00339*	9.56	*H3F3A*	6.73	*GUCY1A3*
22.0	*HMGN4*	13.1	*CHST14*	9.56	*MIR548AG2*	6.64	*CXCR4*
21.7	*SLC2A14*	13.0	*LINC00533*	9.37	*LOC441155*	6.64	*MIR4454*
21.7	*BTN3A2*	12.9	*SSB*	9.37	*KIDINS220*	6.54	*CXorf21*
21.6	*BCAS4*	12.7	*PRSS16*	9.37	*XXYLT1*	6.54	*IQCF1*
21.6	*NANOG*	12.6	*CLEC3A*	9.37	*LOC105369739*	6.54	*CNGB1*
21.3	*DNAJB6*	12.6	*LINC01822*	9.27	*SPRY4-IT1*	6.54	*CCDC179*
21.3	*ZNF692*	12.5	*MIR5188*	9.27	*CPNE8*	6.54	*ENPP2*
21.1	*PRSS16*	12.5	*ZNF184*	9.17	*ZNF592*	6.44	*RBFOX1*
20.6	*A2ML1*	12.5	*ZHX2*	9.08	*LOC101928797*	6.44	*MIR181C*
20.6	*CFAP126*	12.3	*LINC01012*	9.08	*GSN*	6.44	*LOC100506885*
20.4	*LINC01498*	12.2	*LINC01012*	9.08	*MIMT1*	6.34	*DDX11-AS1*
20.3	*ZYG11A*	12.1	*ZNF483*	8.98	*LOC105375075*	6.34	*LOC101929544*
20.3	*NACC1*	12.1	*SMARCA2*	8.98	*KALRN*	6.25	*HULC*
20.2	*ABT1*	12.1	*LINC01012*	8.88	*POU5F1*	6.25	*KIDINS220*
20.2	*TMPO-AS1*	12.0	*SMARCC2*	8.88	*SOX5*	6.25	*SLC39A11*
20.0	*RNY3*	11.8	*HTR1F*	8.88	*LINC01356*	6.15	*LINC01060*
19.8	*LOC100996654*	11.8	*NOBOX*	8.78	*PCDH1*	6.15	*NR2F2*
19.8	*LINC00941*	11.8	*OR1F1*	8.78	*LINC01951*	6.15	*NDUFB6*
19.8	*SLC2A14*	11.8	*FBRS*	8.78	*KRT18*	6.05	*LOC105376360*
19.7	*RN7SL2*	11.7	*SMARCA2*	8.78	*PGAP1*	6.05	*IRX5*
19.5	*MIR6883*	11.7	*SHISA2*	8.78	*RNF11*	6.05	*LOC101928008*
19.5	*ZNF184*	11.6	*DDAH1*	8.69	*CARS*	6.05	*CDH18*
19.4	*RNF112*	11.6	*LRIG1*	8.59	*MIR3977*	6.05	*BASP1*
19.4	*SLC2A14*	11.4	*PLEKHB2*	8.49	*TSPAN9*	5.95	*LOC102725080*
19.3	*PRDM14*	11.4	*LINC01629*	8.49	*PUM2*	5.95	*PMAIP1*
19.3	*LINC01012*	11.4	*MIR5692B*	8.39	*LINC02114*	5.95	*NR2F6*
19.3	*GNG7*	11.4	*HK3*	8.39	*FTO*	5.95	*MIR8084*
19.3	*HIST1H4H*	11.3	*CNN1*	8.39	*ZNF552*	5.95	*LINC02032*
19.1	*OSCP1*	11.3	*MIR5188*	8.39	*BICD1*	5.95	*RNF130*
19.1	*PLXDC1*	11.2	*HSPA6*	8.30	*MACROD2-AS1*	5.95	*ESRP1*
19.1	*MIR193BHG*	11.2	*NIFK-AS1*	8.30	*FSCN1*	5.95	*ZNF565*
19.0	*MIR4638*	11.2	*KPNA2*	8.30	*CCDC129*	5.86	*CBR4*
19.0	*OR1M1*	11.2	*DUSP6*	8.30	*CRHBP*	5.86	*PYDC2*
19.0	*MIR4472-2*	11.1	*MKRN1*	8.20	*CAND1.11*	5.86	*LOC101928797*
19.0	*DPPA5*	11.1	*LINC01012*	8.20	*SMYD3*	5.86	*STARD13*
18.9	*MARCKS*	11.1	*AFF1*	8.20	*MIR4634*	5.76	*NRF1*

18.8	*PLLP*	11.1	*ERCC1*	8.20	*ZFAT-AS1*	5.76	*ARSJ*
18.6	*LOC105376805*	11.1	*NACC1*	8.20	*IL20RB*	5.76	*TPTE*
18.5	*TRIM7*	11.1	*MIR3690*	8.20	*SLC45A1*	5.76	*DDX18*
18.4	*LINC01012*	10.8	*MORC3*	8.10	*EDIL3*	5.76	*KIAA1456*
18.4	*B4GALT5*	10.8	*GRPR*	8.10	*NCEH1*	5.66	*DNAJB6*
18.2	*UBE2D2*	10.8	*GNGT2*	8.00	*SPIDR*	5.66	*OCM*
18.2	*LINC01841*	10.8	*PLEKHG2*	8.00	*MIR3191*	5.66	*RPA1*
18.2	*PCCB*	10.8	*ILF2*	8.00	*LOC100130298*	5.66	*MIR6085*
18.1	*LOC100507468*	10.7	*TIA1*	8.00	*BAMBI*	5.66	*FAM83A*
18.0	*PCDH1*	10.7	*CASP16P*	8.00	*TMEM87B*	5.66	*PRDM14*
18.0	*PSMB2*	10.5	*LINC01448*	7.91	*ZNF724*	5.56	*TSN*
18.0	*FOXK2*	10.5	*SLC35D3*	7.91	*IQCF1*	5.56	*C5orf66-AS1*
18.0	*RASSF8-AS1*	10.5	*APOBEC3F*	7.91	*LOC101927735*	5.47	*SDK1*
17.9	*USP48*	10.4	*RPL36*	7.91	*GREB1L*	5.47	*MIR1915*
17.9	*KIAA1551*	10.4	*MUC4*	7.81	*PMAIP1*	5.47	*HDAC2*
17.7	*LINC01623*	10.4	*LOC100131289*	7.81	*MIR135B*	5.47	*FAM136A*
17.7	*OAT*	10.3	*PIH1D1*	7.81	*LINGO2*	5.47	*TMEM261*
17.6	*NANOGNB*	10.3	*GLOD5*	7.81	*TIFAB*	5.37	*LOC100289230*
17.6	*SRCIN1*	10.2	*RCOR1*	7.81	*LOC100128386*	5.37	*MIR610*
17.6	*SALL4*	10.2	*MIR9-2*	7.71	*ZBTB2*	5.37	*LINC02003*
17.5	*LOC101929011*	10.2	*PLAGL1*	7.71	*CFAP44-AS1*	5.37	*PIN1P1*
17.5	*MIR3143*	10.2	*ZBTB5*	7.71	*CYP4A22*	5.37	*DCTD*
17.3	*ZBTB8OS*	10.2	*TERF1*	7.61	*MIR548AU*	5.37	*LOC100192426*
17.3	*KDM4C*	10.2	*GPD2*	7.61	*MIR548A2*	5.37	*BCL9*
17.2	*LINC01012*	10.0	*HIST1H4H*	7.61	*ZFAT-AS1*	5.37	*ATP6V1G3*
17.2	*CCDC129*	10.0	*GGACT*	7.61	*ADAMTS6*	5.37	*PPM1A*
17.1	*PMS2CL*	9.89	*ZC3HAV1L*	7.61	*TFRC*	5.37	*NPAS3*
17.0	*MIR193A*	9.89	*ANKRD1*	7.61	*TAB2*	5.37	*LOC102546299*
17.0	*ATF1*	9.89	*NANOG*	7.52	*TBCE*	5.37	*LOC101927056*
17.0	*SNORA38B*	9.77	*TRIP4*	7.52	*PDP1*	5.27	*SMYD3*
17.0	*C7orf55-LUC7L2*	9.77	*LOC105374988*	7.52	*DCD*	5.27	*C1orf105*
16.8	*UBE2G1*	9.77	*SIAH2*	7.42	*IGSF5*	5.27	*MIR383*
16.8	*PCGF6*	9.77	*PCLO*	7.42	*ZBTB7C*	5.27	*MGC27382*
16.8	*LINC00443*	9.64	*LINC01947*	7.42	*LOC105374428*	5.27	*LINC01375*
16.8	*ZNF184*	9.51	*UBE2D2*	7.42	*PDZD8*	5.27	*NABP1*
16.8	*SMARCC2*	9.51	*LINC00324*	7.42	*KIZ*	5.17	*MDH1*
16.7	*EEF2K*	9.51	*SLC35F3*	7.32	*KHDRBS3*	5.17	*OR6S1*
16.7	*PMS2P4*	9.38	*RIF1*	7.32	*GBA3*	5.17	*LOC101927847*
16.6	*LINC01447*	9.38	*SPATA45*	7.32	*ENPP2*	5.17	*MIR3191*
16.6	*VSIG10*	9.38	*GRIA3*	7.32	*LINC01267*	5.17	*FIS1*
16.4	*MLXIPL*	9.25	*REST*	7.32	*LOC101927881*	5.17	*ITGA9-AS1*
16.4	*MELK*	9.25	*BTN3A2*	7.32	*LINC02095*	5.17	*WDR36*
16.4	*LINC02016*	9.25	*CLPP*	7.32	*FSCN1*	5.17	*LOC730100*
16.3	*SNX16*	9.25	*LINC00533*	7.32	*TCERG1L*	5.17	*UMODL1-AS1*
16.2	*MTA3*	9.12	*RPA3*	7.32	*MIR6085*	5.08	*ABCB5*
16.2	*AXIN2*	9.12	*ZBTB8B*	7.32	*NUDT12*	5.08	*MACROD2*
16.2	*FOXK2*	9.12	*MIR3675*	7.22	*PLXNA2*	5.08	*CFHR5*
16.2	*ZNF815P*	9.12	*TTC39B*	7.22	*MIR3139*	5.08	*GBA3*
16.1	*ZNF184*	9.00	*LOC284788*	7.12	*CCAT2*	5.08	*TEAD1*
16.1	*RLIM*	9.00	*ALOXE3*	7.12	*LOC728715*	5.08	*DPPA5*
15.9	*BORCS7-ASMT*	9.00	*LOC102724623*	7.12	*UMODL1-AS1*	5.08	*LOC100129216*
15.9	*LOC101926933*	9.00	*MDM4*	7.03	*GPR156*	5.08	*GTF2I*
15.8	*SMU1*	8.87	*JAKMIP2-AS1*	7.03	*AGBL4-IT1*	5.08	*KIAA0513*
15.8	*MPPED2*	8.74	*MIR4666B*	7.03	*LOC102724404*	5.08	*KCTD3*
15.8	*USP7*	8.74	*LINC01589*	7.03	*SEPT9*	5.08	*KYNU*
15.8	*ZYG11A*	8.74	*RRAGC*	7.03	*AQP6*	5.08	*CUEDC1*
15.8	*OR1F1*	8.74	*LOC101928782*	7.03	*EPHA3*	4.98	*PTPRD-AS2*
15.7	*MIR4643*	8.61	*PMS2CL*	7.03	*MIR548XHG*	4.98	*REXO1L2P*
15.7	*AKAP3*	8.61	*COX5A*	6.93	*LSAMP-AS1*	4.98	*MIR548AD*
15.7	*LOC105374988*	8.61	*ASIC2*	6.93	*COL4A1*	4.98	*LINC01923*
15.5	*MIR5188*	8.61	*LOC101929154*	6.93	*MIR4266*	4.98	*MBNL1*
15.5	*RAB11B*	8.61	*ZNF717*	6.93	*C9orf72*	4.98	*PCGEM1*
15.5	*DUSP6*	8.61	*RIMS2*	6.93	*LOC102723886*	4.98	*FREM3*

15.4	*RNF130*
15.3	*VN1R10P*
15.3	*SMARCD2*
15.2	*PARP11*
15.2	*OR6S1*
15.0	*LOC100131289*
15.0	*TIA1*
14.9	*HOXB1*
14.9	*LOC440570*
14.9	*LINC01716*
14.9	*BTN3A2*
14.8	*LINC01623*
14.8	*MIR4634*
14.8	*NPM1*
14.8	*MIS18BP1*
14.6	*ARHGEF3*
14.6	*ANG*
14.5	*ELAVL1*
14.4	*ZBED9*
14.4	*RPN1*
14.3	*PRSS16*
14.3	*HEATR3*
14.3	*ARHGEF10L*
14.3	*TRIM55*
14.1	*SMARCA2*
14.1	*CECR1*
14.1	*MIR21*
14.0	*SUMO2*
14.0	*FCGR2A*
14.0	*SLC25A39*
14.0	*FLJ41278*
14.0	*MKRN1*
14.0	*RBMS3-AS1*
14.0	*PHC1*
14.0	*MIR2117*
13.9	*WNT11*
13.9	*HOXB1*
13.9	*PPM1B*
13.8	*TXLNG*
13.8	*SOX5*
13.6	*SLC2A14*
13.6	*LOC643770*
13.6	*ZNF184*
13.6	*PLEKHB2*
13.5	*MIR4472-2*
13.5	*ATP5G1*
13.5	*SERBP1*
13.5	*ZNF184*
13.5	*NINJ2*
13.5	*CCNH*
13.4	*POM121L2*
13.4	*KLRG2*
13.4	*ZNF839*
13.2	*DHRS7B*
13.1	*MIR5188*
13.1	*SHISA5*
13.1	*CLDN3*
13.0	*LINC00533*
13.0	*GPD2*
12.9	*CNN1*
12.9	*SH2B3*
12.9	*PSMB3*
12.9	*RNU6-7*
12.9	*LINC01775*
12.9	*SSB*
8.48	*RNF112*
8.48	*LINC00922*
8.48	*WNT11*
8.48	*KLRG2*
8.48	*MIR591*
8.48	*TXLNG*
8.48	*HOXB1*
8.35	*ZNF692*
8.35	*COL17A1*
8.22	*SALL4*
8.22	*OTX2*
8.22	*CSF2RA*
8.22	*MIR629*
8.22	*DDX53*
8.22	*CECR1*
8.22	*EDIL3*
8.10	*AK4*
8.10	*KLF9*
8.10	*EDDM3B*
8.10	*LOC100270746*
8.10	*LINC00533*
8.10	*LINC01012*
8.10	*MYO1E*
8.10	*FTO*
7.97	*LINC00533*
7.97	*C19orf25*
7.97	*MIR4268*
7.97	*LINC01320*
7.97	*TRA2B*
7.97	*LOC102546229*
7.97	*MIR548AQ*
7.97	*LOC100507468*
7.97	*TRA2B*
7.97	*ITSN1*
7.84	*SHISA5*
7.84	*LINC01556*
7.84	*RAB5C*
7.84	*HSPA7*
7.71	*MIR3143*
7.71	*XACT*
7.71	*MIR193BHG*
7.71	*MIR3663*
7.58	*SOX6*
7.58	*LINC01867*
7.58	*MIR371A*
7.58	*FEM1A*
7.58	*EPHA3*
7.45	*SEMA3A*
7.45	*RIOX1*
7.45	*LINC01012*
7.45	*LOC101927159*
7.45	*LINC01447*
7.45	*PDCL*
7.45	*DHRS7B*
7.45	*ZNF592*
7.45	*DRD1*
7.45	*FAM60A*
7.45	*MIRLET7I*
7.32	*CDX2*
7.32	*RBM43*
7.32	*GRM3*
7.32	*PABPC4L*
7.20	*FAM181B*
7.20	*SMARCA1*
7.20	*MAOA*
6.93	*SPOCK2*
6.83	*COL23A1*
6.83	*WSPAR*
6.83	*SLC35D2*
6.83	*SCUBE3*
6.83	*PRLH*
6.83	*ZNF521*
6.83	*TNFAIP8*
6.83	*PLXNA2*
6.73	*ITPRIP*
6.73	*LINC00534*
6.73	*LOC101928304*
6.73	*GTF2I*
6.64	*CXCR4*
6.64	*DPPA5*
6.64	*RNF130*
6.54	*GC*
6.54	*MIR1204*
6.54	*KIAA0513*
6.54	*LOC102723672*
6.54	*MIR205*
6.44	*OLFM2*
6.44	*FRMD6*
6.44	*CCZ1B*
6.44	*DMRT1*
6.44	*TFAP2C*
6.44	*LOC100506885*
6.44	*KLRB1*
6.34	*C5orf66-AS1*
6.34	*AGK*
6.34	*GALNT8*
6.34	*COL2A1*
6.34	*C1orf105*
6.34	*LOC101928674*
6.34	*LOC101929544*
6.34	*C17orf64*
6.34	*BMPR1A*
6.25	*TRABD2A*
6.25	*CHCHD6*
6.25	*NMNAT2*
6.25	*LINC01696*
6.25	*CNTLN*
6.25	*SUMO1P1*
6.25	*SLC39A11*
6.15	*TNFRSF6B*
6.15	*PKP1*
6.15	*ZMIZ1-AS1*
6.15	*PXDN*
6.15	*IGF2BP1*
6.15	*LOC105376430*
6.15	*CST5*
6.15	*CNGB1*
6.15	*NR2F2*
6.05	*LINC01496*
6.05	*RIPK2*
6.05	*CHN2*
6.05	*ABCG2*
6.05	*CXorf21*
6.05	*LOC101928008*
6.05	*INPP4A*
6.05	*ALPL*
5.95	*BCAR3*
5.95	*MIR8084*
5.95	*CFL1*
5.95	*LOC100507468*
4.98	*SLC6A15*
4.98	*LOC102467223*
4.98	*DCAF4L2*
4.98	*LINC00603*
4.98	*PSTPIP2*
4.98	*HNF4G*
4.88	*GABRA6*
4.88	*LINC01676*
4.88	*COL23A1*
4.88	*PRDM14*
4.88	*SNTG1*
4.88	*ST6GALNAC1*
4.88	*KCNC2*
4.88	*CUBN*
4.88	*FRMD4A*
4.88	*SRSF10*
4.88	*STMN1*
4.88	*ZNF703*
4.88	*MLN*
4.88	*DGKB*
4.88	*KLF6*
4.88	*CH25H*
4.88	*TBCEL*
4.88	*LRRIQ3*
4.88	*MOG*
4.78	*ALPL*
4.78	*RIN1*
4.78	*PLOD1*
4.78	*PPFIA2*
4.78	*LINC01655*
4.78	*MLLT10P1*
4.78	*TMPRSS11B*
4.68	*LINC01037*
4.68	*MIR1915*
4.68	*LINC02032*
4.68	*TMUB2*
4.68	*ZC2HC1A*
4.68	*MIR7977*
4.68	*LOC105376430*
4.68	*BRWD3*
4.68	*LOC102723886*
4.68	*COL3A1*
4.68	*UST-AS1*
4.59	*USH2A*
4.59	*NRXN1*
4.59	*SGIP1*
4.59	*KCNK2*
4.59	*LINC00971*
4.59	*LOC105369893*
4.59	*DEFB1*
4.59	*SLAMF1*
4.59	*GSX1*
4.59	*BRINP3*
4.59	*LOC101928509*
4.59	*BCAR3*
4.59	*CYP4F35P*
4.59	*SLC6A15*
4.59	*OR2AP1*
4.59	*LINC01267*
4.59	*USP44*
4.59	*SHOX2*
4.59	*PABPC4L*
4.59	*LINC01884*
4.49	*KCNC2*
4.49	*CRB1*

12.7	*CERS4*	7.20	*TLK1*	5.95	*ESRRB*	4.49	*LINC01947*
12.7	*KDELR2*	7.20	*RBM17*	5.95	*LINC01210*	4.49	*CWF19L2*
12.6	*CFAP126*	7.20	*HSPA9*	5.95	*SLC36A4*	4.49	*DOCK3*
12.6	*CCND2*	7.07	*ACTR3B*	5.95	*ZNF565*	4.49	*LINC01720*
12.6	*SMARCA2*	7.07	*DPYD-AS2*	5.95	*SUGCT*	4.49	*TYRP1*
12.6	*MIR589*	7.07	*PMS2P4*	5.86	*FAM222B*	4.49	*PRG4*
12.6	*CLEC3A*	7.07	*PTPRZ1*	5.86	*LMO7-AS1*	4.49	*LINC01815*
12.6	*CCND2*	7.07	*LINC01440*	5.86	*LINC01699*	4.49	*MKRN9P*
12.5	*RCOR1*	7.07	*LOC101928386*	5.86	*GRK5*	4.49	*PRRC2B*
12.5	*SUZ12P1*	7.07	*TPRG1-AS1*	5.86	*FAM188B*	4.49	*UNC80*
12.5	*SEPHS1*	7.07	*NICN1*	5.86	*ITGB1*	4.49	*DOK5*
12.5	*GACAT3*	6.94	*RNF113A*	5.86	*SCGB1A1*	4.49	*LRIG3*
12.5	*ELAVL1*	6.94	*TMEM214*	5.86	*PABPC4L*	4.49	*SNTG1*
12.5	*CFAP126*	6.94	*LOC101928519*	5.86	*CYP1B1*	4.49	*LINC01370*
12.5	*ZHX2*	6.94	*KCMF1*	5.86	*FBXW4*	4.49	*DCN*
12.3	*LINC01012*	6.94	*LOC101929154*	5.86	*UBALD2*	4.39	*SLC6A5*
12.3	*CNR2*	6.94	*LINC01340*	5.86	*SLC39A1*	4.39	*COMMD1*
12.3	*SERBP1*	6.94	*LINC01714*	5.76	*SALL1*	4.39	*DGKB*
12.3	*COX6A1*	6.94	*TOB2P1*	5.76	*DNTT*	4.39	*OR6N1*
12.3	*IER2*	6.81	*RNF187*	5.76	*ESRP1*	4.39	*FRAT2*
12.3	*BISPR*	6.81	*CNTN4*	5.76	*LOC101929011*	4.39	*LINC02127*
12.2	*ZC3HAV1L*	6.81	*RBFOX1*	5.76	*ARSJ*	4.39	*LINC01142*
12.2	*LINC01819*	6.81	*TMPRSS11E*	5.76	*DDX18*	4.39	*LRBA*
12.2	*FBRS*	6.81	*LOC646241*	5.76	*CABLES1*	4.39	*HPVC1*
12.2	*HDAC11-AS1*	6.81	*ZNF777*	5.76	*CAAP1*	4.39	*CLEC14A*
12.2	*UPP1*	6.81	*RAB11FIP2*	5.76	*LOC101928894*	4.39	*LINC01790*
12.2	*DNMBP*	6.81	*LINC00648*	5.76	*NMNAT3*	4.39	*LOC100507468*
12.1	*CLPP*	6.81	*PACRG-AS2*	5.76	*EPHB3*	4.39	*ANKS1B*
12.1	*EEF2*	6.81	*POM121L2*	5.66	*DNAJB6*	4.39	*SKIL*
12.1	*HSPA6*	6.68	*GLRA4*	5.66	*FRAT2*	4.39	*DPP4*
12.1	*HK3*	6.68	*KCND2*	5.66	*OCM*	4.39	*ALG10*
12.1	*ZNF483*	6.68	*BMP7-AS1*	5.66	*RPA1*	4.39	*MIR4445*
12.1	*ADGRL1*	6.68	*C9orf85*	5.66	*SLAMF1*	4.39	*LOC100507468*
12.1	*FXR2*	6.68	*SEPHS1*	5.66	*CFLAR*	4.39	*DPY19L2*
12.1	*GAST*	6.68	*EIF3E*	5.66	*ID1*	4.39	*SLC4A4*
12.0	*PLIN3*	6.68	*RHOU*	5.66	*THBD*	4.39	*MIR4735*
12.0	*RPL36*	6.68	*JARID2*	5.66	*FAM196B*	4.29	*ZBED8*
12.0	*SNORD118*	6.68	*GGA3*	5.66	*PPIF*	4.29	*SYT1*
12.0	*DPRXP4*	6.68	*POLG*	5.66	*BMF*	4.29	*MIR3919*
11.8	*HTR1F*	6.68	*MIR513C*	5.66	*MLN*	4.29	*CA10*
11.8	*NOBOX*	6.68	*BRAT1*	5.66	*LOC105376360*	4.29	*SLC24A2*
11.8	*METTL21A*	6.68	*LINC00324*	5.56	*LOC646730*	4.29	*DCLK2*
11.8	*MIR3690*	6.55	*MIR4699*	5.56	*AOAH-IT1*	4.29	*BASP1*
11.7	*NUP85*	6.55	*CCDC57*	5.56	*DDX11-AS1*	4.29	*LINC01851*
11.7	*TTLL6*	6.55	*RHBDD2*	5.56	*DDX3X*	4.29	*PKIA*
11.7	*SHISA2*	6.55	*LINC01623*	5.56	*FBXL19-AS1*	4.29	*GPR149*
11.7	*CERS5*	6.55	*LINC00269*	5.56	*PLPP3*	4.29	*SLC36A4*
11.7	*PINK1*	6.55	*VWC2*	5.56	*ADAMTSL4*	4.29	*LINC01822*
11.7	*ALOXE3*	6.55	*UBE2G1*	5.56	*TSPAN18*	4.29	*TIA1*
11.6	*ILF2*	6.55	*MIR4654*	5.56	*DET1*	4.29	*LOC102467226*
11.6	*FAM212B-AS1*	6.55	*DAPK1*	5.56	*KCTD15*	4.29	*MKRN9P*
11.6	*APOBEC3F*	6.55	*ZNF184*	5.56	*ASIC2*	4.29	*MIR3974*
11.6	*LINC01822*	6.55	*MC4R*	5.56	*EGFEM1P*	4.29	*MIR181B1*
11.6	*SLC2A14*	6.55	*PLS3*	5.56	*PNPT1*	4.29	*ZNF804A*
11.6	*SIAH2*	6.55	*ADAMTS19-AS1*	5.56	*ADAMTS14*	4.29	*PXDNL*
11.4	*LINC01629*	6.55	*LINC00533*	5.47	*CCDC50*	4.29	*ST3GAL1*
11.4	*TEX43*	6.55	*SERPINI1*	5.47	*NCOR2*	4.29	*FRMD6-AS1*
11.4	*LOC102723557*	6.43	*CREB5*	5.47	*TMEM170B*	4.29	*KITLG*
11.4	*YIPF4*	6.43	*MIR6087*	5.47	*LINC01696*	4.29	*LOC105369860*
11.4	*CHMP6*	6.43	*TERC*	5.47	*KRTCAP3*	4.29	*SPRED2*
11.4	*MORC3*	6.43	*LINC01381*	5.47	*MATR3*	4.29	*LMO7-AS1*
11.4	*LINC01448*	6.43	*HOOK1*	5.47	*HULC*	4.29	*MIR4735*
11.4	*CP*	6.43	*LINC01320*	5.47	*SLC2A1-AS1*	4.29	*SI*
11.4	*PWWP2A*	6.43	*AFF2*	5.47	*HNF1B*	4.29	*TMEFF2*

11.4	*RFX1*
11.3	*FBN3*
11.3	*POLR2G*
11.3	*TLE2*
11.3	*MUC4*
11.3	*GGACT*
11.2	*ABCA13*
11.2	*RPUSD3*
11.2	*LHFPL4*
11.2	*EIF4B*
11.2	*LINC00941*
11.2	*CAND2*
11.2	*NIFK-AS1*
11.2	*TTC39B*
11.1	*UIMC1*
11.1	*RIF1*
11.1	*LINC01783*
11.1	*AFF1*
11.1	*GADD45GIP1*
11.1	*ERCC1*
10.9	*WDR66*
10.9	*CROCC*
10.9	*MOG*
10.9	*DDAH1*
10.9	*CLEC4C*
10.9	*MGC12916*
10.9	*LRIG1*
10.9	*MIR3675*
10.8	*ZMYND8*
10.8	*GRPR*
10.8	*PLEKHG2*
10.8	*UBXN11*
10.8	*MSH6*
10.8	*VDAC1*
10.8	*ATPIF1*
10.8	*UNC13B*
10.8	*MIR4472-2*
10.7	*IGFBP4*
10.7	*FCHO1*
10.7	*APTR*
10.7	*LINC01857*
10.7	*LINC00922*
10.5	*ARID3A*
10.5	*TMEM214*
10.5	*MTMR14*
10.5	*VAMP2*
10.5	*SLC35D3*
10.4	*MAN1C1*
10.4	*RPL6*
10.4	*OR2B2*
10.4	*TNRC18*
10.4	*LOC100507468*
10.4	*LINC01947*
10.4	*ZNF184*
10.4	*MELK*
10.4	*LINC01267*
10.4	*WSB1*
10.4	*RAF1*
10.4	*RNF112*
10.4	*ANG*
10.4	*UHRF1BP1L*
10.4	*RRAGC*
10.4	*LHX5*
10.3	*CASP16P*
10.3	*TIMP4*

6.43	*MYNN*
6.43	*CHSY3*
6.43	*SARS*
6.30	*ABCA1*
6.30	*NTN1*
6.30	*SERBP1*
6.30	*TBC1D32*
6.30	*GFRA1*
6.30	*LINC00972*
6.30	*UBXN11*
6.30	*MIR3162*
6.17	*RCC1*
6.17	*LINC01609*
6.17	*TMEM106B*
6.17	*MORF4L1*
6.17	*METTL21A*
6.17	*PTPRG*
6.17	*TYRP1*
6.17	*SHOX2*
6.17	*FBXW2*
6.17	*PFKFB4*
6.17	*LEFTY2*
6.17	*RNASE12*
6.04	*LOC101927139*
6.04	*MYLIP*
6.04	*KDM4B*
6.04	*LINC01716*
6.04	*POLR2G*
6.04	*EOMES*
6.04	*DAP*
6.04	*LINC00906*
6.04	*NAALADL2*
6.04	*ID3*
6.04	*LARP1B*
6.04	*EYA1*
6.04	*COMMD7*
6.04	*MYOF*
6.04	*DDX43*
5.91	*CRLF2*
5.91	*SLTM*
5.91	*DLGAP1-AS2*
5.91	*PABPC1P2*
5.91	*SNX16*
5.91	*LINC01036*
5.91	*DPP10*
5.91	*MIR5188*
5.91	*SGIP1*
5.91	*LOC101929555*
5.91	*LOC101929570*
5.91	*MIR1263*
5.91	*TRPC7*
5.91	*MIR4426*
5.91	*SRSF10*
5.91	*TDGF1*
5.91	*LOC101928909*
5.91	*SMU1*
5.78	*RN7SL1*
5.78	*CD99L2*
5.78	*MIR4459*
5.78	*ETV1*
5.78	*RPS24*
5.78	*LMX1B*
5.78	*RMND5B*
5.78	*STK10*
5.78	*SAMD5*

5.47	*PRPF6*
5.47	*STARD13*
5.37	*ASB1*
5.37	*GPX5*
5.37	*LINC02003*
5.37	*GDF6*
5.37	*GALNT2*
5.37	*XRCC5*
5.37	*GRHPR*
5.37	*PPM1A*
5.37	*RARRES3*
5.37	*CUBN*
5.37	*LOC101927056*
5.37	*ARID1B*
5.37	*TMUB2*
5.27	*PKDCC*
5.27	*FAM86DP*
5.27	*DDX11-AS1*
5.27	*LRRC4B*
5.27	*UXS1*
5.27	*IRX6*
5.27	*IER2*
5.27	*PAG1*
5.27	*PDE2A*
5.27	*PSORS1C2*
5.27	*PRRC2B*
5.27	*LOC101928540*
5.27	*MIR3664*
5.27	*NEAT1*
5.27	*LOC102724933*
5.27	*CASC18*
5.27	*WI2-2373I1.2*
5.27	*RARG*
5.27	*ALX1*
5.17	*AKAP1*
5.17	*MIR569*
5.17	*ALDH7A1*
5.17	*ATP6V1C2*
5.17	*DKK1*
5.17	*GREB1L*
5.17	*ST3GAL1*
5.17	*JUP*
5.17	*ZNF302*
5.17	*C11orf58*
5.17	*CDH10*
5.17	*LOC100507468*
5.17	*WBSCR17*
5.17	*CDH4*
5.17	*RRM1*
5.17	*RFK*
5.17	*OPRM1*
5.17	*LINC01070*
5.17	*MIR4427*
5.08	*SLC28A3*
5.08	*CSF1*
5.08	*CHCHD6*
5.08	*LINGO2*
5.08	*CFAP126*
5.08	*HSPA8*
5.08	*USP32*
5.08	*LOC102724890*
5.08	*NRP1*
5.08	*HNRNPAB*
5.08	*LOC100130298*
5.08	*ECE1*

4.29	*LINC01070*
4.29	*FZD4*
4.29	*KCNQ5*
4.29	*MIR548AE1*
4.29	*YTHDC2*
4.29	*LINC01111*
4.29	*PDE4B*
4.29	*MIR149*
4.29	*MIR4999*
4.29	*LRFN5*
4.29	*LINC01620*
4.29	*LINC02010*
4.29	*XIRP2*
4.29	*FUNDC2P2*
4.20	*MIR8065*
4.20	
4.20	*LINC01419*
4.20	*PTPRR*
4.20	*IZUMO3*
4.20	*PTCHD1*
4.20	*C1orf140*
4.20	*NKAIN3*
4.20	*TRIM2*
4.20	*NR4A3*
4.20	*MGAT4C*
4.20	*DUSP10*
4.20	*LOC440982*
4.20	*CASP8*
4.20	*CYP1B1*
4.20	*ADAMTS20*
4.20	*MAP4K5*
4.20	*LINC01170*
4.20	*LINC01322*
4.20	*ZNF335*
4.20	*LINC01239*
4.10	*NRP1*
4.10	*MIR4735*
4.10	*GXYLT1*
4.10	*LINC01609*
4.10	*FGF20*
4.10	*DGKB*
4.10	*IGSF5*
4.10	*BACH1-IT2*
4.10	*RCC2*
4.10	*SEMA6D*
4.10	*FAM19A2*
4.10	*FGFR3*
4.10	*KCNIP4-IT1*
4.10	*CDCA7L*
4.10	*DIRC1*
4.10	*LINC00524*
4.10	*LINC01031*
4.10	*LINC01935*
4.10	*NFATC1*
4.10	*NFIB*
4.10	*LINC01239*
4.10	*LINC01554*
4.10	*PELO*
4.10	*LOC102723895*
4.10	*MROH9*
4.10	*LOC100129138*
4.10	*PLSCR2*
4.10	*MTAP*
4.10	*SP3*
4.10	*DNAH7*

10.3	*GLOD5*
10.3	*PFKFB4*
10.3	*PIH1D1*
10.3	*MIR648*
10.3	*RPEL1*
10.3	*HNF1A-AS1*
10.3	*SPATA45*
10.2	*LINC01164*
10.2	*RCC2*
10.2	*SRCIN1*
10.2	*LOC105369723*
10.2	*ZBTB5*
10.2	*TERF1*
10.2	*RPN1*
10.2	*CERS4*
10.2	*WWTR1-AS1*
10.2	*ADGRL1*
10.2	*NANOG*
10.2	*MIR9-2*
10.2	*PLAGL1*
10.2	*STYK1*
10.2	*BCAT1*
10.0	*ZNF184*
10.0	*ZNF335*
10.0	*SLC44A1*
10.0	*ZNF675*
10.0	*CASC21*
10.0	*ZMYND8*
10.0	*RAB5C*
10.0	*LYZL1*
10.0	*BASP1*
10.0	*FGD4*
10.0	*LOC284788*
10.0	*WNT5B*
10.0	*DENND2A*
10.0	*ATF7IP*
9.89	*FAM60A*
9.89	*MIR5188*
9.89	*TNFAIP8L1*
9.89	*TERC*
9.89	*SPNS3*
9.89	*SRCIN1*
9.89	*MACF1*
9.89	*ANKRD1*
9.89	*LOC105369632*
9.89	*RPH3A*
9.89	*ZNF184*
9.77	*KIF2C*
9.77	*TGFBR2*
9.77	*PXN*
9.77	*OR6S1*
9.77	*PCLO*
9.77	*GRIA3*
9.77	*UBE2G1*
9.77	*LOC105374988*
9.77	*RAD52*
9.77	*TRIP4*
9.77	*RP9P*
9.77	*MORF4L1*
9.77	*ZFP36L2*
9.77	*RHBDD2*
9.77	*SPEN*
9.77	*EIF2AK1*
9.64	*SLC2A14*
9.64	*C19orf25*
5.78	*EPHA3*
5.78	*RIPK1*
5.78	*YWHAE*
5.78	*LINGO2*
5.78	*MTF2*
5.78	*SNUPN*
5.78	*WDR59*
5.78	*LINC01623*
5.78	*MIR371A*
5.65	*KLF4*
5.65	*SLC44A1*
5.65	*PLOD2*
5.65	*OR1F1*
5.65	*SSTR2*
5.65	*FAM212B-AS1*
5.65	*SLC2A3*
5.65	*PRUNE1*
5.65	*RPL34-AS1*
5.65	*AACSP1*
5.65	*NRXN3*
5.65	*LAMA2*
5.65	*TMEM106B*
5.65	*OSCP1*
5.65	*NXPH1*
5.65	*TMEM14EP*
5.65	*NATD1*
5.65	*LOC100996251*
5.65	*SOX2-OT*
5.65	*OR5AR1*
5.65	*PIM2*
5.53	*LOC100132831*
5.53	*ZMYND8*
5.53	*TRAPPC8*
5.53	*TMEM2*
5.53	*LINC01012*
5.53	*ASMT*
5.53	*LRP1B*
5.53	*YIPF5*
5.53	*FOXN3*
5.53	*LINC01242*
5.53	*LOC105369860*
5.53	*PCLO*
5.53	*C17orf112*
5.53	*SPEN*
5.53	*SNORD12*
5.53	*OTUD4*
5.53	*CCDC62*
5.53	*ANKS1B*
5.40	*SFRP2*
5.40	*CWC27*
5.40	*LINC01756*
5.40	*CASP16P*
5.40	*DHX15*
5.40	*NEGR1*
5.40	*PHF12*
5.40	*ASGR2*
5.40	*LOC101928834*
5.40	*LINC01320*
5.40	*CDKL3*
5.40	*TMEM261*
5.40	*SKAP2*
5.40	*SPATA16*
5.40	*IAPP*
5.40	*FAT4*
5.40	*LOC100506474*
5.08	*LINC01063*
5.08	*RIMS1*
5.08	*KYNU*
4.98	*OTUD4*
4.98	*TTC25*
4.98	*KDELR2*
4.98	*NUDCD1*
4.98	*ZFAT*
4.98	*PLAGL1*
4.98	*WWP2*
4.98	*ETV4*
4.98	*LINC01139*
4.98	*C20orf85*
4.98	*GNPDA2*
4.98	*TRIM24*
4.98	*KIF15*
4.88	*ZNF608*
4.88	*GC*
4.88	*SLC36A4*
4.88	*MIR3917*
4.88	*RSPO3*
4.88	*PDK1*
4.88	*RBFOX1*
4.88	*FAM19A5*
4.88	*PSKH2*
4.88	*LMX1B*
4.88	*LINC01090*
4.88	*CUEDC1*
4.88	*NSD1*
4.88	*COL4A1*
4.88	*KLF6*
4.88	*ISG20*
4.88	*NBPF3*
4.88	*TBCEL*
4.88	*CTSO*
4.78	*LINC00964*
4.78	*SP4*
4.78	*RHOB*
4.78	*ZBTB10*
4.78	*LINGO2*
4.78	*TADA3*
4.78	*TMEM132D*
4.78	*NDUFS5*
4.78	*TENM3*
4.78	*CNDP1*
4.78	*KIAA1456*
4.78	*CENPN*
4.78	*LINC00551*
4.78	*PTPRS*
4.78	*EEF1A1*
4.78	*MIR4792*
4.78	*TYRO3*
4.78	*LOC101927043*
4.78	*SLAMF7*
4.78	*MIR2053*
4.78	*PRSS36*
4.78	*SPATA6*
4.78	*FUZ*
4.78	*LINC01291*
4.78	*USP32*
4.78	*BMPR1A*
4.78	*DEFB131*
4.78	*KIAA1614*
4.78	*LOC646241*
4.68	*FAM84B*
4.10	*MIR2053*
4.00	*PTPRD*
4.00	*TMEM178A*
4.00	*P2RY1*
4.00	*FAM46A*
4.00	*OR2L5*
4.00	*KCNB2*
4.00	*FGF13*
4.00	*APBB2*
4.00	*NUDT12*
4.00	*LINC01343*
4.00	*LOC102723833*
4.00	*FRG1BP*
4.00	*LOC105377143*
4.00	*LINC01467*
4.00	*CEBPZ*
4.00	*MIR5688*
4.00	*LOC100506474*
4.00	*SI*
4.00	*LRRC4B*
4.00	*SOX2-OT*
4.00	*DKK1*
4.00	*LOC101927849*
4.00	*LINC01324*
4.00	*LINGO2*
4.00	*ELAVL2*
4.00	*LOC105376633*
4.00	*ADGRB3*
4.00	*RELN*
4.00	*FOXN3-AS2*
4.00	*MIR1-1HG*
4.00	*LINC01473*
4.00	*SATB2*
4.00	*MIR205*
4.00	*NLN*
4.00	*PRG4*
4.00	*LOC105373782*
3.90	*LRP12*
3.90	*UGT2A3*
3.90	*CHRM3*
3.90	*LINC01948*
3.90	*LINC01923*
3.90	*BRINP3*
3.90	*PRDM14*
3.90	*LINC01995*
3.90	*PSAT1*
3.90	*STARD7*
3.90	*LINC01467*
3.90	*LOC102723831*
3.90	*SFRP2*
3.90	*MIR6827*
3.90	*MIR4735*
3.90	*CDAN1*
3.90	*TUSC1*
3.90	*LOC102724053*
3.90	*TOX*
3.90	*LOC100129434*
3.90	*OR4A5*
3.90	*LOC105375972*
3.90	*LOC100506474*
3.90	*KCNC2*
3.90	*GOLIM4*
3.90	*PRRX1*
3.90	*LINC01239*
3.90	*HDAC9*

9.64	*SYT6*	5.40	*MIR3686*	4.68	*MIR4454*	3.90	*RAB17*
9.64	*DNM1L*	5.40	*GPRIN3*	4.68	*PYGL*	3.90	*BSPRY*
9.64	*RIOX1*	5.40	*PER4*	4.68	*MIR1915*	3.90	*GLRA3*
9.64	*SLC2A14*	5.40	*PRRC2C*	4.68	*UBQLN4*	3.90	*LGR5*
9.64	*MIR1303*	5.40	*ATF6*	4.68	*LINC00303*	3.90	*STMN2*
9.64	*BRDT*	5.40	*LOC101929926*	4.68	*ITGB5*	3.90	*UBE2N*
9.64	*PIK3CB*	5.40	*PTBP2*	4.68	*SRD5A2*	3.90	*TRHR*
9.64	*GDF3*	5.40	*LRRC7*	4.68	*C8orf58*	3.90	*DOK5*
9.64	*GCNT2*	5.40	*LOC101927434*	4.68	*APP*	3.90	*LINC01014*
9.51	*ZBED9*	5.40	*LINC01242*	4.68	*FGF13*	3.90	*LINGO2*
9.51	*RPA3*	5.40	*CASC21*	4.68	*MIR548AQ*	3.90	*RANBP17*
9.51	*YWHAE*	5.40	*ATR*	4.68	*PHTF2*	3.90	*LOC102546299*
9.51	*ASIC2*	5.40	*MIR4521*	4.68	*HEG1*	3.90	*EGFEM1P*
9.51	*SLC35F3*	5.40	*LINC00276*	4.68	*TSPAN18*	3.90	*FAM196B*
9.51	*HCG27*	5.40	*LINC01947*	4.68	*BRWD3*	3.90	*CADM2-AS2*
9.51	*NTN1*	5.40	*HNF1A-AS1*	4.68	*MIR4463*	3.90	*PLCB1*
9.51	*TRIM71*	5.40	*PRSS16*	4.59	*SERBP1*	3.90	*MAML3*
9.51	*BRAT1*	5.27	*PRKACB*	4.59	*TFDP2*	3.90	*THADA*
9.51	*LOC102546229*	5.27	*VPS41*	4.59	*AGO3*	3.90	*TNFSF18*
9.51	*MYNN*	5.27	*TYRP1*	4.59	*LOC101927847*	3.90	*SLC16A7*
9.51	*LINC01267*	5.27	*ZNF184*	4.59	*POMC*	3.90	*LINC02141*
9.38	*LINC01381*	5.27	*SLC29A2*	4.59	*LOC101928254*	3.90	*LINC01239*
9.38	*MIR23A*	5.27	*ZNRF1*	4.59	*SNAPC1*	3.90	*EEF1A1*
9.38	*PEMT*	5.27	*SEMA3E*	4.59	*AMOTL2*	3.90	*MMP16*
9.38	*VAMP1*	5.27	*PRR16*	4.59	*FGF18*	3.90	*PDPN*
9.25	*SNURF*	5.27	*LOC101927356*	4.59	*LINC01005*	3.90	*P2RY1*
9.25	*NANOG*	5.27	*MUC19*	4.59	*ZBTB5*	3.90	*LOC440982*
9.25	*PGPEP1*	5.27	*LINC02032*	4.59	*MIR548AG2*	3.90	*CNGB3*
9.25	*LINC00620*	5.27	*HIST1H4H*	4.59	*FGFR1*	3.90	*MIR548AD*
9.25	*LINC00533*	5.27	*SGK1*	4.59	*FAM86EP*	3.90	*GBE1*
9.25	*CLEC7A*	5.27	*MIR4699*	4.59	*NKAIN1*	3.90	*KCNN2*
9.25	*LOC100507468*	5.27	*DCN*	4.49	*YWHAZ*	3.90	*RNF133*
9.25	*CLINT1*	5.27	*DOCK3*	4.49	*LINC01962*	3.90	*EPDR1*
9.25	*BMPR2*	5.27	*CACHD1*	4.49	*LRRN3*	3.90	*TMEM139*
9.25	*PRSS16*	5.27	*TOX*	4.49	*LINC00552*	3.90	*ISG20*
9.25	*GTF2I*	5.27	*TTC27*	4.49	*CWF19L2*	3.90	*LOC100507377*
9.25	*LINC00533*	5.27	*LINC01947*	4.49	*TRERF1*	3.90	*FYB*
9.25	*FLNB*	5.27	*MSH6*	4.49	*LINC01170*	3.90	*NTS*
9.25	*REST*	5.27	*PRICKLE1*	4.49	*PSAP*	3.90	*SLC24A2*
9.25	*SENP2*	5.27	*CFD*	4.49	*PBX3*	3.90	*CDC14C*
9.25	*CDH1*	5.27	*PPM1B*	4.49	*ZNF826P*	3.90	*LINC00971*
9.25	*LOC100270746*	5.27	*FGF12*	4.49	*LINC01488*	3.90	*MIR2053*
9.25	*KDM4B*	5.27	*SPRED2*	4.49	*SSUH2*	3.90	*TFCP2L1*
9.25	*VWF*	5.27	*LINC00299*	4.49	*SSUH2*	3.90	*LINC01222*
9.12	*AP2A2*	5.27	*MIR7157*	4.49	*MIR205HG*	3.90	*LOC401134*
9.12	*OLFM2*	5.27	*XK*	4.49	*THSD4-AS2*	3.90	*MIR7641-2*
9.12	*TP53*	5.27	*LINC01322*	4.49	*MAP4K4*	3.90	*FAM188B*
9.12	*SLC2A14*	5.27	*CCDC171*	4.49	*HUS1*	3.81	*KCNC2*
9.12	*CASC17*	5.27	*MIR548AD*	4.49	*HUS1*	3.81	*RPS29*
9.12	*HSPB1*	5.27	*HES7*	4.49	*KPNA2*	3.81	*PKIA*
9.12	*DFNA5*	5.27	*DCUN1D1*	4.49	*TMCC1*	3.81	*CNTNAP4*
9.12	*PRR13*	5.27	*JAK2*	4.39	*FOLR1*	3.81	*PITPNM2*
9.12	*CCDC9*	5.27	*LINC00693*	4.39	*SPARC*	3.81	*ZIC4*
9.12	*PUM1*	5.27	*SNORA38B*	4.39	*LINC01101*	3.81	*HDGF*
9.12	*LOC101927637*	5.27	*LINC00533*	4.39	*ESCO1*	3.81	*MIR4300*
9.12	*FOXJ2*	5.27	*KANK1*	4.39	*LOC105369739*	3.81	*LOC102723883*
9.12	*TRAPPC8*	5.27	*ZNF714*	4.39	*TMEM72*	3.81	*KCNV1*
9.12	*LRP6*	5.27	*CTR9*	4.39	*PLCD4*	3.81	*GRM5*
9.12	*DAZL*	5.27	*SULT6B1*	4.39	*SSBP3*	3.81	*MIR4735*

Genes are annotated according to distance of ChIP-seq peak to the nearest transcription start site (TSS)

9. Publications

2019 **Epigenetic drugs and their molecular targets in testicular germ cell tumours**
Jostes S, Nettersheim D, Schorle H
Nature Reviews Urology

2018 **Deciphering the molecular effects of romidepsin on germ cell tumours: DHRS2 is involved in cell cycle arrest but not apoptosis or induction of romidepsin effectors.**
Nettersheim D, Berger D, Jostes S, Skowron M, Schorle H
J Cell Mol Med. 2018 Nov 20

2018 **Signals and Transcription Factors for Specification of Human Germ Cells**
Jostes S, Schorle H
Stem Cell Investigations 2018; 5:13

2017 **Xenografting of Cancer Cell Lines for In Vivo Screening of the Therapeutic Potential of HDAC Inhibitors**
Nettersheim D, Jostes S, Schorle H
Methods Mol Biol. 2017

2016 **Re-visiting the Protamine-2 locus: deletion, but not haploinsufficiency, renders male mice infertile.**
Schneider S, Balbach M, Jikeli J, Fietz D, Nettersheim D, Jostes S, Schmidt R, Kressin M, Bergmann M, Wachten D, Steger K, Schorle H
Sci Rep. 2016 Nov 11;6:36764

2016 **The bromodomain inhibitor JQ1 triggers growth arrest and apoptosis in testicular germ cell tumours in vitro and in vivo**
Jostes S, Nettersheim D, Fellermeyer M, Schneider S, Hafezi F, Honecker F, Schumacher V, Geyer M, Kristiansen G, Schorle H
J Cell Mol Med. 2016 Dec 27

2016 **A signalling cascade including ARID1A, GADD45B and DUSP1 induces apoptosis and affects the cell cycle of germ cell cancers after romidepsin treatment**
Nettersheim D, Jostes S, Fabry M, Honecker F, Schumacher V, Kirfel J, Kristiansen G, Schorle H
Oncotarget. 2016 Aug 27.

2016 **Elucidating human male Germ Cell Development by studying Germ Cell Cancer**
Nettersheim D, Jostes S, Schneider S, Schorle H
Reproduction. 2016 Oct 152(4):R101-13

2016 **The cancer/testis-antigen PRAME supports the pluripotency network and represses somatic germ cell differentiation programs in seminomas**
Nettersheim D, Arndt I, Sharma R, Riesenberg S, Jostes S, Schneider S, Hölzel M, Kristiansen G, Schorle H
Br J Cancer. 2016 Aug 9;115(4):454-64

2016 **SOX2 is essential for in vivo reprogramming of seminoma-like TCam-2 cells to an embryonal carcinoma-like fate**
Nettersheim D, Heimsoeth A, Jostes S, Schneider S, Fellermeyer M, Hofmann A, Schorle H
Oncotarget. 2016 Jul 26;7(30):47095-47110

2015 **BMP Inhibition in Seminomas Initiates Acquisition of Pluripotency via NODAL Signaling Resulting in Reprogramming to an Embryonal Carcinoma**
Nettersheim D, Jostes S, Sharma R, Schneider S, Hofmann A, Ferreira HJ, Hoffmann P, Kristiansen G, Esteller MB, Schorle H
PLoS Genet. 2015 Jul 30;11(7):e1005415

10. Acknowledgements

Allen voran möchte ich mich bei meinem Doktorvater Prof. Dr. Hubert Schorle bedanken. Bereits 2013 gab er mir die Möglichkeit seine Arbeitsgruppe und die hier angestrebten wissenschaftlichen Projekte und Ziele im Rahmen eines Labor-Praktikums kennen zu lernen. Gerne habe ich hier auch das Projekt meiner anschließenden Masterarbeit begonnen, welches ich im Rahmen der Doktorarbeit weiterführen und ausbauen konnte. Prof. Dr. Schorle hat mich vertrauensvoll auf meinem wissenschaftlichen Weg begleitet und mir zu jeder Zeit das Gefühl vermittelt mit Fragen oder Problemen an ihn herantreten zu können. Für seine Hilfe und seine geleistete Vorbereitung auf meinen wissenschaftlichen Werdegang bin ich sehr dankbar.

Außerdem gilt mein Dank Priv. Doz. Dr. Reinhard Bauer für die freundliche Bereitschaft das 2.-Gutachten meiner Arbeit zu übernehmen. Zudem bedanke ich mich bei Prof. Matthias Geyer für eine erfolgreiche Kollaboration, sowie die Zusage Teil meiner Prüfungskommission zu sein und bei Prof. Dr. Ian Brock für die Bereitschaft als fachfremdes Prüfungsmitglied der Kommission anzugehören.

Der Sander Stiftung danke ich für die finanzielle Unterstützung des SOX2/SOX17 Projekts, ohne welches die letzten beiden Jahre meiner Promotion nicht möglich gewesen wären. Der Monika Kutzner Stiftung danke ich für die finanzielle Unterstützung des JQ1 Projekts. Außerdem bedanke ich mich bei GlaxoSmithKline, dem DAAD und dem Bonner Forum Biomedizin für die Erstattung von Reisekosten und Konferenzgebühren. Mithilfe dieser Gelder war es mir möglich meine wissenschaftlichen Ergebnisse im nationalen und internationalen Rahmen zu diskutieren und mich mit anderen Wissenschaftlern auf diesem Gebiet auszutauschen.

Ferner gilt mein Dank allen aktuellen und ehemaligen Mitarbeitern der Pathologie. Besonders Prof. Dr. Daniel Nettersheim hat mich während seiner Zeit als Post Doc unter Prof. Schorle immer tatkräftig unterstützt und mir bei der Projektplanung, sowie dem Schreiben von Publikationen hilfreich zur Seite gestanden. Ich möchte mich auch besonders bei Gaby Beine, Franziska Kaiser, Simon Schneider, Jan Langkabel, Blanca Randel, Anna Pehlke und Caroline Schuster bedanken. Auch dank ihnen war die Zeit in der Pathologie ein tolles Erlebnis für mich und ich bin dankbar für so viel Freundlichkeit und Zusammenhalt innerhalb der Arbeitsgruppe. Nicht zuletzt möchte ich mich bei meiner Familie, meinem Partner und bei meinen Freunden bedanken, welche auch außerhalb der Arbeitsgruppe immer ein offenes Ohr für mich hatten und mich während dieser herausfordernden Zeit unterstützt haben.